Quantification of fucoidan isolated from *Laminaria hyperborea* using two different colorimetric assays and qNMR method

Erling Sæbø Fagnastøl

Department of chemistry

University of Bergen

2022

Image front page: Laminaria hyperborea, picture by Alginor.

Acknowledgements

I would first like to thank my main supervisor, associate professor Monica Jordheim for the guidance and support throughout the research period. I would also like to thank external supervisor, research & development manager at Alginor, Georg Kopplin for his supervision and encouragement.

I am grateful for the Research Council of Norway and Alginor for their financial support, and for all support given by the technical staff at the Department of Chemistry (UiB). I sincerely appreciate the opportunity of being a part of the Alginor FucoMed project, which may lead to higher sustainable utilization of the riches along the Norwegian coast.

A special thanks goes to the industrial PhD candidate Marie Wekre (UiB, Alginor ASA) for sharing her valuable laboratory experience, and to Alginor researcher Collin C.V. Danker for his experience with the NMR instrumentation at the Department of Chemistry (UiB).

List of selected abbreviations:

Seaweeds:	
F. ves.	*Fucus vesiculosus,* eng: bladderwrack, nor:blæretang
L. hyp.	*Laminaria hyperborea, eng:* tangle/cuvie, nor: stortare

Chemicals:	
$(CH_3)_2CO$	Acetone
Calcium formate	≥99,9% Calsium formate from Sigma Aldrich Ca(HCOO)2
CH_3COOH	Acetic acid
Crude fucoidan (OEWA-00038)	Fucoidan from *L. hyp.* that has been extracted and is less filtered than the fine fucoidan (Alginor)
D_2O	≥99,9% Deuterium oxide from Bruker
Factor Xa	Lyophilized bovine FXa containing Tris buffer, EDTA, NaCl, dextran sulphate and bovine serum albumin.
Fine fucoidan (OEWA-00289)	Fucoidan from *L. hyp.* that has been extracted and more finely filtered than the crude fucoidan (Alginor)
Fucoidan standard	≥95% fucoidan from *Fucus vesiculosus*. In all experiments except NMR, it was assumed that the fucoidan was 95% pure.
HCl	Hydrochloric acid
KHP	Potassium hydrogen phthalate
L-FDH	L-Fucose dehydrogenase suspension, stable for > 2 years below -10C
L-Fucose	Fucoidan that has been hydrolyzed and desulphated into L-fucose units
L-Fucose Standard	≥99,9% fucose from Sigma Aldrich
L-Fucose colorimetric assay Buffer	Plus sodium azide, stable for > 2 years at 4C, pH 9,5
L-Fucose colorimetric assay standard	L-Fucose standard solution (0,5mg/ml), stable for > 2 years at 4C
NADP+	Nicotinamide-adenine dinucleotide phosphate, freeze dried powder
NaOH	Sodium hydroxide
S-2732	Chromogenic substrate, Suc-Ile-Glu(γ-pip)-Gly-Arg-pNA • HCl lyophilized with detergent and mannitol as bulking agent
Water	Deionized water (Deionized at the University of Bergen)

Other:	
6-hh	6-hours hydrolyzation
24-hh	24-hours hydrolyzation
48-hh	48-hours hydrolyzation
Col. assay	Colorimetric assay
DP	Degree of polymerization
DS	Degree of sulphation
GHz	Giga Hertz

kDa	Kilodalton
LOD	Limit of Detection
MDa	Megadalton
MHz	Mega Hertz
MT^{-1}	Metric tons
NMR	Nuclear Magnetic Resonance Spectroscopy
NNP	Norwegian NMR Platform
qNMR	Quantitative Nuclear Magnetic Resonance Spectroscopy
R^2	Coefficient of determination
SDG-14	Sustainable Development Goal 14: Life below water
SEC	Size Exclusion Chromatography
S/N	Signal to Noise ratio
UiB	University of Bergen
UV-VIS	Ultraviolet-Visible light Spectroscopy

Abstract

In this thesis, a colorimetric heparin assay and quantitative NMR (qNMR) are used for fucoidan quantification and compared against an established colorimetric enzymatic L-fucose assay. For the L-fucose colorimetric assay, the assay procedure was followed as described by the manufacturer. The fucoidan quantification of the fucoidan standard (≥ 95 %) (Sigma Aldrich/Merck, obtained from *Fucus vesiculosus*) was assumed to be 95% pure and the weight is based on this fucoidan purity. The heparin colorimetric assay, initially a method for quantification of heparin in blood plasma was adapted from microplate UV-VIS to cuvette UV-VIS by either quadrupling or quintupling the volumes in the procedure. A high purity fucoidan standard (≥ 95 %) (Sigma Aldrich/Merck, obtained from *Fucus vesiculosus*) was used to prepare a fucoidan standard curve, and optimization of the standardization conditions was performed. The fucoidan content of a fine (OEWA-00289) and a crude (OEWA-00038) fucoidan sample, obtained from *Laminaria hyperborea (L. hyp*.) by Alginor, were determined using the optimized heparin col. assay. For the qNMR experiments, calcium formate was selected as a standard mainly based on the expected lack of overlapping signals with the ^{1}H signals from the fucoidan structure. The fucoidan standard (≥95%) (Sigma Aldrich/Merck) and the fine and crude fucoidan samples from Alginor were quantified with the qNMR method.

The L-fucose colorimetric assay gave a reasonable yield for the fucoidan standard (98.0±0.17%) with high accuracy and precision, close to the qNMR yield (98.7%). The heparin colorimetric assay gave high accuracy in the fine fucoidan (OEWA-00289) sample (57.6 ±3.4%) and decent precision. The result was almost identical to the result from the L-fucose assay (57.1 ±0.7%) and qNMR (56.8%). The heparin assay gave low accuracy and low precision when quantifying the crude fucoidan (OEWA-00038) (46.5 ±5.3%) compared to the L-fucose assay (28.7±0.40%) and qNMR (33.4%).

For fucoidan quantification of cruder solutions with more contaminants, it appears that the precision and accuracy of the heparin col. assay is lowered. The heparin col. assay has however proven to be a direct and rapid method of quantifying fucoidan samples from *L. hyp*. The established L-fucose colorimetric assay appears to benefit from the fact that impurities in the fucoidan samples are removed when hydrolyzing the fucoidans into L-fucose monomers with 1M HCl. Hydrolyzing fucoidan samples for 48 hours at 65°C gives high accuracy and precision but is time consuming. To overcome this time-consuming step, the temperature can be increased, and time spent hydrolyzing can be lowered, this will however lower precision and accuracy. The qNMR method appears to be highly accurate quantifying fucoidan samples of high purity and less affected by contaminants in cruder fucoidan samples compared to the heparin assay. All three methods were proven to be capable of quantifying fucoidan samples of different purity.

Table of contents

Acknowledgements 3
List of selected abbreviations: 4
Abstract 6
List of figures 9
List of tables 11
Chapter 1 - Introduction 12
1.1 Motivation 12
1.2 Macroalgae 13
1.2.1 *Laminaria hyperborea* 17
1.3 Polysaccharides/carbohydrates in *Laminaria hyperborea* 18
1.3.1 Alginate 19
1.3.2 Laminaran 20
1.3.3 Fucoidan 20
1.4 Comparison of heparin and fucoidan 24
Chapter 2 – Experimental methods 26
2.1 Extraction 26
2.2 Ultraviolet-Visible (UV-VIS) Spectroscopy 27
2.3 Colorimetric assays 28
2.3.1 L-fucose colorimetric assay quantification 29
2.3.2 Heparin colorimetric assay 33
2.4 Nuclear Magnetic Resonance (NMR) Spectroscopy 37
2.4.1 Quantitative Nuclear Magnetic (qNMR) Spectroscopy 38
Chapter 3 – Results and discussion 42
3.1.1 Initial test analysis – quantitative assays 42
3.2 L-fucose colorimetric assay standardization 42
3.2.1 L-fucose standard curve 42
3.2.2 Quantifying the fucoidan standard using L-fucose col. assay 44
3.2.3 Quantification of fine fucoidan (OEWA-00289) 46
3.2.4 Quantification of crude fucoidan (OEWA-00038) 46
3.3 Heparin colorimetric assay 48
3.3.1 Standard curves obtained with Sigma Aldrich fucoidan and drift checks for parallels 48
3.3.2 Quantification of fucoidan from fine fucoidan (OEWA-00289) 53
3.3.3 Quantification of fucoidan from crude fucoidan (OEWA-00038) 55
3.3.4 Improving the standard curve 56

3.3.5 Standardization at room temperature 58
3.4 Quantification of fucoidan using the quantitative NMR method 61
3.4.1 qNMR of L-Fucose (≥99.9%) standard 63
3.4.2 qNMR analysis of fucoidan standard 67
3.4.3 qNMR of fine fucoidan (OEWA-00289) sample 68
3.4.4 qNMR of crude fucoidan (OEWA-00038) sample 69
Chapter 4 – Conclusion and further work 71
Sources 74
Appendix 1: Drift checks of selected L-fucose col. assay experiments 84
Appendix 2: Drift check of optimized and room temperature heparin col. assay standard curves 90
Appendix 3: ^{1}H NMR and qNMR spectrums 92

List of figures

Figure 1: Macrocystis pyrifea, aka. giant kelp (Brauder, retrieved 28.01.2022) 14
Figure 2: Seaweed global market share (Piconi, 2020) 14
Figure 3: A fine-tuned global distribution dataset of brown seaweed (J. Assis, 2020) 15
Figure 4: Laminaria hyperborea (Mortensen, last accessed 01.04.2022) 17
Figure 5: The littoral zones where seaweeds are known to be (J. R. Dodson, 2013) 17
Figure 6: Laminaria hyperborea breaking the ocean surface at low tide (algaebase.org) 18
Figure 7: Components and structure of alginate (sciencedirect – alginate, last accessed 04.05.2022). 19
Figure 8: The figure shows the two types of laminaran chains with either mannitol (A) or glucose (B) attached. 20
Figure 9: Two suggested general fucoidan structures, type I and type II, based on findings from 9 different seaweed sources (Cumashi, 2007). 21
Figure 10: Suggested structural fragment of 25 fucose residues applied as building blocks for a full-scale structural model (DP = 750, Rw = 37nm) of Fucoidan from Laminaria Hyperborea (Kopplin, 2019) 23
Figure 11: Repeating units in the polysaccharides heparin (left) and fucoidan (fucose residues) (right). 24
Figure 12: Hydrolyzation of fucoidan causes depolymerization and desulphation of the polysaccharide into L-fucose units. 29
Figure 13: Reaction principle of the L-fucose col. assay. 30
Figure 14: NADP+ and NADPH wavelength difference at 340 nm 30
Figure 15: Absorbance of hydrolyzed and desulphated fucoidan measured periodically using L-fucose col. assay (Ahmad, 2015). 31
Figure 16: General structure of Heparin (left) and Fucoidan (right). 33
Figure 17: UV-VIS spectra of pNA (Baraniraj, 2011). 35
Figure 18: qNMR method overview (Quantitative NMR, retrieved 28.03.2022) 39
Figure 19: Potassium phthalate monobasic (left), Calcium formate (middle), and fucoidan fracture (right). 40
Figure 20: Standard curve L-fucose with two parallels, formula of P2 was used. 43
Figure 21: Drift check of L-fucose standard curve P1. 44
Figure 32: Heparin col. assay standard curve using Sigma Aldrich fucoidan solution 1, P1. 49
Figure 33: Drift check of the heparin col. assay standard curve P1. 49
Figure 34: Heparin col. assay standard curve using Sigma Aldrich fucoidan solution 1, P2. 50
Figure 35: Heparin col. assay standard curve using Sigma Aldrich fucoidan P2. 50
Figure 36: Heparin col. assay standard curve using Sigma Aldrich fucoidan solution 1, P3. 51
Figure 37: Heparin col. assay standard curve using Sigma Aldrich fucoidan P3. 51
Figure 38: Comparison of heparin col. assay standard curves using Sigma Aldrich fucoidan P1, P2 and P3. 52
Figure 39: Drift check of fine fucoidan with the heparin col. assay. Measurements done every 60 seconds 54
Figure 40: Drift check of crude fucoidan with the heparin col. assay. Measurements every 30 seconds. 55
Figure 41: Standard curve with Sigma Aldrich fucoidan solution 2 P1. 57
Figure 43: Standard curve with Sigma Aldrich fucoidan solution 2 P2. 57
Figure 45: Comparison of standard curves with Sigma Aldrich fucoidan solution 2 P1 and P2. 58
Figure 46: Standard curve with Sigma Aldrich fucoidan solution 3 P1 with room temperature. 59
Figure 48: Standard curve with Sigma Aldrich fucoidan solution 3 P2 with room temperature. 59
Figure 50: Comparison of standard curves P1 and P2 with T=293K. 60
Figure 51: Standard curve comparison of fucoidan solution 2 (P1 and P2) and fucoidan solution 3 performed at room temperature (P1 T=293K and P2 T=293K). 60
Figure 52: 1H NMR of L-fucose with calcium formate as standard. The alpha and beta C6 proton and the beta and alpha methyl group is highlighted. 62
Figure 22: Drift check of L-fucose standard curve P2. 84
Figure 23: Drift check of the three parallels of the 6-hh fucoidan standard. 84
Figure 24: Drift check of the three parallels of the 24-hh fucoidan standard. 85
Figure 25: Drift check of the three parallels of the 48-hh fucoidan standard. 85
Figure 26: Drift check of the three parallels of the 6-hh fine fucoidan. 86
Figure 27: Drift check of the three parallels of the 24-hh fine fucoidan. 87
Figure 28: Drift check of the three parallels of the 48-hh fine fucoidan. 87

Figure 29: Drift check of the three parallels in 6-hh fucoidan crude. 88
Figure 30: Drift check of the three parallels in 24-hh fucoidan crude. 88
Figure 31: Drift check of the three parallels in 48-hh crude fucoidan. 89
Figure 42: Drift check for standard curve with Sigma Aldrich fucoidan solution 2 P1 90
Figure 44: Drift check for standard curve with Sigma Aldrich fucoidan solution 2 P2. 90
Figure 47: Drift check of standard curve with Sigma Aldrich fucoidan solution 3 P1 with room temperature. 91
Figure 49: Drift check of standard curve with Sigma Aldrich fucoidan solution 3 P2 with room temperature. 91
Figure 53: T1 experiment of fucose (≥99,9%), with KHP as internal standard and D2O as solvent. 92
Figure 54: ^{1}H NMR of fucose (≥99,9%), with KHP as standard and D2O as solvent. 92
Figure 55: ^{1}H NMR of fucose (≥99,9%) with calcium formate as standard and D2O as solvent P1. 93
Figure 56: ^{1}H NMR of fucose (≥99,9%) with calcium formate as standard and D2O as solvent P1, broad integration. 93
Figure 57: ^{1}H NMR of fucose (≥99,9%) with calcium formate as standard and D2O as solvent P2. 94
Figure 58: ^{1}H NMR of fucose (≥99,9%) with calcium formate as standard and D2O as solvent P2, broad integration. 94
Figure 59: ^{1}H NMR of fucose (≥99,9%) with calcium formate as standard and D2O as solvent P3, considered an outlier. 95
Figure 60: qNMR of fucoidan (≥95%) from Fucus vesiculosus, with calcium formate as standard and D2O as solvent. 95
Figure 61: qNMR of fine fucoidan from Alginor, with calcium formate as standard and D2O as solvent. 96
Figure 62: qNMR of crude fucoidan from Alginor, with calcium formate as standard and D2O as solvent. 96

List of tables

Table 1: Biochemical composition of crude extract obtained from L. hyp. using hydrothermal assisted extraction (Ahmad, 2015) 19
Table 2: Specifications of the Shidazu UV-1800 UV-VISible Scanning Spectrophotometer; 115 VAC, which was used in analysis. 28
Table 3: Theoretical Mw values of Fucoidan, Fucose and the loss of one or two NaSO3-groups. 32
Table 4: Overview of the Sigma Aldrich fucoidan solutions used in standardization of heparin colorimetric assay. 36
Table 5: Parameters of proton T1 NMR test experiment. 40
Table 6: Parameters of 1H qNMR experiments. 40
Table 7: Values used to make the L-fucose standard curve (P1) 43
Table 8: Values used to make the L-fucose standard curve (P2) 43
Table 9: L-fucose quantification of Sigma Aldrich Fucoidan (≥95%) with assumed purity of 95% 45
Table 10: L-fucose quantification of highly filtered fucoidan from L. hyp. (Alginor) 46
Table 11: L-fucose quantification of less filtered fucoidan from L. hyp.. (Alginor) 46
Table 12: Relevant concentrations of fucoidan (≥95%) from solution 1 and their respective absorbances used to standardize heparin col. assay. 48
Table 13: Fine fucoidan (Alginor) solution using heparin col. assay 53
Table 14: Crude fucoidan (Alginor) solution using heparin col. assay. 55
Table 15: Relevant concentrations of fucoidan (≥95%) from solution 2 and their respective absorbances used as an attempt to optimize standardization of heparin col. assay. 56
*Table 16: Relevant concentrations and their respective absorbances for standardization of Sigma Aldrich fucoidan (≥95%) solution 3 with T=293K. *= Outliers.* 58
Table 17: ^{1}H NMR results from Sigma Aldrich L-Fucose (99,9% purity) Calculation of yield is done using the average calculated concentration of the methyl- and alpha group. 63
Table 18: ^{1}H NMR results from Sigma Aldrich L-Fucose (99,9% purity) Calculation of yield is done using the average calculated concentration of the methyl- and alpha group. 64
Table 19: ^{1}H NMR results from Sigma Aldrich Fucose (99,9% purity) Calculation of yield using the average calculated concentration of the methyl- and alpha group. 65
Table 20: ^{1}H NMR results from Sigma Aldrich Fucose (99,9% purity) P2 broad integration Calculation of yield is done using the average calculated concentration of the methyl- and alpha group. 66
Table 21: ^{1}H NMR results from Sigma Aldrich Fucose (99,9% purity) P3. Calculation of yield is done using the average calculated concentration of the methyl- and alpha group. 66
Table 22: qNMR of Fucoidan standard from Fucus vesiculosus ≥95% 67
Table 23: qNMR of the fine fucoidan from Alginor. 68
Table 24: qNMR of the crude fucoidan from Alginor. 69
Table 25: Summary of the average yield from all quantification methods. 71
Table 26: Advantages and disadvantages of the methods explored. 72

Chapter 1 - Introduction

1.1 Motivation

For the past decades there has been a growing interest in utilizing available natural resources in a more sustainable way. Among the marine resources that are easily available, seaweeds are of great interest as a source of food, for pharmaceutical and industrial applications, and as fertilizer (seaweed.ie, 16.01.2022; Buschmann, 2017). The major utilization of these plants is found in Asia, where most species (e.g. *Kappaphycus alvarezii, Eucheuma, Saccharina japonica* etc.) are harvested for food while some species, such as *Gracilaria,* are harvested for agar (McHugh, 2003). Seaweed farming in Asia has been an alternative to fishing which provides improved economic conditions and relieves pressure on fishing, which may be even more important in a sustainable oriented future. Harvesting or growing industrial-scale volumes of seaweeds would potentially provide a sufficient, sustainable biomass to be processed into a magnitude of products through biorefineries (Buschmann, 2017).

One of the common seaweeds found in the northern hemisphere is the brown seaweed *Laminaria hyperborea (L. hyp.)*. The seaweed has been harvested for the alginate industry and has a potential in cultivation due to its high growth rate and having no land competition to terrestrial farming. Using *L. hyp.* only for alginate is wasteful as the seaweed contains other valuable polysaccharides such as laminarin and fucoidan. To make use of more of the seaweed than just alginate, a total utilization method should be implemented. This would also be in line with Sustainable Development Goal 14 – *Life below water*, especially section 14.1; reduce marine pollution and 14.7; increase the economic benefits from sustainable use of marine resources (Goal 14: DoESA, 2022; Goal 14: Life below water, 2022).

Roughly 5% of *L. hyp.* consists of fucoidan (Carvalho, 2018; Alginor). Fucoidan has numerous properties that are valuable in food, pharmaceutics, and health products. The properties of fucoidan depends on the mass weight of the polysaccharide chains and its sulphation degree (Kopplin, 2018). Some of the fucoidan is relatively similar to heparin, a naturally occurring glycosaminoglycan used in medication. Heparin is similar to fucoidan both in structure and in properties such as its anticoagulant effect (Grauffel, 1989; Cumashi, 2007). Fucoidan might even replace heparin as an anticoagulant in treatment of thrombosis, with the benefit of no risk of hemorrhage side effect (Soon-Ki, 2012).

For industries to achieve total utilization of *L. hyp.*, reliable and cheap quantification methods of the desired compounds from the raw material are needed. One way to quantify fucoidan is with a commercially available Megazyme L-Fucose colorimetric assay (col. assay). The fucoidans are then hydrolyzed into fucose units which can be quantified with the col. assay through UV-VIS spectroscopy. This is an expensive and time-consuming method. In this master thesis, two approaches that are more

direct are examined: heparin col. assay and qNMR. Commercialized heparin col. assay has to the authors knowledge not before been used to quantify fucoidans. The heparin col. assay takes advantage of the anticoagulant properties of fucoidans and its similarities to heparin. The anticoagulant properties are known to depend on the sulphate content, and with a high sulphate content from *L. hyp.* fucoidans the heparin col. assay may prove to be usable for quantification. The sulphate groups are dyed with cationic blue dye and the concentration is determined with UV-VIS spectroscopy.

For the first time known to the author, qNMR will be used to quantify fucoidans. This is a well-recognized and widely applied analytical tool that has been applied for the quantification of polysaccharides for the past two decades (De Souza, 2017). Suitable standards will be chosen to quantify the C-6 alpha proton and the methyl group protons.

Finding reliable, accurate, fast, and cheap solutions to quantify fucoidan may prove challenging because the structure is not yet determined and because of its relatively viscous nature and vulnerability to change if the pH is changed. The purpose of this thesis is to advance the knowledge of quantification of polysaccharides from marine macroalgae with the use of rapid quantification methods. The thesis is part of the FucoMed project by Alginor ASA in collaboration with the Department of Chemistry at the University of Bergen (UiB). The project is financed by the Research Council of Norway. Monica Jordheim (UiB) is lead advisor and Georg Kopplin is co-supervisor.

1.2 Macroalgae

Today there are more than 164 000 species of algae that have been identified, about 12 000 of them being macroalgae (Guiry, 2012; Kulshreshtha, 2020; Algaebase.org, accessed 22.12.2021). The macroalgae vary in size, forms, pigments, and functional compounds. They can be classified according to their ecology, habitat, size, pigments, polysaccharides, cell culture, composition, and morphology. Macroalgae, also known as seaweeds, are a polyphyletic group of multicellular algae that consists of *chlorophyceae* (green algae), *rhodophyceae* (red algae) and *phaeophyceae* (brown algae). As the name indicates, macroalgae are macroscopic in size, in contrary to microalgae which is microscopic in size, often unicellular, and are best known by the blue-green algae that sometimes bloom and contaminate rivers and streams. While singular microalgae are not visible to the naked eye - macroalgae are, and some can grow to enormous lengths, such as the brown seaweed *Macrocystis pyrifera,* shown in figure 1, which can grow up to 45m long (North, 1978). Usually though, red, and green seaweeds are small, ranging from a few cm to a meter, while brown seaweeds are usually larger, thicker leather-like seaweeds that range from 30-60 cm to 2-4 m long (McHugh, 2003).

Figure 1: Macrocystis pyrifea, aka. giant kelp (Brauder, retrieved 28.01.2022)

Seaweeds are important marine bioresources around the world, being used in human consumption, fertilizers, hydrocolloids extraction, animal feed additive, extracts for cosmetics and pharmaceuticals, biofuels, and wastewater treatment (McHugh, 2003; Rocha, 2018). Hydrocolloids such as alginate, agar and carrageenan can be produced by red and brown seaweed and is used as thickening and gelling agents. A distribution of some of the seaweed uses is shown in figure 2. Though the interest for marine algae is rising due to their bioactive natural substances with potential health benefits, they are still identified as an underexplored resource (Pangestuti, 2011; Rajauria, 2017).

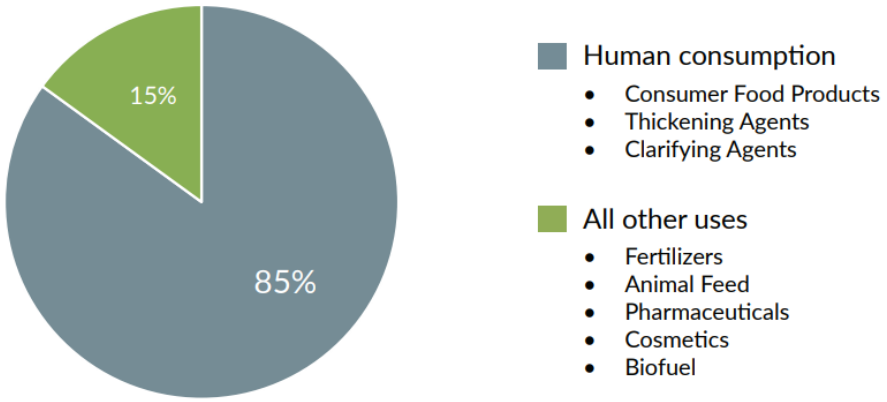

Figure 2: Seaweed global market share (Piconi, 2020).

Seaweeds grow in the ocean as well as in rivers, lakes, and other water bodies. Algae are the main contributor for production of oxygen through photosynthesis, as this process is only carried out by cyanobacteria, algae and plants found on land (Delwiche, 2007). Farming seaweed may thus help lower the amount of carbon dioxide in the atmosphere.

There are about 2000 brown algae and most of them are marine. Brown algae are usually found in colder waters where they thrive in the intertidal and sublittoral zones of the oceans (Kasco, last accessed 21.12.2021). The brown algae around the world have been mapped out and can be seen in figure 3.

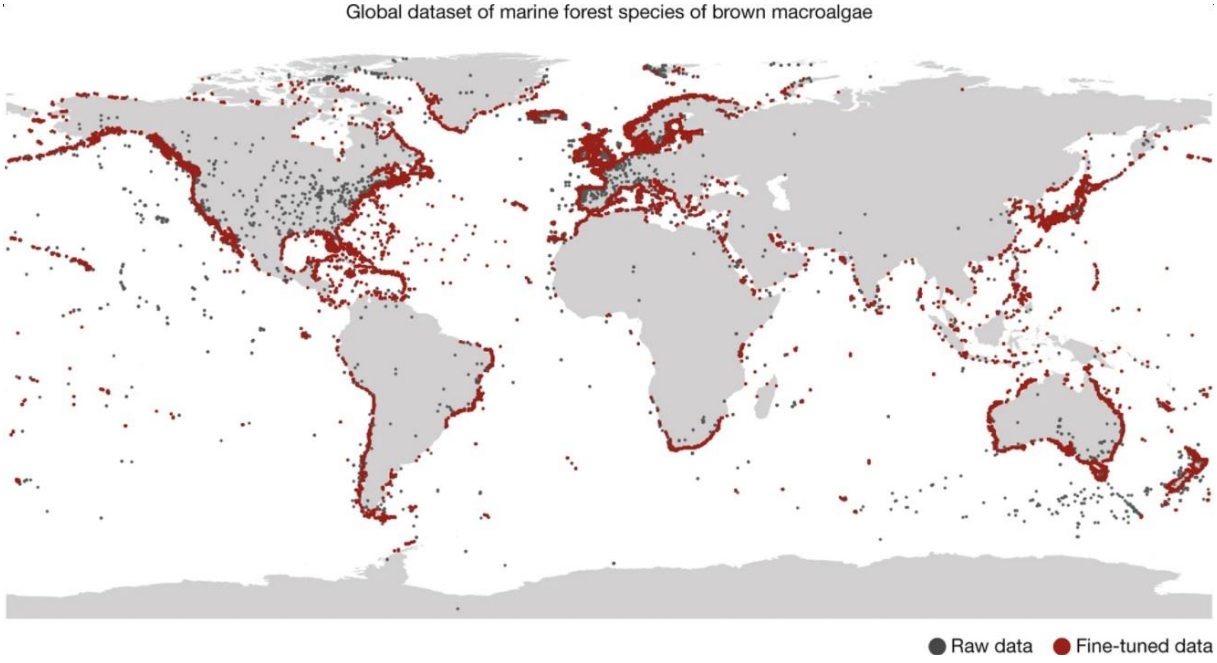

Figure 3: A fine-tuned global distribution dataset of brown seaweed (Assis, 2020).

Traditional use of seaweed has been traced back to the fourth century in Japan and the sixth century in China (McHugh, 2003; Buschmann, 2017). However, when the nationals from these countries migrated to other parts of the world and shared their culture, demand for consumable seaweed in other countries increased steadily, especially in North America, South America, and Europe.

Seaweeds can be collected from the wild but is now increasingly cultivated. Seaweeds can have high crop productivities per unit area, with growth rates up to half a meter per day in some species. Marine macroalgae are autotrophic organisms that utilize dissolved carbon dioxide and nutrients (e.g., dissolved inorganic nitrogen and phosphorus) in combination with light for growth and do not require feed nor fertilizer (Stévant, 2017). Furthermore, the fact that macroalgal growth rates exceed those of terrestrial plants, have sharpened the interest in cultivation of seaweed biomass (Brinkhuis, 1987),

shown by a doubling of the global growth of seaweed production from 2006 to 2015 (Piconi, 2020). Coastal habitat and capacity for aquaculture both in the ocean and in land-based systems means the seaweed industry does not need to compete with terrestrial crops for diminishing land, fresh water, or nutrient resources, making the commercialization of macroalgal product highly attractive (Lorbeer, 2013).

In 2016 the four countries Indonesia, South Korea, China, and Japan together stood for more than 90% of the seaweed consumption worldwide with 162 000 metric tons (MT^1). In 2018 China and Indonesia together produced 86% of all consumable seaweeds. Indonesia was the leading exporter in 2016 with a 58% market share. Today, more than 95% of the global consumable seaweed production is imported from Asian countries even though most marine waters provide perfectly capable conditions for growing seaweeds locally (Piconi, 2020).

Due to their size, macroalgae possess an increased ability to detoxify contaminants, because their large surface area may provide an enlarged biosorption area for the toxic compounds. Macroalgae are considered to have a potential to become a major feed stock of renewable energy sources, such as bioethanol, biodiesel, or biogas. This is because these algal cells contain 15-20% polysaccharides, a higher quantity than found in terrestrial plants (Kraan, 2013). Using macroalgae as a renewable energy source might be a waste though, since they often contain compounds that would likely be more valuable as food, pharmaceutical, cosmetics and industrial use.

Cultivation of kelp and macroalgae in Norway is in an early phase and the cultivation facilities are small. The first concession for cultivation of algae was assigned in 2014. After five years this grew to 574 concessions distributed in 97 locations. In 2019, 16 companies cultivated 111 tons of *saccharina latissima* and *alaria esculenta.* These are among the easier species to cultivate. The kelp is currently being cultivated to be used as food, feed and to be manufactured in industries. Although cultivation is in an early phase and the production is relatively low, there is a high interest and several actors involved (Nordhaug, 2020).

Including fjords and islands, the 100 000 km Norwegian coastline provide a suitable habitat with optimal growth conditions for brown seaweed (Ahmad, 2015; Steen, 2019). They thrive in the littoral zone, more specifically upper sublittoral and intertidal zones, in depths with sufficient light to drive photosynthesis, but in clear water they can grow at depths around 30-50m (Hurd, 2014). Among the brown algae species, *ascophyllum nodosum* and *Laminaria hyperborea* have been harvested in Norway for their industrial applications in pharmaceutical, cosmetics, agriculture, nutraceutical, and more predominately - alginate production (McHugh, 2003; snl stortare, 2021). In production of alginate the ocean is polluted due to use of the toxic chemical formaldehyde and considerable algae biomass is

discarded as waste. A total utilization approach would be a more sustainable way of bioprocessing the algae by preventing pollution of toxic chemicals, (Wekre, Kopplin and Jordheim, 2020) and would also be in line with the SDG – 14 as mentioned earlier.

1.2.1 *Laminaria hyperborea*

Laminaria hyperborea (L. hyp.), also known as tangle and cuvie, is a kelp in the Laminariaceae family and is categorized as brown algae. It consists of a holdfast, a stipe, and the laminate blade that is deeply divided into linear segments which are renewed every year (Steen, 2019). The color is yellowish brown, and the older leaves are covered in epiphytes. An illustration of the macro algae is shown in figure 4.

The depths of where *Laminaria hyperborea* is found mainly depends on light penetration and its availability to the algae. It is usually found between 0-24 meters depth but has been found at depths of 32 m (Kain & Jones, 1976).

Figure 4: Laminaria hyperborea (Mortensen, last accessed 01.04.2022)

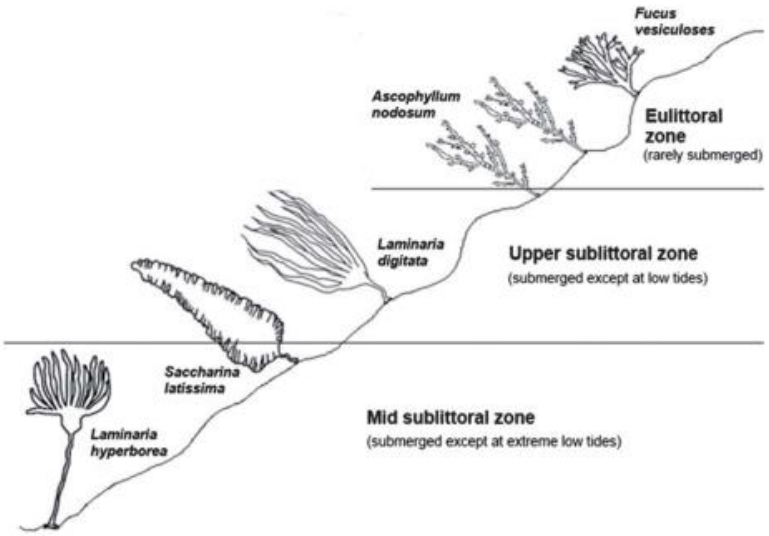

Figure 5: The littoral zones where seaweeds are known to be (Dodson, 2013)

The seaweed is found along the coast of Ireland, Britain, France, and Norway. About 60 million tons *L. hyp.* grow along the Norwegian coastline. The seaweed is often found in dense forests 1-2m tall in the sublittoral zone (McHugh, 2003), shown in figure 5. Since it usually thrives in mid sublittoral zone, at low tide it may break the water surface, as seen in figure 6. In Norway, it is mainly harvested to be used in the alginate industry. Harvesting is executed by rotation every fifth year, allowing the beds to recover. This harvesting method had proven to remove all the adult kelp plants while small kelp plants

were left undisturbed. With the improved light conditions, they can grow to a height of at least 1 m within 2-3 years. 150 000 tons of *L. hyp.* is harvested yearly in Norway (Steen, 2019; snl stortare, 2021; fiskeridirektoratet, 2021).

Figure 6: Laminaria hyperborea breaking the ocean surface at low tide (algaebase.org)

To extract valuable compounds from *Laminaria hyperborea* more research in extraction optimization, purification processes, and characterization and quantification of polyphenols is required. Polyphenols are high molecular weight compounds with numerous health promoting activities that may reduce risk of chronic diseases such as cardiovascular diseases, cancer, as well as protecting against diabetes, obesity, and Alzheimer's disease (Wekre & Jordheim, 2019; Mateos, 2020).

1.3 Polysaccharides/carbohydrates in *Laminaria hyperborea*

Though *L. hyp.* is mainly used in the alginate industry for its high yield of alginate, there are other valuable polysaccharides present, namely the bioactive polysaccharides called fucoidan and laminarin. An overview of in *L. hyp.* composition is shown in table 1. The structures of the polysaccharides in seaweed vary according to the season, age of population, species, and geographic location (Graham, 2000). Laminarin and fucoidan are mostly interesting for their potential biological activities whereas alginate is mostly used as an ingredient in food.

Table 1: Biochemical composition of crude extract obtained from L. hyp. using hydrothermal assisted extraction (Ahmad, 2015)

Component	Composition (dry weight extract [mg/g])
Laminaran	368.0 ⊥ 2.1
Fucoidan	171.2 ⊥ 0.7
Alginate	189.7 ⊥ 0.2
Mannitol	85.3 ⊥0.2
Protein	15.0 ⊥ 0.8
Dry matter	15.6 ⊥ 0.3
Ash	3.4 ⊥ 0.2

1.3.1 Alginate

Alginate is an anionic polysaccharide mainly found in brown algae. It is made from two copolymers, guluronic acid and mannuronic acid, seen in figure 7. With traits such as high stability, gelling properties, and high viscosity, alginate makes for an important industrial polysaccharide (Angra, 2021). Alginate can be used in textiles, healthcare applications, fish food, printing and to make paint, dye, welding rods, mold release (Mollah, 2021; ArtMolds, last accessed 04.02.2022). In Norway *Laminaria digitata*, and more recently *Laminaria hyperborea,* is being harvested for alginate extraction. In recent years however, the harvesting has halted in Canada and United Kingdom because of government restrictions. Alginate also has numerous applications in the pharmaceutical industry such as stabilizing agents, gels, and localized drug delivery. Today, alginate hydrogels are widely used for tissue drug delivery (sciencedirect – alginate, last accessed 04.05.2022).

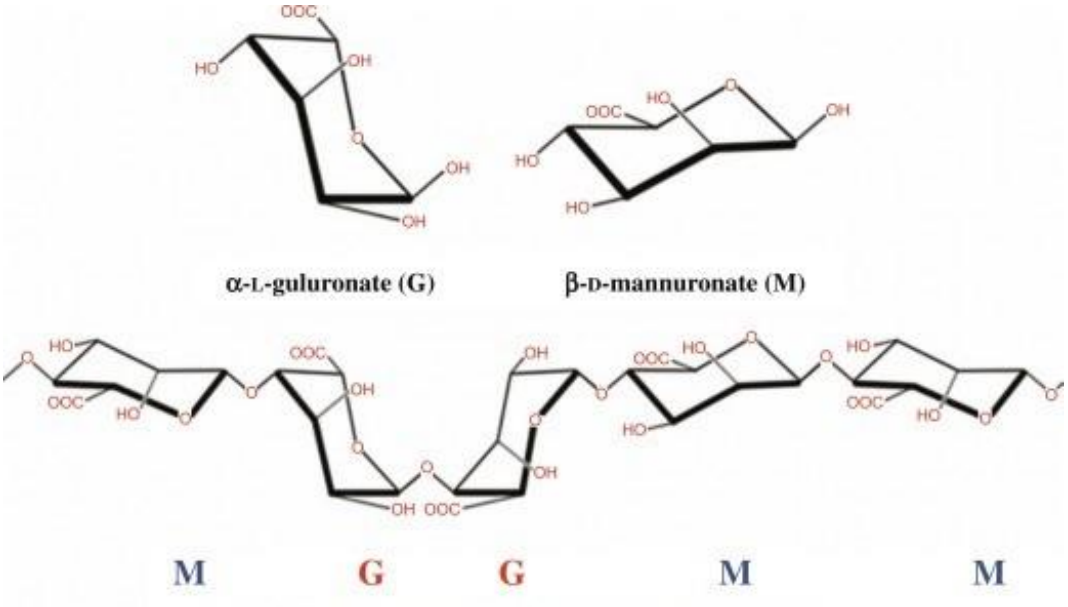

Figure 7: Components and structure of alginate (sciencedirect – alginate, last accessed 04.05.2022).

1.3.2 Laminaran

Unlike plants where the main storage is the polymeric carbohydrate known as starch, seaweed like *Laminaria hyperborea* stores laminaran (hence the name *Laminaria*) in the form of chains. There are two types of laminaran chains, M or G, which differ in their reducing end, as seen in figure 8. G chains end with a glucose residue whereas M chains end with mannitol residue (Rioux, 2007). Laminaran is composed of (1,3)-β-D-glucan with β(1,6) branching (Nelson, 1974; Rioux, 2007).

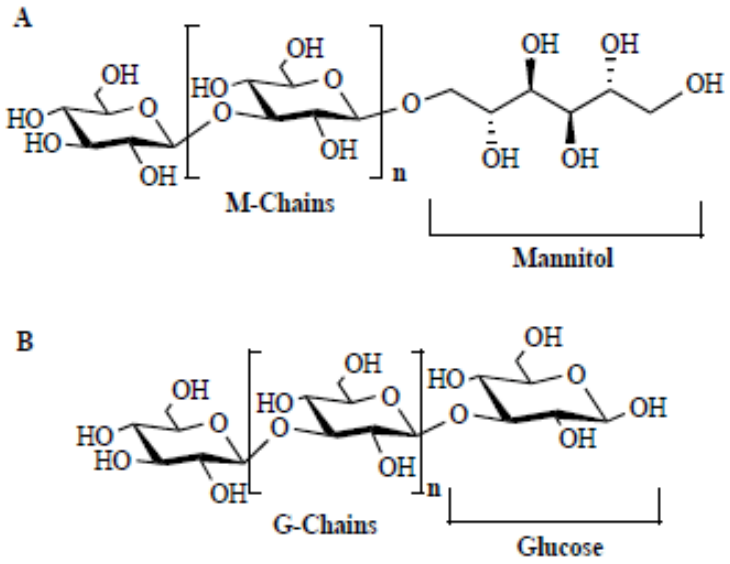

Figure 8: The figure shows the two types of laminaran chains with either mannitol (A) or glucose (B) attached.

The composition and structure vary according to algae species (Chizhov, 1998). The molecular weight of laminaran is approximately 5 kDa depending on the degree of branching. Since the molecular weight of laminaran is lower than other polysaccharides present in seaweed, it can be separated using dialysis with different molecular weight cutoff membranes (Kadam, 2014). Highly branched laminarin is soluble in cold water while lower levels of branching induce solubility only in warm water (Ahrazem & Leal, 2002). Laminaran is used in food, but it is more interesting for its biological activities. It has been reported to exhibit several biologic activities such as anti-inflammatory, anti-apoptotic, anti-tumor antioxidant and anticoagulant activities (Bohn, 1995; Balboa, 2013; Zargarzadeh, 2020).

1.3.3 Fucoidan

Fucoidans are polysaccharides containing a substantial amount of L-fucose and sulphate ester groups (Li, 2008). Fucoidans are constituents of brown seaweed and some marine invertebrates such as sea urchins and sea cucumbers. The polysaccharides were first isolated from brown algae by Kylin in 1913 (Kylin, 1913; Li, 2008). Because of its many bioactivities, Fucoidan has numerous applications in the health sector. The polysaccharides have antioxidant, anticomplementary, blood lipids reducing,

antitumor anticancer and antiviral properties, as well as pro- and anticoagulant properties and activity against hepatopathy, uropathy and renalpathy, gastric protective effects and therapeutic potential in surgery (Bertau, 2003; Kusaykin, 2008; Li, 2008; Chen, 2016; Kopplin, 2018). Fucoidan may have applications in anticoagulant drugs, antithrombotic drugs or functional food and medicinal biological materials with few side effects. Fucoidans may also serve as research reagents to investigate and distinguish among a variety of interrelated events, such as coagulation, bleeding, thrombosis, and platelet aggregation (Mourao, 2005; Li, 2008). The antioxidant activity of fucoidan has been found to be influenced by change in the extraction temperature of fucoidan as well as the sulphate content (Ardiana, 2020). Low molecular weight fucoidan has been found to be effective for its anti-inflammatory response, while middle and high molecular weight fucoidan has been found to be more effective for its anticoagulant activity, which is related to the altering of sulphate groups by changing Mw to control the binding properties (Hwang, 2016; Tsai, 2017).

The chemical structure and molecular weight of fucoidan differ depending on the species from which it is extracted, growth environment, season of harvesting and the method of extraction used (Fitton, 2015; Chollet, 2016). Fucoidans isolated from most brown algae are branched and have one of two types of backbone, as seen in figure 9 (Cumashi, 2007). Type I chains has repeating (1→3)-linked α-L-fucopyranose residues, whereas type II chains consist of alternating (1→3)- and (1→4)-linked α-L-fucopyranose residues.

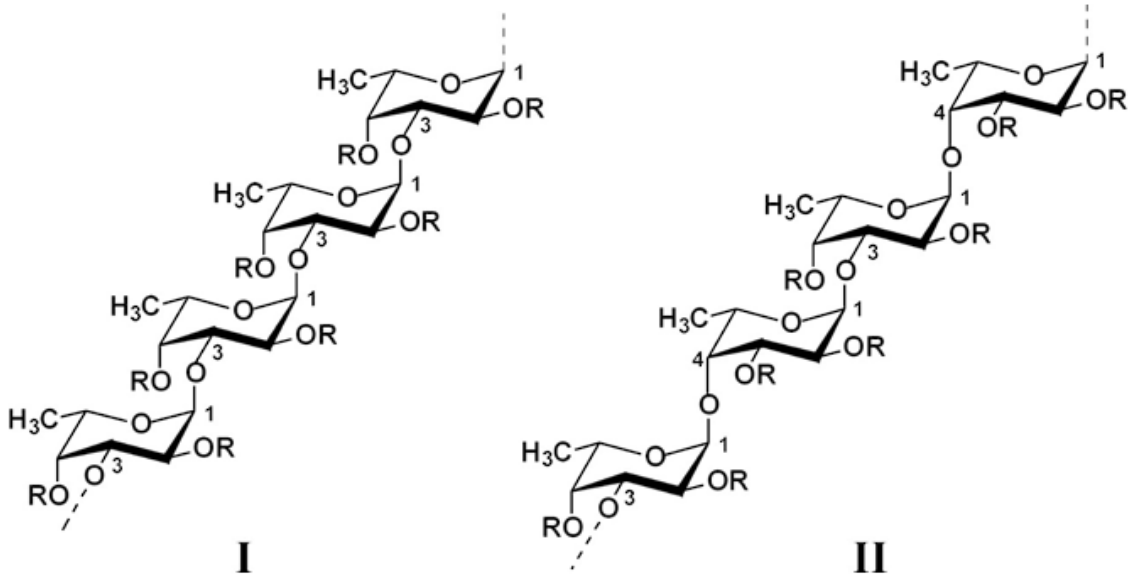

Figure 9: Two suggested general fucoidan structures, type I and type II, based on findings from 9 different seaweed sources (Cumashi, 2007).

Fucoidans may contain other sugars than fucose such as xylose, arabinose, rhamnose, glucose, galactose and uronic acid or even protein and acetyl groups. Both molecular weight as well as the varied percentage shared in sugar and non-sugar components makes the analysis of fucoidan structure difficult (Fitton, 2016; Cunha, 2016).

Isolating fucoidan is a challenging task, one that often results in degradation of the molecular weight of the fucoidans. However, with size exclusion chromatography with multi-angle light scattering (SEC-MALS), a molecular weight average of 469,2 ±1,9 kDa, and a molecular number average of 218,6 ±0,9 kDa were determined (Kopplin, 2018). This corresponds to a degree of polymerization (DP) of 720. The DP is then calculated based of every monomer unit containing two fucose units, both disulphated, giving each monomer a molecular weight of roughly 625 Da. Both type I and type II fucoidan chain types are then accommodated for.

The fucoidans from *L. hyp.* are among the most highly sulphated fucoidans with a degree of sulphation at 1,7 (53,8% of the total mass weight) (Kopplin, 2018). In other words, each fucoidan fucose unit consist of 1,7 sulphate groups, meaning it is usually disulphated. Raman spectroscopy has determined the sulphate groups to be located axial at 4C and equatorial 2C.

Fucoidan is similar to heparin in structure and its ability to inhibit thrombin activity. It may thus be able to replace heparin as anticoagulant since heparin has an unfortunate high chance of causing hemorrhage (Grauffel, 1989; Cumashi, 2007). Compared to other sulphated polysaccharides, fucoidans are highly available from cheap sources. Thus, fucoidans have been gaining researchers attention to develop drugs, pharmaceutics, cosmetics, and functional food.

The bioactivity of the fucoidan is mainly determined by the mass weight of the polysaccharide and the sulphation degree (Li, 2008; Wang, 2019). It has also been demonstrated that the anticoagulant effects of the polysaccharides depend predominantly on the degree of sulphation, to lesser extend on the molecular weight, whereas branching and sugar composition showed no significant influence on coagulation (Matsuraba, 2005; Nazarenko, 2010). Fucoidans have a large variety of glycosidic linkages, branching points, and their random distribution results in a heterogeneous structure. A detailed structural elucidation of fucoidan is a challenging task because of heterogeneity and nonrepeating motifs (Kopplin, 2018). The primary structure cannot be determined due to lack of repeating units but, with a coalescence of analytical techniques, a sensible approximation of a hypothetical structure can be given, as seen in figure 10.

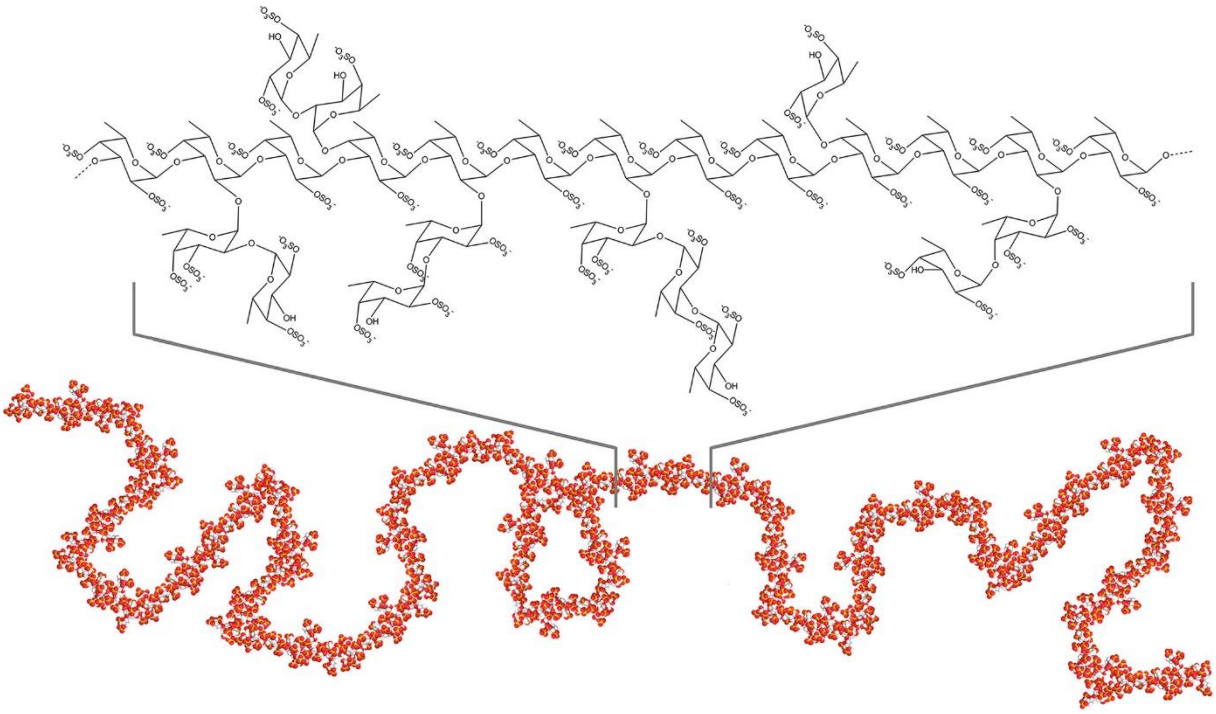

Figure 10: Suggested structural fragment of 25 fucose residues applied as building blocks for a full-scale structural model (DP = 750, Rw = 37nm) of Fucoidan from Laminaria Hyperborea (Kopplin, 2019)

Raman spectrometry and mass spectrometry analysis has revealed that sulphate groups are usually found at the C-2 position. Though, disulphated structures also occur in some fucoidan alongside C-4 and C-3 monosulphated fucose units (Anastyuk, 2010; Synytsya, 2010; Bilan, 2013).

Industries that aim to make use of fucoidans from *L. hyp.* needs to find suitable quantification methods to quantify the fucoidans. Preferably the methods can also quantify different DP fucoidans, considering the change in properties when the structural integrity is changed. Because of variations in its structure, molecular weight, and its sulphation degree, there are variations in fucoidans properties.

One way to quantify fucoidan is by hydrolyzing the sugar, thus breaking up the fucoidan units into fucose units. Hydrolyzing also has the advantage of removing impurities in the process. The fucose units can be quantified with commercialized fucose col. assays with high accuracy and high precision. This can, however, be time consuming and expensive since hydrolyzation for many hours is required to fully break up the fucoidans. Additionally, filtration and pH neutralization are required.

Quantifying sulphated polysaccharides can also be done using a solid-phase colorimetric method. It has been shown that methylene blue dye binding heparin is not affected by pH among 2 and 12 (Liu, 2006). Dye binding requires a macromolecular form with both carboxyl and sulphate-rich groups. The carboxyl groups without sulphate groups give no responses. After staining the sulphate groups with methylene blue, the polysaccharides are immobilized into filter paper, and consequent using optic

density (at A_{663} nm) measurement of the eluted dye from filter paper. This allows for determination of 1-20 ug fucoidan in presence of potentially interfering compounds such as alginic acid, salts, proteins, DNA and detergents. Many of the colorimetric determination methods of sulphated polysaccharides are based on interactions with cationic dyes such as dimethyl methylene blue, methylene blue, and toluidine blue in a solution (Farndale, 1986; Beutlev, 1993; Soedjak, 1994; Liu, 1998; Matsubara, 2005; Lee, 2012; Ustyuzhaina, 2014). Heparin col. assays follow the same quantification principle, using dye to quantify the sulphate groups. The change in absorbance upon binding to the sulphate groups can be measured with UV-VIS spectrometer.

1.4 Comparison of heparin and fucoidan

Naturally occurring heparin is one of the sulphated polysaccharides that is most used as an anticoagulant, but long-term use may cause hemorrhage (Soon-Ki, 2012). Heparin may also cause virus-based infections due to that it is mostly obtained from animals. Marine sourced sulphated polysaccharide fucoidan is an alternative anticoagulant without the hemorrhage downside (Soon-Ki, 2012). Along with fucoidans anticoagulant activity, other biological activities such as antivirus, anticancer, antitumor, anti-inflammatory, and antioxidant activities have been observed. These properties make fucoidan an attractive polysaccharide for numerous biomedical applications. (Ozaltin, 2016).

As mentioned, fucoidan and heparin are similar in structure, as seen in figure 11. With the similarities in structure and properties a hypothesis can be proposed.

Hypothesis: The shared anticoagulant properties of Heparin and fucoidan and similarities in structure, combined with anticoagulants dependency on a high sulphation degree and polymer length, could mean that highly sulphated and high Mw fucoidan from *L. hyp.* is eligible for quantification the same way heparin is quantified in heparin col. assays.

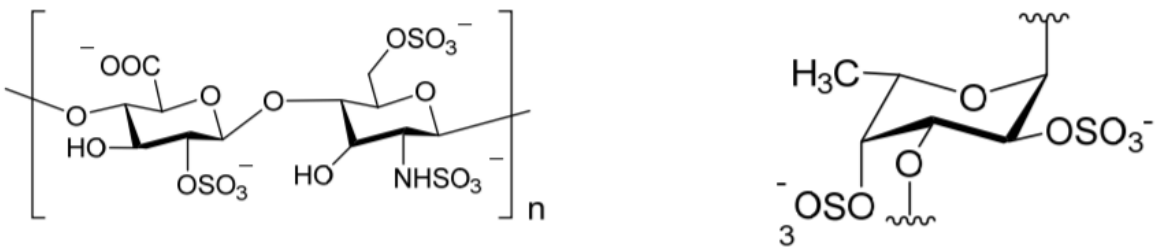

Figure 11: Repeating units in the polysaccharides heparin (left) and fucoidan (fucose residues) (right).

Contrarily to other polysaccharides, the mechanism of anticoagulant activity of fucoidan is related to the interactions with the natural thrombin inhibitors of antithrombin (AT III) and heparin cofactor II (HCII), activated factor II (thrombin), and activated factor X (Chromogenix, 1999). The effect of the anticoagulant activity of fucoidan depends on its structural properties, such as sulphation degree and pattern, monosaccharide composition and its molecular weight. Heparin has a lower anticoagulant activity than fucoidan and using heparin may cause hemorrhage side effects. The same side effect is not seen with fucoidan (Grauffel, 1989; Soon-Ki, 2012). On the other hand, the structure of fucoidan is not properly defined yet, which limits its current applications.

Chapter 2 – Experimental methods

The goal is to find efficient and suitable methods for quantification of fucoidan in fucoidan extracts obtained from *Laminaria hyperborea*. The methods should aim to have a high degree of reliability, accuracy (relationship between experimental and true value), precision (distribution of data values), as well as being cost and time efficient. Fucoidans from *L. hyp* have a high sulphation degree and well filtered fucoidans have been found to have around 1.7 sulphate groups per monomer (Kopplin, 2018). In this thesis, all calculations are done with the assumption of each fucoidan monomer being disulphated. Due to difficulties in extracting and isolating the fucoidan, the more isolated the fucoidans are, the lower molecular weight and sulphation degree is expected. According to Alginor, molecular weight of fucoidans in *L. hyp.* may range from 10 kDa to several MDa.

2.1 Extraction

Extracting biopolymers from the cell wall of brown seaweed is a challenging task. The yield, the structural features and the chemical nature of the polysaccharides are highly dependent on the conditions on which they are extracted (Li, 2008). A variety of methods have been tested in isolating high quality fucoidan, but the precise structure is still debatable due to difficulties in the extraction and purification process (Ragan & Jensen, 1979). The seaweeds are usually extracted for crude fucoidan with acid as extraction solvent to avoid a release of alginic acid (Geiselman & McConnell, 1981).

The extraction treatment employed affects the composition resulting in change in the properties of the fucoidan substances (Ale & Meyer, 2013). Extraction with alkaline conditions will generally result in alginic acid. Extracting with hot water maintains the stability and the overall charge of the molecule, making higher quality fucoidan which better retains its bioactivity. Acid treatment used as a major step in the extraction of fucoidans causes degradation and affects the compositions integrity. Using acidic solvents give a higher fucoidan yield in comparison to water, but the acid may remove the sulphate groups and break up the polysaccharide into fucose fractions. Using acid at a concentration that minimizes loss of structural integrity or using greener solvents such as water, may be the most efficient way to extract high molecular weight fucoidan with sulphate groups intact. Mild extraction procedures must be implemented to preserve the native fucoidan structure and thus bring out the distinct and valuable biological properties.

Precipitation of alginate by divalent ions (such as Ca^{2+} or Ba^{2+}) is a common pre-treatment step during fucoidan extraction (Zayed, 2020). An acidic medium (pKa below carboxylic groups) also helps in

precipitation of alginate as alginic acid. Therefore, traces of alginate are frequently detected in crude fucoidan extracts from brown algae. Precipitation can be performed by adding $CaCl_2$. After precipitation, NaOH can be added (to pH of ~13) to the solution (50-70 °C) to break down the alginate. Polyphenols can make the solution brown, which may be a result of degradation.

Extraction of fucoidan from *L. hyp.* have been shown to be close to equally efficient with acidic solvent (0,1 M HCl) at 80°C for 2 hours and for 24 hours (Ahmad, 2015). Extraction with acid gives a 5/2 ratio of fucoidan compared to extraction with water. Varying the temperature and solvent could be investigated further. The crude fucoidan analyzed in this thesis is extracted and filtered by Alginor.

2.2 Ultraviolet-Visible (UV-VIS) Spectroscopy

UV-VIS spectroscopy is an analytical technique that measures the number of discrete wavelengths of UV or visible light that are absorbed by or transmitted through a sample in comparison to a reference or blank sample. This property is influenced by the composition of the sample and can provide information on what is in the sample and at what concentration. Many molecules contain chromophores which will absorb specific wavelengths of ultraviolet or visible light. Using the Beer Lamberts law, the absorption of spectra generated from these samples at given wavelengths can be related directly to the concentration of the sample. Normally UV and UV-VIS spectra are recorded at high and low pH and the results of both for the samples under question compared with known standards (Tomasik, 1998; De Caro, 2015; Justin, 2021; ScienceDirect – UV-VIS, last accessed 03.03.2022).

UV-VIS is the preferred method to analyse the samples as the analytes are highly conjugated and are thus suitable for UV-VIS. In quantitative analysis, UV-VIS offers high sensitivity with a detection limit of 10^{-4} to 10^{-6} M, high accuracy (1-5%) and is relatively simple to use. The technique allows sample recovery and good discrimination between pure compounds without the need for derivatisation. Furthermore, the device is cheap and accessible (ScienceDirect – UV-VIS, last accessed 03.03.2022).

Kinetic UV-VIS method was performed to check for drift caused by the instrument or the samples. This is done by measuring the absorbance of a wavelength specific for the analyte as a function of time. When using the col. assays, if the reaction leading to a change in absorbance had not properly finished, a change in absorbance over time would be visible. This is especially useful for the heparin col. assay since the reaction is stopped after 120 seconds of reaction with the dye. A change in absorbance would mean the reaction was not properly stopped.

A check for drift is performed whenever UV-VIS is used. This is especially useful when using the heparin col. assay to see if the reaction has not been properly stopped with acetic acid. The UV-VIS used in this

thesis was the Shidazu UV-1800 UB/Visible Scanning Spectrophotometer; 115 VAC. It provides 1 nm resolution in a compact double-beam instrument. Features such as full functionality from 190 to 1100 nm, built-in validation software and was run through a computer. Check table 2 for detailed specifications.

Table 2: Specifications of the Shidazu UV-1800 UV-Visible Scanning Spectrophotometer; 115 VAC, which was used in analysis.

Stray light	<0.02%T at 340 nm, 400 nm; <1.0 %T at 198 nm
Source lamp	Deuterium; tungsten-halogen
Beam type	Double
Bandwidth	1.0 nm
Minimum wavelength	190 nm
Maximum wavelength	1100 nm
Wavelength accuracy	± 0.1 nm
Wavelength reproducibility	± 0.1 nm
Photometric drift	<0.0003 A/hr
Detector	Silicon photodiode

2.3 Colorimetric assays

There are several colorimetric (col.) assays used to measure analytes in different ways. These assays range from simple pH measurements to more complex pharmaceutical or pesticide compounds which can be valuable in applications such as health monitoring and water testing (Abels, 2021). Col. assays usually utilize laboratory spectrophotometry. This allows for development of calibration curves and consistent absorbance measurements. The concentration of the analyte can be determined quantitatively by comparing the absorbance at wavelengths that are specific to the chromophore of interest to the calibration curve.

With the fast development of clinical laboratory techniques, assays with increased accuracy and sensitivity have been developed. Enzymatic assays are one of the assays that can avoid the disadvantages of low sensitivity and many of the interfering factors that may occur with the colorimetric method (sciencedirect – colorimetry, last accessed 12.05.2022). The crude extract from *L. hyperborea* will include a decent amount of laminarin, mannitol and other carbohydrates as well as

polyphenols which may create interference in detecting fucose. Thus, the method used to quantify fucoidan from a crude extract needs to be specific.

2.3.1 L-fucose colorimetric assay quantification

In this colorimetric method, harsh acidic conditions are used to depolymerize and desulphate fucoidan into monomeric fucose. The fucose monomers can be quantified with a commercially available L-fucose col. assay from Megazyme which specifically quantifies fucose in the presence of other sugars and impurities. The L-fucose col. assay is a simple, rapid, and reliable method for the measurement and analysis of L-Fucose in plant extracts, biological samples, and other materials (Megazyme.com assay protocol, last accessed 28.01.2022). The col. assay can be used in measurement of α-L-fucosidases that do not act on chromogenic substrates (Wu, 2021). The quality control criteria for accuracy and repeatability are to be within 2% of the expected value using pure analytes (Megazyme.com, 28.01.2022). However, the level of accuracy is obviously analyst and sample dependent. The detection limit of the L-Fucose col. assay is 0.68 mg/L which is derived from an absorbance difference of 0.020 with the maximum sample volume of 2.00 ml. The assay is linear over the range of 0.5 to 100 µg of L-fucose per assay. The col. assay is stable under recommended storage conditions for more than 2 years.

Extracted and filtered fucoidan are hydrolyzed with heat into fucose units, as seen in figure 12. Fucoidan is depolymerized and desulphated in these harsh acidic conditions. The L-fucose units can then be quantified by using the L-fucose col. assay and UV-VIS spectrophotometer.

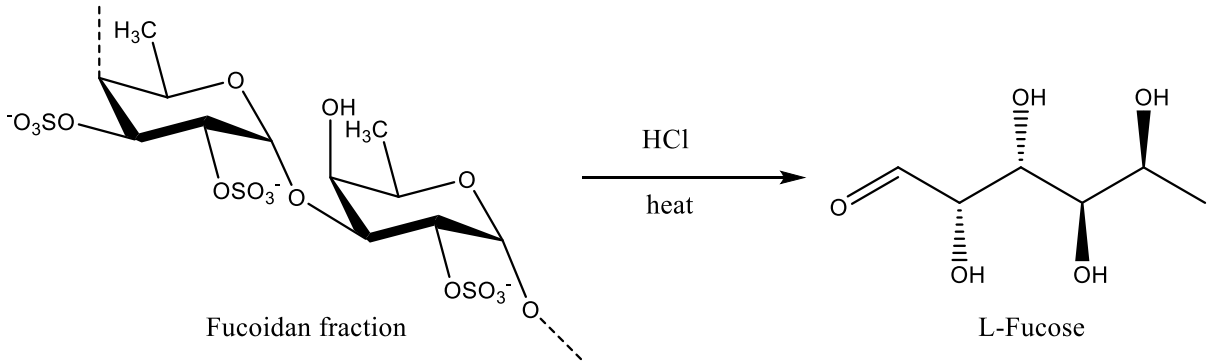

Figure 12: Hydrolyzation of fucoidan causes depolymerization and desulphation of the polysaccharide into L-fucose units.

L-fucose is oxidized by the enzyme L-fucose dehydrogenase (L-FDH) in the presence of nicotinamide adenine dinucleotide phosphate ($NADP^+$) to L-fucono-1,5-lactone with the formation of reduced nicotinamide adenine dinucleotide phosphate (NADPH), as shown in figure 13.

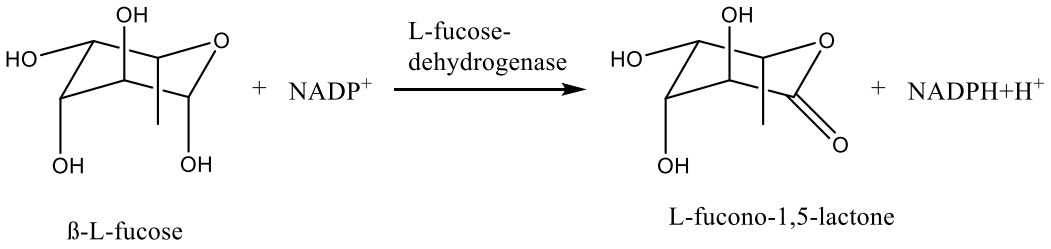

Figure 13: Reaction principle of the L-fucose col. assay.

The amount of NADPH in this reaction is stoichiometrically equal to the amount of L-fucose in the solution. The reduced NADPH gives an increase in the absorbance at 340 nm wavelength, as shown in figure 14.

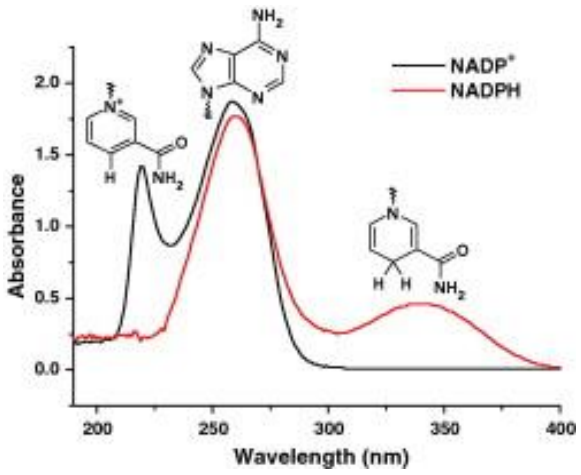

Figure 14: NADP+ and NADPH wavelength difference at 340 nm (Ruyck, 2007)

To quantify fucoidan a standard curve will be obtained with the fucose standard included in the Megazyme col. assay. With the standard curve in place, a known amount of high purity Fucoidan (≥95%) from *Fucus vesiculosus* delivered from Sigma Aldrich will be hydrolyzed to fucose, pH neutralized and checked against the standard curve.

Publications determining fucoidan by hydrolyzing fucoidan into L-fucose units have been found to hydrolyze the fucoidan samples between 1 and 24 hours, at 70 or 80°C (Ahmad, 2015; Turan, 2017). Periodically analyzed samples of hydrolyzed and desulphated *L. hyp.* fucoidan (delivered by Nova Matrix) with 1M HCl at 80°C indicates that hydrolyzation should be done at least for 5 hours for complete hydrolysis, as seen in figure 15 (Ahmad, 2015). This is the main reason hydrolyzation times will be done for 6 hours at 80°C, and for 24 and 48 hours at 60°C. Practical reasons, such as temperature

control and water bath evaporation, were also taken into consideration when optimizing the hydrolyzation.

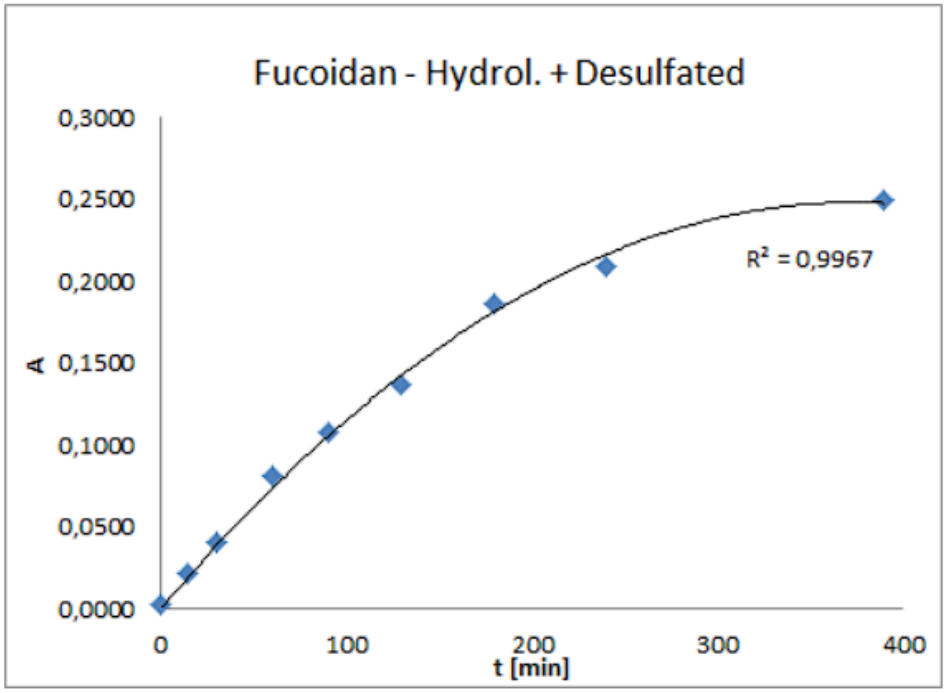

Figure 15: Absorbance of hydrolyzed and desulphated fucoidan measured periodically using L-fucose col. assay (Ahmad, 2015).

Procedure: L-fucose (0.5mg/ml) provided from the Megazyme col. assay was used as standard. Samples of the standard were diluted with water into five different concentrations ranging from 0.02 to 0.1 mg/ml. In each cuvette series the following was added; sample solution at different concentrations (0.1 ml), buffer (plus sodium azide, pH 9.5 0.02% w/v) (0.4 ml), NADP+(0.1 ml) and distilled water (2 ml). The solution in the cuvettes were mixed with a glass staff. After three minutes of incubation, absorbance (blank) was measured at 340 nm three times at 1 minute interval between each reading. With the blank measured UV-VIS measurements were paused and L-fucose dehydrogenase (0.05 ml) was added to the cuvettes and mixed with a glass staff. After 10 minutes the reaction was assumed to be finished and UV-VIS measurements were resumed. 9 readings of the product were performed with 1 minute interval between each reading, in total 12 readings were performed at 340 nm. The standard curve was quality checked with three parallels and drift check.

When following the procedure of the L-fucose col. assay, equation 1.1 is used to calculate the concentration of L-fucose.

(1.1) $$c = \frac{V \cdot Mw}{\varepsilon \cdot d \cdot v} \cdot \Delta A_{L-fucose}$$

$$c = \frac{2.65 \cdot 164.16}{6300 \cdot 1.0 \cdot 0.1} \cdot \Delta A_{L-fucose}$$

$$c = 0.6905 \cdot \Delta A_{L-fucose}$$

Where c is concentration [g/L], V is final volume [mL], Mw is molecular weight of L-fucose, ε is the extinction coefficient of NADPH at 340 nm (6300 $lmol^{-1}cm^{-1}$), d is light path [cm], v is sample volume [mL], and $\Delta A_{L\text{-}fucose}$ is measured absorbance at 340 nm subtracted by the blank absorbance at same wavelength before adding L-FDH.

After standardizing the L-fucose col. assay the fucoidan standard can be tested to see if the fucoidan yield is close to what is specified. The amount of L-fucose can easily be calculated back to fucoidan by using the Mw ratio of L-fucose units per disulphated fucoidan monomer, as shown in table 3 below. This factor was calculated based on the loss of two $NaSO_3$ groups per monomer.

Table 3: Theoretical Mw values of fucoidan, L-fucose, one and two NaSO3-groups and the L-fucose/fucoidan relation

Mw (Monosulphat or disulphate groups) [g/mol]	103.053	206.106
Mw (Fucose) [g/mol]	164.16	164.16
Mw (Mono- or disulphated fucoidan) [g/mol]	267.213	370.266
Mw percentage of sulfur in the sugar [%]		55.664
Factor Mw calculating back from Fucose to Fucoidan		0.4434

Procedure: Samples of fucoidan (≥95% pure) delivered from Sigma Aldrich is weighed with an assumption of 95% purity. The fucoidan was hydrolyzed in a water bath for either 6, 24 or 48 hours in HCl (1M, 20-30 ml). For the 6-hour hydrolyzation (6-hh) water bath temperature will be at 80°C based of figure 15 above. For the 24- and 48-hour hydrolyzation (24-hh and 48-hh respectively) water bath temperature will be at 60°C to see if lower temperature with longer hydrolyzation time gives a higher or more accurate yield. The pH of the hydrolyzed acidic L-fucose solutions is measured with litmus paper and neutralized with NaOH (1M) to a pH from 1 to around 7. The now neutral 6h, 24h and 48h solutions are each filtered and diluted with distilled water to 100 ml in a volumetric flask. From each of the hydrolyzed solutions, 3 parallels of the solutions were taken for UV-VIS measurements. Apart

from diluting the concentrations, the UV-VIS measurements were done the same way as the L-fucose standard.

If the col. assay proves to be accurate for the fucoidan standard, tests to check the fucoidan content of cruder samples of *Laminara hyperborea* delivered from Alginor can be performed the same way as the fucoidan standard.

2.3.2 Heparin colorimetric assay

Heparin has a relatively similar structure compared to fucoidan, as seen in figure 16. Heparin and fucoidan are also similar with respect to their polysaccharide nature and high negative charge density due to sulphation (Pozharitskaya, 2018). Given the similarities in the structures of heparin and fucoidan, the heparin col. assay may be able to quantify fucoidan similarly to how it quantifies heparin. The heparin col. assay could then potentially be a cheaper, faster, and a more accurate and precise way to quantify fucoidan in a sample. The heparin col. assay method is a simple and direct approach which is sensitive below 1 IU per ml, 9 times more sensitive than metachromatic dyes (Warttinger, 2017). In traditional dye binding assays, the affinity measurements of protein interactions are typically performed at room temperature or lower, with little or no consideration of the potential impact of the temperature on these interactions. Higher temperatures favor conformational change and gives more stable ATIII-heparin complexes (Zhao, 2018).

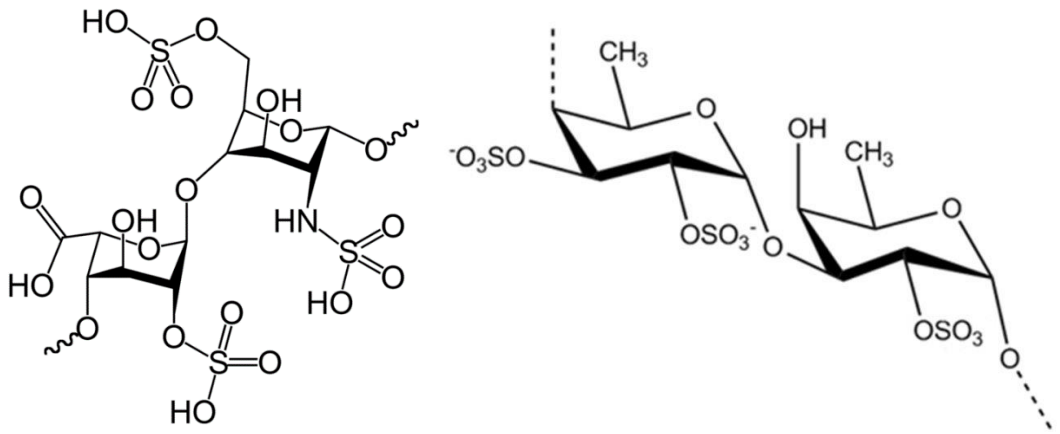

Figure 16: General structure of Heparin (left) and Fucoidan (right).

The basis for heparin's anticoagulant activity in plasma is that it binds to antithrombin. Antithrombin is the main inhibitor of the coagulation cascade in plasma. When binding, a confirmational change in the antithrombin molecule is induced. This accelerates the antithrombin inhibition of several serine proteases such as factors IXa, Xlla, Xla, Xa and thrombin (diapharma, last accessed 29.04.2022).

For quantitative determination of unfractionated heparin or low molecular weight heparin in human citrated plasma, a heparin col. assay can be used. Heparin is a frequently used antithrombotic therapeutic. The biological activity of heparin lies in its capability to accelerate the inhibitory effect of antithrombin (AT) on the coagulation proteases. The amount of low molecular weight heparin or unfractionated heparin is determined from the anti-FXa activity expressed by the [AT•Heparin] complex formed in plasma.

I. $Heparin + AT \rightarrow [AT \bullet \text{Heparin}]$
II. $[AT \bullet \text{Heparin}] + \text{FXa (excess)} \rightarrow [FXa \bullet \text{AT} \bullet \text{Heparin}] + \text{FXa (residual)}$
III. $FXa\ (residual) + S2732\ \rightarrow Peptide + pNA$

S-2732: Chromogentic substrate, Suc-Ile-Glu(γ-pip)-Gly-Arg-pNA • HCl lyophilized with detergent and mannitol as bulking agent.

Factor Xa: Lyophilized bovine FXa containing Tris buffer, EDTA, NaCl, dextran sulphate and bovine serum albumin.

Factor Xa (FXa) is added to a mixture of undiluted plasma and the chromogenic substrate S-7232. When heparin and AT are complexed, two competing reactions occur simultaneously:

1. Inhibition of FXa by the [AT•Heparin] complex.
2. Reaction of FXa with S-2732 resulting in cleavage of pNA.

The pNA release measured at 405 nm is inversely proportional to the heparin level in the sample. By subtracting the wavelength at 490 nm, any impurities pre-reaction should be neglected, as seen in the UV-VIS spectra of pNA in figure 17. This is the reason 490 nm was chosen for the blank measurements. Whether or not the heparin col. assay can be used to quantify the amount of fucoidan in a given sample in water without human citrated plasma, is yet to be tested.

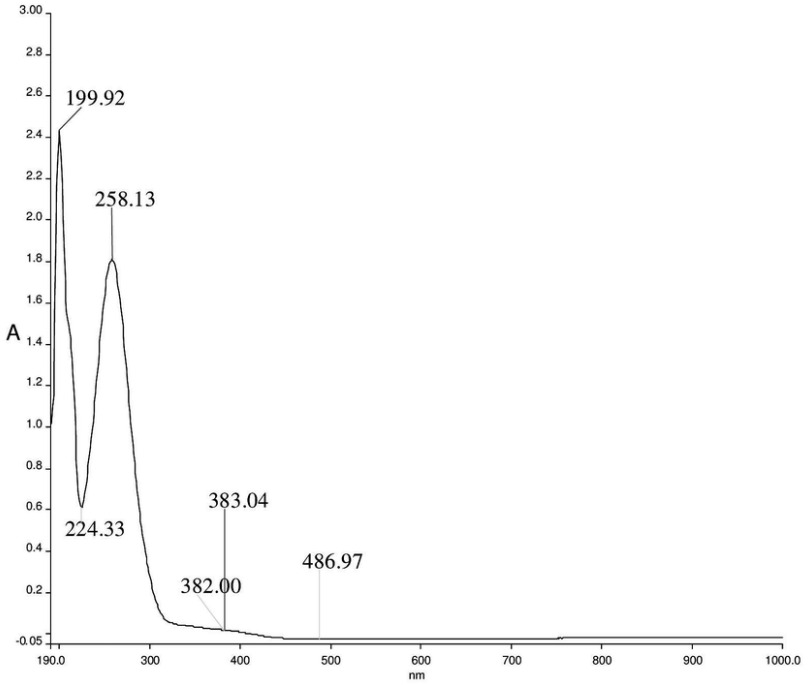

Figure 17: UV-VIS spectra of pNA (Baraniraj, 2011).

To reduce the influence from heparin antagonists, such as platelet factor 4, dextran sulphate is included in the reaction mixture.

As mentioned in the introduction, fucoidan is relatively similar to heparin in structure and shares many of its properties such as anticoagulant and antithrombin activities. With the similarities in structure and properties, it is possible that the already developed heparin col. assay is also able to quantify fucoidan with the same principles.

Principle of the method used in this quantification experiment:

I. $Fucoidan + AT \rightarrow [AT \bullet \text{Fucoidan}]$
II. $[AT \bullet \text{Fucoidan}] + \text{FXa (excess)} \rightarrow [FXa \bullet \text{AT} \bullet \text{Fucoidan}] + \text{FXa (residual)}$
III. $FXa\ (residual) + S2732\ \rightarrow Peptide + pNA$

The spearman correlation coefficient (r_s) between anti-Xa activity and heparin concentration has been determined by spiking plasma samples to be 1.0. Variation of the coefficient was at most 5% within run as well as day-to-day variability (Bürki, 2018). Though the heparin col. assay seems to be reliable, these tests were done in plasma, and the accuracy and reliability may differ when using the assay without plasma.

To quantify fucoidan with the heparin col. assay, a standard curve will be obtained by using a high purity (≥95%) fucoidan standard from *Fucus vesiculosus* delivered from Sigma Aldrich. The procedure delivered from the Heparin col. assay was adapted from microplate UV-VIS to manual assay cuvette UV-VIS by simply quadrupling the volumes of the procedure. Beyond this, the recommended procedure provided by the producer was followed.

The mass weight of the Sigma Aldrich fucoidan standard is unknown (Sigma Aldrich: product number F8190). A cruder fucoidan from the same seaweed, *Fucus vesiculosus*, delivered by the same manufacturer has mass weight ranging from 20 kDa to 200 kDa, with an average of 134 kDa (Burbach, 2016). The anticoagulant properties of heparin and fucoidan depend on the molecular weight and DS of the polysaccharide (Reis, 2008; Kopplin, 2018). This could have an impact on the heparin col. assay standard curve, and thus also on the amount of fucoidan that is quantified in the fine and crude fucoidan solution.

In the following procedures three different fucoidan standard solutions are used to make standard curves. The concentration and use of each fucoidan solution is listed in table 4.

Table 4: Overview of the Sigma Aldrich fucoidan solutions used in standardization of heparin colorimetric assay.

Solutions of Sigma Aldrich Fucoidan (≥95%) from *F. ves.*	Concentration [mg/ml]	Use
1	1.028	Standardizing heparin col. assay, quantification of both crude fucoidan samples from Alginor.
2	2.02	Optimize standard curves and reproduce achieved results.
3	2.20	Establish a standard curve in room temperature and find out if temperature is a variable.

Procedure of fucoidan solution 1: A sample of Fucoidan (≥95% pure) from Sigma Aldrich was weighed (25.7 mg) and diluted in water (25 ml) to achieve a working concentration of 1.028 mg/ml. The working sample (1.03 mg/mL) along with dilutions of the working sample (0.8, 0.6, 0.4, and 0.2 mg/ml) were used to make the standard curve. The volumes in the procedure of the col. assay were quadrupled to give a volume suitable for the UV-VIS cuvettes as well as to prevent bubbles. The recommended procedure in the heparin col. assay manual was followed. A volume of the samples (0.60 ml) was transferred to separate test tubes, mixed with distilled water (1.2 ml), and incubated for 6 minutes at 37°C. Pre-heated S-2732 (0.2 ml, 37°C) was mixed into each test tube, followed by pre-heated Factor Xa (0.2 ml, 37°C) and shaken thoroughly for 2 minutes. Change in colour from colourless to slight blue was observed. The reaction was stopped with 20% acetic acid (0.2 ml) and UV measurements were taken. Absorbance at 490 nm were measured and subtracted to the absorbance measured at 405 nm.

12 readings were performed at 30 second intervals and a standard curve with three parallels was obtained as well as a check for drift. The same procedure was followed for the crude (OEWA-00038) and fine fucoidan (OEWA-00289) samples with different working concentrations.

Procedure of fucoidan solution 2: A sample of Fucoidan (≥95% pure) from Sigma Aldrich was weighed (20.2 mg) and diluted in water (10 ml) to achieve a working concentration of 2.02 mg/ml. The working sample along with dilutions of the working sample (1.8, 1.4, 1.0 and 0.6 mg/ml) were used to make the improved standard curve. The volumes in the procedure of the col. assay were quintupled to give a volume suitable for the UV-VIS cuvettes as well as to easily prevent bubbles. The recommended procedure in the heparin col. assay manual was followed. A volume of the samples (0.75 ml) was transferred to separate test tubes, mixed with distilled water (1.5 ml), and incubated for 6 minutes at 37°C. Pre-heated S-2732 (0.25 ml, 37°C) was mixed into each test tube, followed by pre-heated Factor Xa (0.25 ml, 37°C) and shaken thoroughly. Change in colour from colourless to slight blue was observed. The reaction was stopped with 20% acetic acid (0.25 ml) and UV measurements were taken. Absorbance at 490 nm were measured and subtracted to the absorbance measured at 405 nm. 12 readings were performed at 30 second intervals and a standard curve with three parallels was obtained as well as check for drift.

Procedure of fucoidan solution 3: A sample of Fucoidan (≥95% pure) from Sigma Aldrich was weighed (22.0 mg) and diluted in water (10 ml) to achieve a working concentration of 2.20 mg/ml. The working sample along with dilutions of the working sample (1.8, 1.4, 1.0 and 0.6 mg/ml) were used to make the room temperature standard curve. The volumes in the procedure of the col. assay were quintupled to give a volume suitable for the UV-VIS cuvettes as well as to easily prevent bubbles. The recommended procedure in the col. assay manual was followed. A volume of the samples (0.75 ml) was transferred to separate test tubes, mixed with distilled water (1.5 ml). S-2732 (0.25 ml, 20°C) was mixed into each test tube, followed by pre-heated Factor Xa (0.25 ml, 37°C) and shaken thoroughly. Change in color from colorless to slight blue was observed. The reaction was stopped with 20% acetic acid (0.25 ml) and UV measurements were taken. Absorbance at 490 nm were measured and subtracted to the absorbance measured at 405 nm. 12 readings were performed at 30 second intervals and a standard curve with three parallels was obtained as well as a check for drift.

2.4 Nuclear Magnetic Resonance (NMR) Spectroscopy

NMR spectroscopy is one of the most essential and useful tools to analyze and elucidate the structure of polysaccharides (Yao, 2021). The “Web of Science” database shows a clear uptrend of articles related to the use of NMR spectroscopy. During the past decades the strength of the superconducting

magnets that provide ^{1}H resonance frequencies have increased drastically from below 100 MHz in the 1960's to up to 1.2 GHz in 2020 (Castaing, 2021). Today, 300 and 600 MHz NMR spectrometers are routinely used in many research laboratories and industries. Stronger magnets and high-end electronics and computers have made the technique more accurate and sensitive by lowering the signal to noise ratio (S/N) and increasing the resolution of the spectrums.

2.4.1 Quantitative Nuclear Magnetic (qNMR) Spectroscopy

NMR spectroscopy directly observes the nuclear spins of the atoms in a molecule. Thus, in principle the technique has quantitative capabilities and can be used in quantification analysis (JEOL – qNMR, last accessed 27.03.2022). Quantitative NMR (qNMR) is used for determination of concentration and purity of molecules.

There are basically three types of qNMR applications.

1. The concentration of products and impurities down to ppm level
2. Purity determination of standards for other techniques like HPLC. This requires high accuracy and precision.
3. Composition of complex mixtures. Many compound classes at the same time (e.g. metabolomics).

The first method, determination of concentration, is the qNMR application used in this thesis. The concentration of the analyte can be determined with a known concentration of a standard in the sample, illustrated in figure 18.

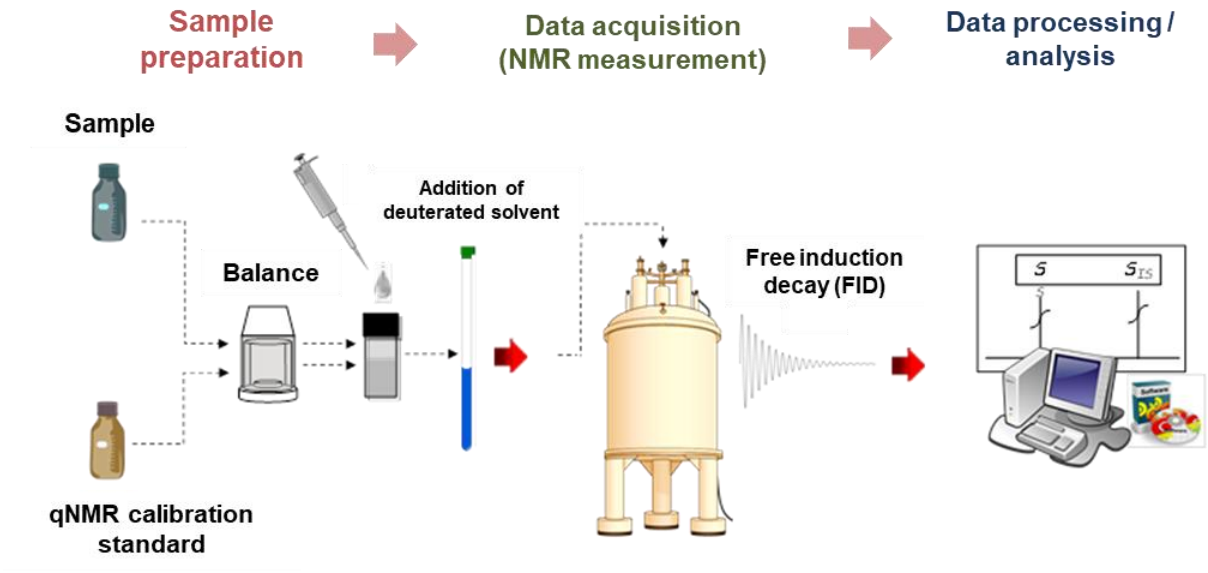

Figure 18: qNMR method overview (Quantitative NMR, retrieved 28.03.2022)

NMR signal intensities are expressed as equation (1.2). Where I_A and I_B represent the area of the integrated NMR peaks of the standard and the analyte, H_A and H_B represent the number of protons the standard and analyte integral represent, and C_A and C_B represent the concentration of the standard and the analyte.

(1.2) $$\frac{I_A}{I_B} = \frac{H_A C_A}{H_B C_B}$$

If the sample varies over time (e.g., biological variation), or is subject to sample inhomogeneity, this will have an impact on the qNMR results. Some standards may also change over time. Inaccurate weighing and pipetting are some of the common errors with an inexperienced operator. Especially since you need the weight of both the analyte and the internal standard. As long as the sample is homogenous, only a duplicate analysis (two samples with one measurement for each sample) is necessary to exclude incidental sample preparation errors (Schoenberger, 2019).

The NMR and qNMR experiments were performed at a Bruker AVANCE NEO 600 MHz instrument which was installed in 2017 at the Norwegian NMR platform (NNP) building. The instrument is equipped with a cryogenic prove with four RF-channels (1H, 13C, 15N, and 31P). It features new generation of electronics (NEO), which gives improved dynamic range, quicker control, and scalability. The automatic sample changer (SampleJet) automatically switches the samples. NNP also provides 850 MHz analysis. The added quality of resolution from 850 MHz is not necessary for the experiment.

The salts potassium phthalate monobasic (KHP) and calcium formate, figure 19, are standards that are suited for qNMR experiments with fucoidan. KHP has two *meta* and two *para* protons that should in total give rise to two signals with the same area and at slightly different chemical shifts. Calcium

formate should give one signal from its two protons. KHP operates at 8.2 ppm – 7.5ppm and has a pH of 4. The pH could be a problem since fucoidans composition is vulnerable to pH change. Calcium formate does not have this issue and could therefore be used instead. Calcium formate operates at 8.5 – 7.5 ppm and is a slightly cheaper standard than KHP.

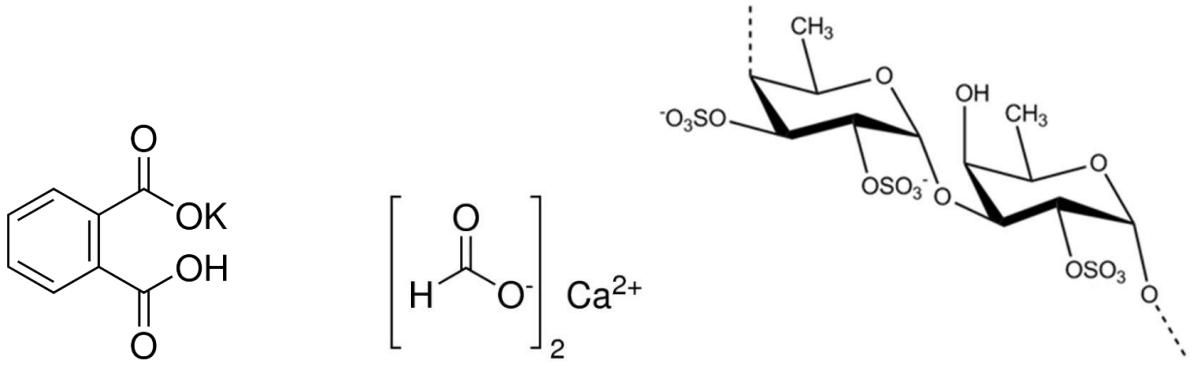

Figure 19: Potassium phthalate monobasic (left), Calcium formate (middle), and fucoidan fracture (right).

When quantifying fucoidan, the C6 alpha proton and the three protons in the methyl group are the protons used for quantification against the protons in the standard. The C6 beta proton is in the aromatic "forest" and is thus impossible to integrate. The area found from integration of the peaks, the measured known concentrations of the standard and analyte, as well as the proton relation is used in equation (1.2) to calculate the concentration of the analyte.

The parameters of the T1 and 1H qNMR experiments are shown in table 5 and table 6.

Table 5: Parameters of proton T1 NMR test experiment.

NS	8
P1	8
D1	10
TE	298
1TD	10
2TD	16384
1SW	2
2SW	19,8368
O1P	6.175
O2P	6.175
SI	8192
AUNM	au_zg
ANMP	proc_2dt1
FNTYPE	0

Table 6: Parameters of 1H qNMR experiments.

NS	128
P1	8
D1	30
TE	298
1TD	65536
2TD	65536
1SW	19,8368
2SW	19,8368
O1P	6,175
O2P	6,175
SI	65536
AUNM	au_zgpc
ANMP	proc_1d
FNTYPE	0

Procedure: One parallel with L-fucose with KHP was first analyzed, followed by one parallel with calcium formate. The standard that gave the least deviation in yield had two more parallels taken and was chosen to be used for fucoidan qNMR experiments.

One parallel of fucose (11.1 mg) and KHP (2.6 mg), and a total of three parallels of fucose (11.4 mg, 2.9 mg, and 5.5 mg) and calcium formate (0.5 mg, 0.9 mg, and 1.6 mg) was respectively weighed and diluted with deuterium oxide (0.75 ml) into separate 20 ml sample glasses and stirred thoroughly. The parallels were pipetted into 5 mm tubes and capped with coded closed caps provided by Bruker. Samples were placed in the NMR apparatus, proton NMR was performed with iconNMR and a spectrum was obtained.

One parallel of fucoidan (5.1 mg) and calcium formate (0.8 mg) was weighed and diluted with deuterium oxide (0.75 ml) into a 20 ml sample glass and stirred thoroughly. The solution was pipetted into 5 mm tubes and capped with coded closed caps provided by Bruker. The same parameters for fucoidan as for L-fucose.

The same procedure was followed for fine fucoidan (4.5 mg) with $Ca(HCOO)_2$ (2.8 mg), and crude fucoidan (1.4 mg) with $Ca(HCOO)_2$ (1.5 mg). Spectrums are shown in appendix 1. Number of scans (NS) was set to 128 seconds for the qNMR experiments since it requires only a few minutes longer.

Chapter 3 – Results and discussion

3.1.1 Initial test analysis – quantitative assays

In the initial testing of practical issues related to the colorimetric method set-up, samples volume, reaction time and instrument drift were some of the factors of main concern. After attempts to standardize L-fucose with an available microplate UV-VIS instrument and a cuvette UV-VIS instrument, it was concluded that cuvettes were the most user friendly. This was mainly due to the viscous nature of the solutions, making it easier to pipette into the larger volume cuvettes without quantitative error. Cuvette UV-VIS was further used for both L-fucose and heparin col. assay. The assays are based on time dependent reactions leaving a colored product to be detected, this warrants training in operating fast and efficient to get reliable and linear results. The laboratory work constituted of much trial and error in learning how to use the col. assays and pipettes properly, especially with the heparin col. assay. For the col. assay UV-VIS measurements, checks for drift were performed in all series by measuring the absorbance 12 times in 30 or 60 second intervals. The drift checks were important to determine if the reaction had finished properly. The initial measured absorbance was always used in the calculations.

With the L-fucose col. assay, temperature control and evaporation of the water bath and fucoidan solution were optimization problems that took time to overcome due to the long hydrolyzation times. Through trial and error, an appropriate volume of 1M HCl was determined that would not evaporate overnight. To limit evaporation of the water bath, an improvised lid of aluminum foil was made around the bottle neck of the volumetric flasks as to not react with the HCl vapor.

3.2 L-fucose colorimetric assay standardization

The L-fucose col. assay was standardized with the L-fucose standard included in the assay. The measured values and resulting calibration curves are given in concentration (mg/ml) and is shown together with drift checks in section 3.2.1. The fucoidan yield of the fucoidan standard (≥95%) and the fine (OEWA-00289) and crude fucoidan (OEWA-00038) were determined and is shown in section 3.2.2, 3.2.3 and 3.2.4 respectively.

3.2.1 L-fucose standard curve

The two parallels of the standard curves are shown in table 7 and 8. The concentration of the dilutions, their respective volume, absorbance, theoretical mass, and calculated concentration is listed in the five series.

Table 7: Values used to make the L-fucose standard curve (P1).

Fucose standardization of L-Fucose col. assay P1					
	Serie 1	Serie 2	Serie 3	Serie 4	Serie 5
Absorbance	0.1442	0.1198	0.0907	0.0618	0.0301
Concentration (Fucose) [mg/ml]	0.1	0.08	0.06	0.04	0.02
Volume total (ml)	0.1	0.1	0.1	0.1	0.1
Mass Fucoidan [mg]	0.01	0.008	0.006	0.004	0.002
Megazyme calculation method for concentration [mg/ml]	0.100	0.083	0.063	0.043	0.021

Table 8: Values used to make the L-fucose standard curve (P2).

Fucose standardization of L-Fucose col. assay P2					
	Serie 1	Serie 2	Serie 3	Serie 4	Serie 5
Absorbance	0.1513	0.1191	0.0911	0.0583	0.0306
Concentration (Fucose) [mg/ml]	0.1	0.08	0.06	0.04	0.02
Volume total (ml)	0.1	0.1	0.1	0.1	0.1
Mass Fucoidan [mg]	0.01	0.008	0.006	0.004	0.002
Megazyme calculation method for concentration [mg/ml]	0.104	0.082	0.063	0.040	0.021

The standard curve obtained from P1 (blue) and P2 (orange) along with their respective equation is shown in figure 20.

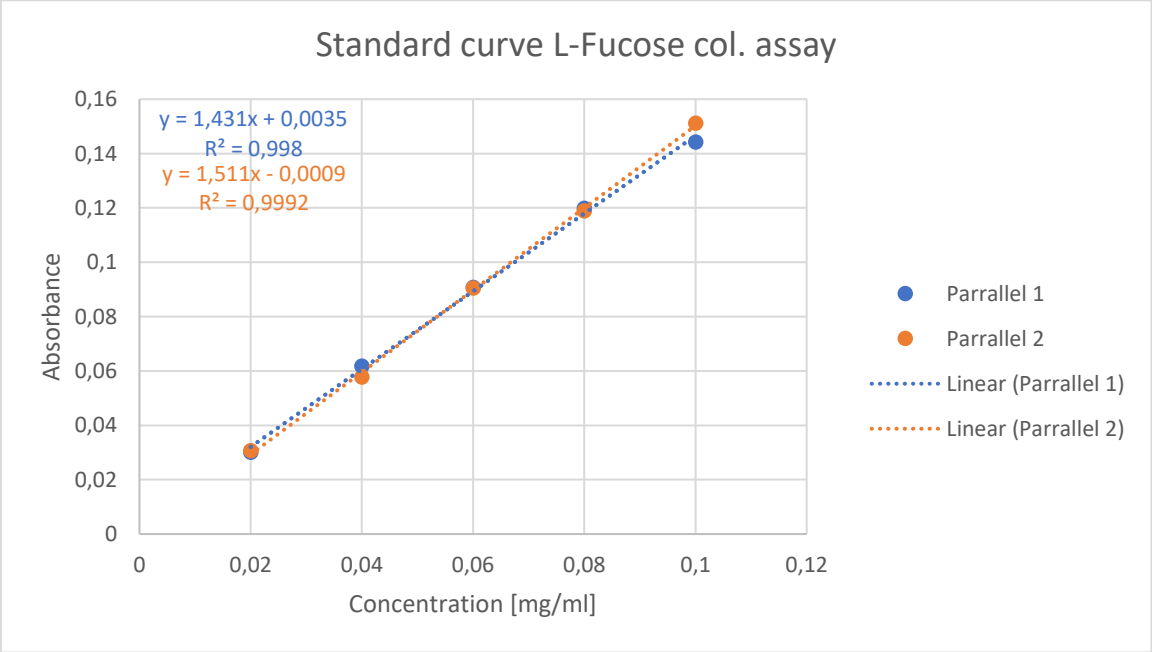

Figure 20: Standard curve L-fucose with two parallels, formula of P2 was used.

The drift check for parallel 1 is shown in figure 21 while parallel 2 is shown in figure 22 in appendix 1. Drift checks that gave little or no drift for L-fucose experiments can be seen in the appendix 1.

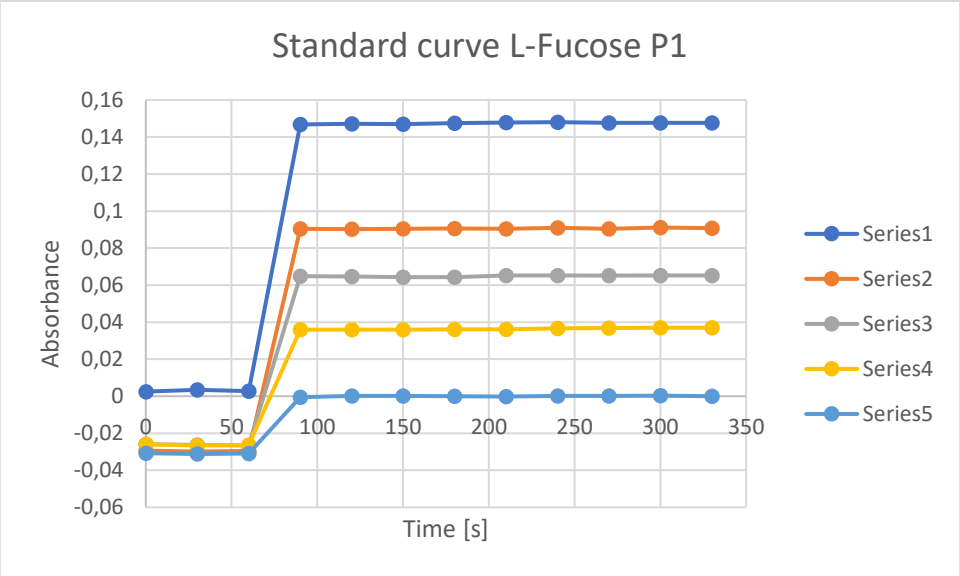

Figure 21: Drift check of L-fucose standard curve P1.

In table 7 and 8 the yield of the L-fucose is highlighted in yellow. The concentration of fucoidan is highlighted in green and were calculated using the col. assays method of calculation that is shown in equation (1.1). The same highlighting colors will be used in other tables when quantifying the fucoidan standard and the cruder fucoidan solutions. The L-fucose standard provided by the L-fucose col. assay was used to make an exemplary standard curve, as shown in figure 20. Using either the standard curve or the assays own calculation method gave strikingly equal yield of L-fucose. The made standard curve should thus give results intended by the L-fucose col. assay manufacturer. For every L-fucose col. assay experiment, the amount of L-fucose detected was calculated back to fucoidan by the fucoidan/L-fucose ratio (0.4434) shown in table 7 and 8. The standard curves parallels P1 and P2 are almost identical. Due to a slightly higher number in coefficient of determination (R^2), the formula of P2 was chosen as standard curve. There was no drift detected in either P1 or P2, as shown in figure 21 and 22.

3.2.2 Quantifying the fucoidan standard using L-fucose col. assay

For quantification of the (≥95%) fucoidan standard from Sigma Aldrich with the L-fucose kit, an assumption was made that the fucoidan was 95% pure. The fucoidan standard was weighed in at a mass (9 mg) that would give a concentration suitable for the standard curve without the need of extrapolation. The fucoidan standard was hydrolyzed in water bath with 1M HCl at 80°C for 6 hours or 60°C for 24 or 48 hours. The acidic solutions were filtered and neutralized with 1M NaOH to a pH around 7 into a volumetric flask. The volumetric flask was filled to the meniscus and quantification with the L-fucose col. assay could commence. The same procedure is done for the fine (OEWA-00289)

and crude (OEWA-00038) fucoidan samples. Parameters used to quantify the fucoidan standard (≥95%) are shown in table 9. The drift checks from all parallels are shown in appendix 1.

Table 9: L-fucose quantification of Sigma Aldrich Fucoidan (≥95%) with assumed purity of 95%

Sigma Aldrich Fucoidan solution, assuming purity = 95%									
	6-hour hydrolyzation			24-hour hydrolyzation			48-hour hydrolyzation		
	P1	P2	P3	P1	P2	P3	P1	P2	P3
T(water bath) [C]	80	80	80	65	65	65	65	65	65
m(Sigma Aldrich Fucoidan)[mg]	9	9	9	9	9	9	9	9	9
V(Total) [ml]	100	100	100	100	100	100	100	100	100
C(Sigma Aldrich Fucoidan) [mg/ml]	0.09	0.09	0.09	0.09	0.09	0.09	0.09	0.09	0.09
Absorbance	0.053	0.058	0.063	0.055	0.052	0.052	0.058	0.058	0.058
C(Fucose) Using std. Curve	0.035	0.039	0.042	0.037	0.035	0.035	0.039	0.039	0.039
m(Fucose) calculating back w/ std. Curve [mg]	3.534	3.925	4.236	3.700	3.501	3.494	3.918	3.905	3.911
Factor: Fucose/Fucoidan	0.443	0.443	0.443	0.443	0.443	0.443	0.443	0.443	0.443
m(Fucoidan) [mg]	7.970	8.851	9.553	8.344	7.896	7.881	8.836	8.806	8.821
Fucoidan in Crude [%]	88.56	98.34	106.14	92.71	87.73	87.57	98.18	97.85	98.01
Average [%]	97.7 ±8.81			89.3 ±2.92			98.0 ±0.17		

As seen from table 9, the L-fucose col. assay provided seemingly accurate and reliable results for the Sigma Aldrich fucoidan standard (≥95%) from *Fucus vesiculosus*. The yield of the 48-hour hydrolyzation (48-hh) proved to be the most stable and had little variation between the parallels, as seen in table 9. It has thus been confirmed that 65°C is a high enough temperature to hydrolyze fucoidan if enough time is spent hydrolyzing. Hydrolyzing the fucoidan standard for 6 hours at 80°C gave a high yield, as was expected from figure 15. However, the shorter the time spent hydrolyzing the standard, the higher the standard deviation appears to be. The variation in the yield of the parallels of the 6-hour hydrolyzation (6-hh) was higher than the 24-hh, and much higher than the 48-hh, though the average yield of the 6-hh was similar to the 48-hh. If the standard is 95% pure as assumed, an average yield of 100% should be achieved. The average yield for the 48-hh is 98% and appears thus to be 2% off from expected value. However, since the limit of detection (LOD) for the L-fucose assay is 2%, the 48-hh is within expected yield. In other words, with 95% purity assumed and a LOD at 2%, 100% of the fucoidan standard was hydrolyzed and desulphated into L-fucose units with the 48-hh. As can be seen from figure 23, 24 and 25 in appendix 1, hardly any drift was detected.

3.2.3 Quantification of fine fucoidan (OEWA-00289)

Parameters used to quantify the fine fucoidan from Alginor are shown in table 10. The drift check of all parallels can be observed in appendix 1.

Table 10: L-fucose quantification of highly filtered fucoidan from L. hyp. (Alginor)

Fine fucoidan OEWA-00289	6-hour hydrolyzation			24-hour hydrolyzation			48-hour hydrolyzation		
	P1	P2	P3	P1	P2	P3	P1	P2	P3
T(water bath) [C]	80	80	80	65	65	65	65	65	65
m(Crude)[mg]	198	198	198	197	197	197	198	198	198
V(Total) [ml]	100	100	100	100	100	100	100	100	100
C(Crude) [mg/ml]	1.98	1.98	1.98	1.97	1.97	1.97	1.98	1.98	1.98
Absorbance	0.678	0.697	0.713	0.695	0.685	0.689	0.752	0.752	0.768
C(Fucose) Using std. Curve	0.449	0.462	0.472	0.461	0.454	0.456	0.499	0.498	0.509
m(Fucose) calculating back w/ std. Curve [mg]	44.92	46.17	47.23	46.06	45.40	45.64	49.85	49.79	50.85
Factor: Fucose/Fucoidan	0.443	0.443	0.443	0.443	0.443	0.443	0.443	0.443	0.443
m(Fucoidan) [mg]	101.32	104.12	106.51	103.87	102.39	102.93	112.44	112.30	114.69
Fucoidan in Crude [%]	51.17	52.59	53.79	52.73	51.98	52.25	56.79	56.72	57.92
Average [%]	52.5 ±1.31			52.3 ±0.38			57.1 ±0.68		

The fucoidan yield of the fine fucoidan solution from *L. hyp.* was similar for 6-hh and 24-hh, as seen in table 10. The highest yield was again given by the 48-hh, with roughly 5% more fucoidan detected than for both the 6-hh and the 24-hh. Variance between the parallels were relatively low for all hydrolyzation times with the largest variance for the 6-hh. Drift checks in the parallels showed little to no drift, as can be seen in figure 26, 27 and 28 in appendix 1.

3.2.4 Quantification of crude fucoidan (OEWA-00038)

Parameters used to quantify the crude fucoidan from Alginor is shown in table 11. The drift checks from all parallels are shown in appendix 1.

Table 11: L-fucose quantification of less filtered fucoidan from L. hyp. (Alginor).

Crude Fucoidan OEWA-00038	6-hour hydrolyzation			24-hour hydrolyzation			48-hour hydrolyzation		
	P1	P2	P3	P1	P2	P3	P1	P2	P3
T(water bath) [C]	80	80	80	65	65	65	65	65	65
m(Crude)[mg]	217	217	217	204	204	204	217	217	217
V(Total) [ml]	100	100	100	100	100	100	100	100	100
C(Crude) [mg/ml]	2.17	2.17	2.17	2.04	2.04	2.04	2.17	2.17	2.17
Absorbance	0.399	0.392	0.397	0.303	0.317	0.319	0.411	0.414	0.422

C(Fucose) Using std. Curve	0.265	0.260	0.263	0.201	0.210	0.211	0.273	0.274	0.280
m(Fucose) calculating back w/ std. Curve [mg]	26.48	26.00	26.32	20.13	21.01	21.14	27.27	27.43	27.99
Factor: Fucose/Fucoidan	0.443	0.443	0.443	0.443	0.443	0.443	0.443	0.443	0.443
m(Fucoidan) [mg]	59.72	58.64	59.36	45.40	47.39	47.69	61.51	61.87	63.12
Fucoidan in Crude [%]	27.52	27.02	27.35	22.26	23.23	23.38	28.35	28.51	29.09
Average [%]	27.30 ±0.25			22.95 ±0.61			28.65 ±0.39		

The fucoidan yield from the crude fucoidan had a somewhat similar trend to the fucoidan standard, with a low yield detected for the 24-hh and high yield for both the 6-hh and 48-hh. In contrast to the fucoidan standard, the crude fucoidan yield had low deviation for all hydrolyzations. The yield of the 6-hh was relatively similar compared to the 48-hh, and in contrary to the fucoidan standard, with low deviance between their respective parallels. It would thus seem that the increased temperature made up for the less time spent hydrolyzing. No sign of drift was observed when quantifying the crude fucoidan, as can be seen in figure 29, 30 and 31 in appendix 1.

Interpreting the results of the fucoidan standard and the fine and crude fucoidan, it should be taken into consideration that the water bath in the 6-hh was 15 C° higher than the 24-hh and 48-hh. The added time spent hydrolyzing could make up for the lower temperature. The average yield of the 24-hh was lower than the average yield of the 6-hh for all fucoidan samples. The standard deviation of the 24-hh was however lower in general compared to the 6-hh. In figure 15, hydrolyzation of fucoidan at 80 C° were done at several intervals within 400 minutes before determining the fucoidan yield with L-fucose col. assay. After 300 minutes, the change in absorbance was minor. Thus, the 6-hh method should have adequate time to break the polysaccharide into L-fucose groups, which is also shown in the results in this thesis. However, when hydrolyzing at 65 C°, 24 hours seem to be insufficient time for a high yield. 48 hours of hydrolyzation provided the highest yield with the least variance.

The L-fucose col. assay has previously been used to determine fucoidan in a sample and was also proven to be successful in this thesis. To compare the L-fucose col. assay with the heparin col. assay and qNMR, the results from the 48-hh samples are used since this was the method that gave the highest yield and the least variation. To which extent temperature and hydrolyzation time affects the results can be researched further.

Publications determining fucoidan by hydrolyzing fucoidan into L-fucose units have been found to hydrolyze the fucoidan samples between 1 and 24 hours, at 70 or 80°C (Ahmad, 2015; Turan, 2017). From the results in this thesis, it would make sense to always use the 48-hh as it gave the highest yield and a generally low deviation, and it is thus likely to be closer to true value. The fucoidan yield of the

Sigma Aldrich standard from *F. ves.*, as well as the fine (OEWA-00289) and crude (OEWA-00038) fucoidan is then found to be 98.0 ±0.17%, 57.1 ±0.68% and 28.7 ±0.40% respectively.

3.3 Heparin colorimetric assay

The heparin col. assay is normally used in automated microplates. Because of the fucoidan solutions viscous nature, the manual was adapted to be used with cuvettes at the UV-VIS instrument. This would limit human error when pipetting the solutions. The volumes in the manual procedure were simply quadrupled or quintupled to give samples with appropriate volume for the cuvettes. Since the procedure of the heparin col. assay was done according to the manual, strict timing was required when performing the experiment. This includes timing the preheating, pipetting, stirring and reaction time with a stop clock according to the manual. After much practice pipetting in a mechanically timed fashion, a standard curve was obtained.

3.3.1 Standard curves obtained with Sigma Aldrich fucoidan and drift checks for parallels

The Sigma Aldrich fucoidan standard from *F. ves*. was used to make the standard curve. For the standardization used in the quantifications, fucoidan solution 1 was used, see table 4.

Table 12: Relevant concentrations of fucoidan (≥95%) from solution 1 and their respective absorbances used to standardize heparin col. assay.

Sigma Aldrich fucoidan standardization with heparin col. assay					
	Serie 1	Serie 2	Serie 3	Serie 4	Serie 5
V [ml]	0.6	0.6	0.6	0.6	0.6
C (Fucoidan) [mg/ml]	1.028	0.8	0.6	0.4	0.2
P1 Absorbance	0.7263	0.7409	0.768	0.7628	0.813
P2 Absorbance	0.7839	0.8256	0.8211	0.8589	0.8468
P3 Absorbance	0.6911	0.692	0.7193	0.7433	0.7381

The first parallel of the heparin col. assay standard curve and its formula are shown in figure 32.

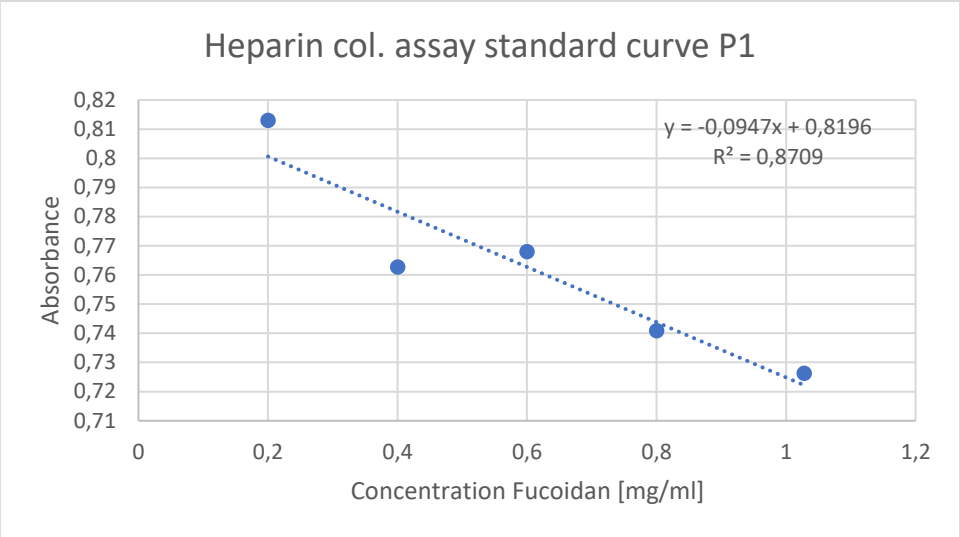

Figure 22: Heparin col. assay standard curve using Sigma Aldrich fucoidan solution 1, P1.

The drift check of the first parallel is shown in figure 33. Drift is detected in series 4 and 5.

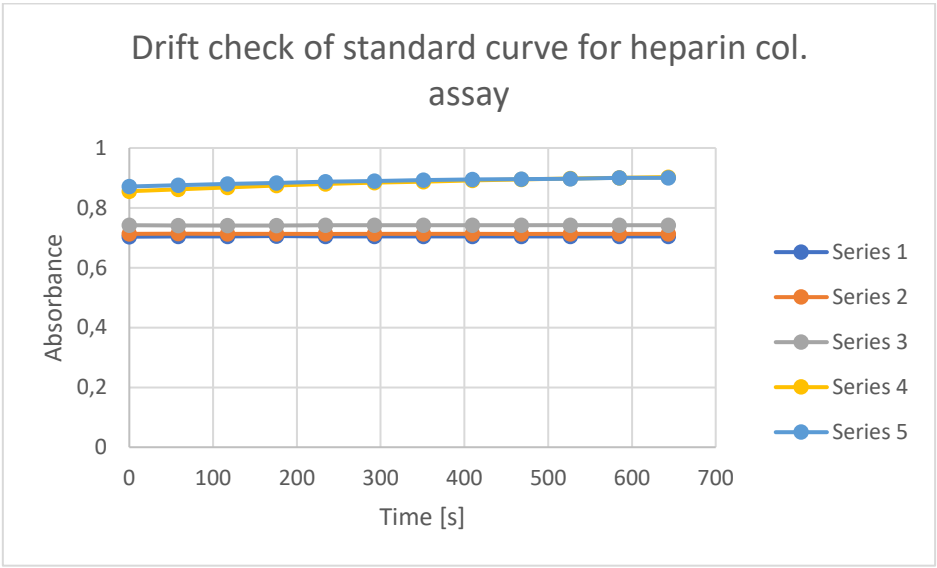

Figure 23: Drift check of the heparin col. assay standard curve P1.

The second parallel of the heparin col. assay standard curve and its formula are shown in figure 34.

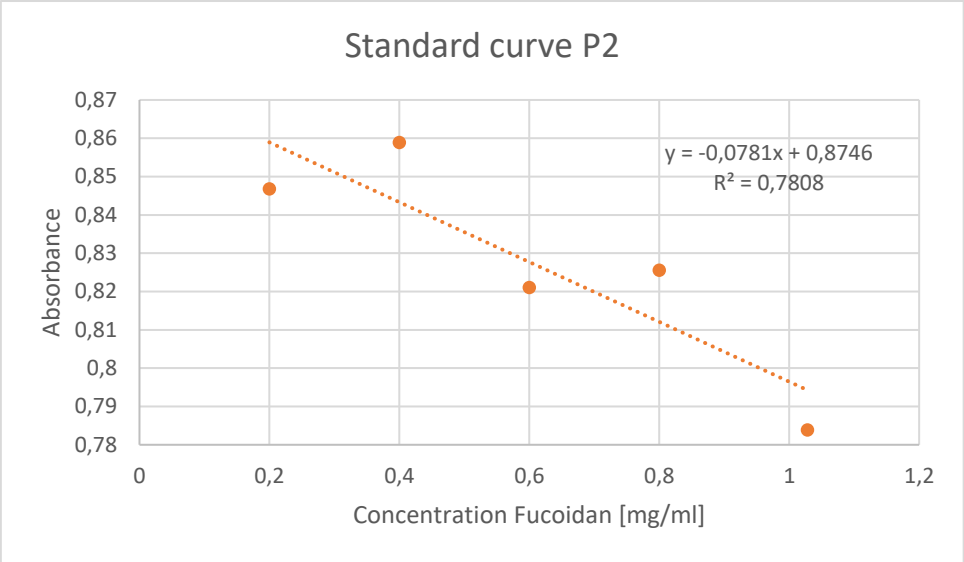

Figure 24: Heparin col. assay standard curve using Sigma Aldrich fucoidan solution 1, P2.

The drift check of said parallel is shown in figure 35. Drift is detected in series 4.

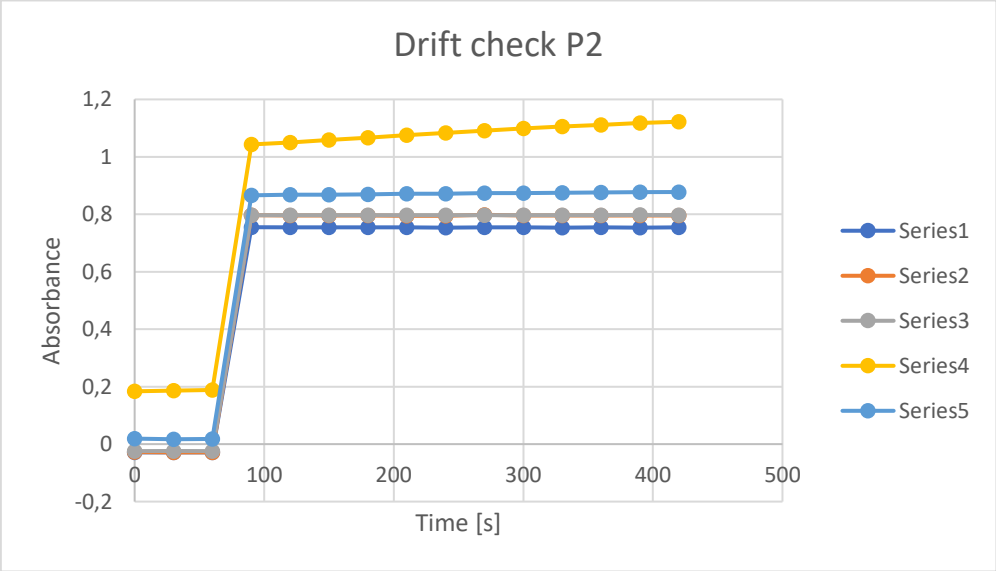

Figure 25: Heparin col. assay standard curve using Sigma Aldrich fucoidan P2.

The third parallel of the heparin col. assay standard curve and its formula are shown in figure 36.

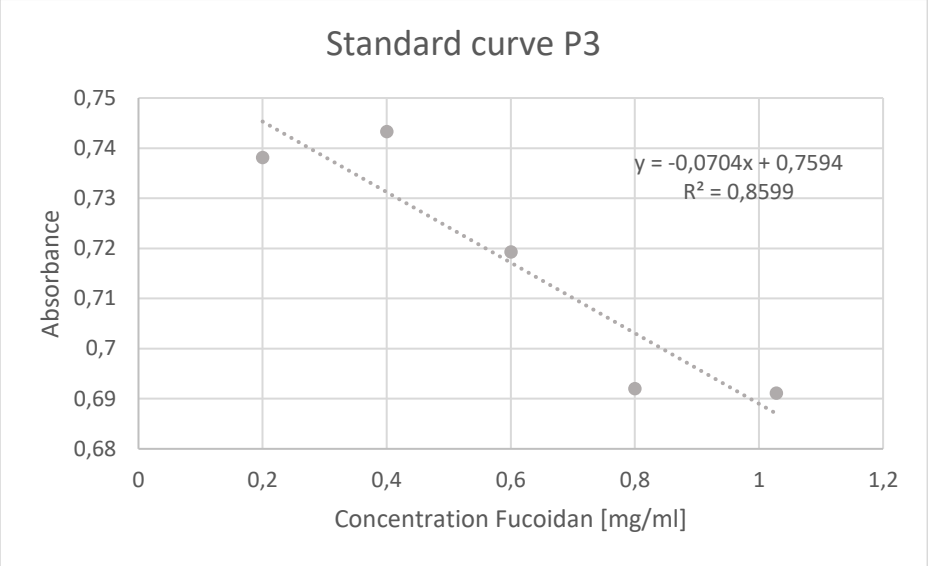

Figure 26: Heparin col. assay standard curve using Sigma Aldrich fucoidan solution 1, P3.

The drift check of said standard curve parallel is shown in figure 37.

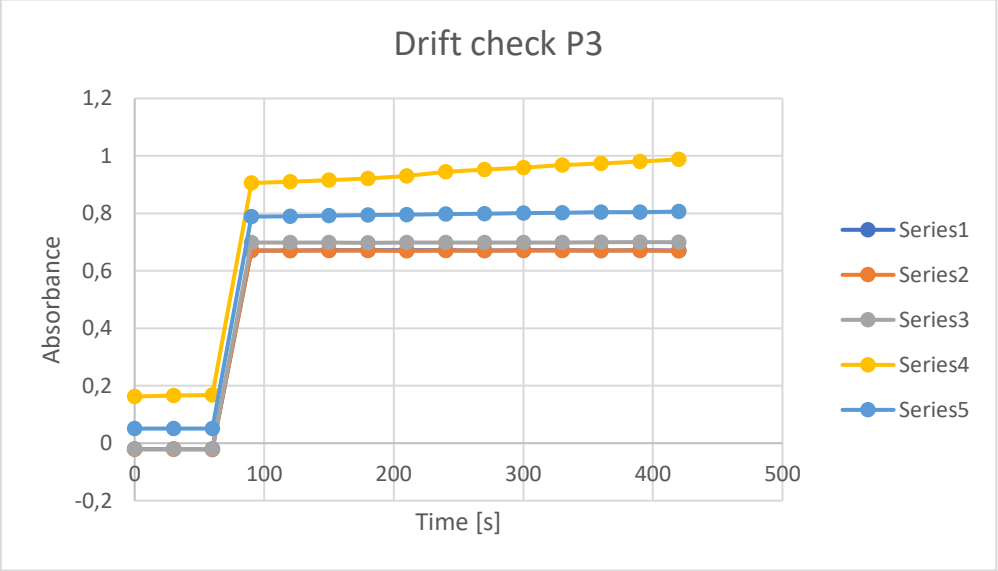

Figure 27: Heparin col. assay standard curve using Sigma Aldrich fucoidan P3.

A comparison of the three standard curve parallels is presented in figure 38.

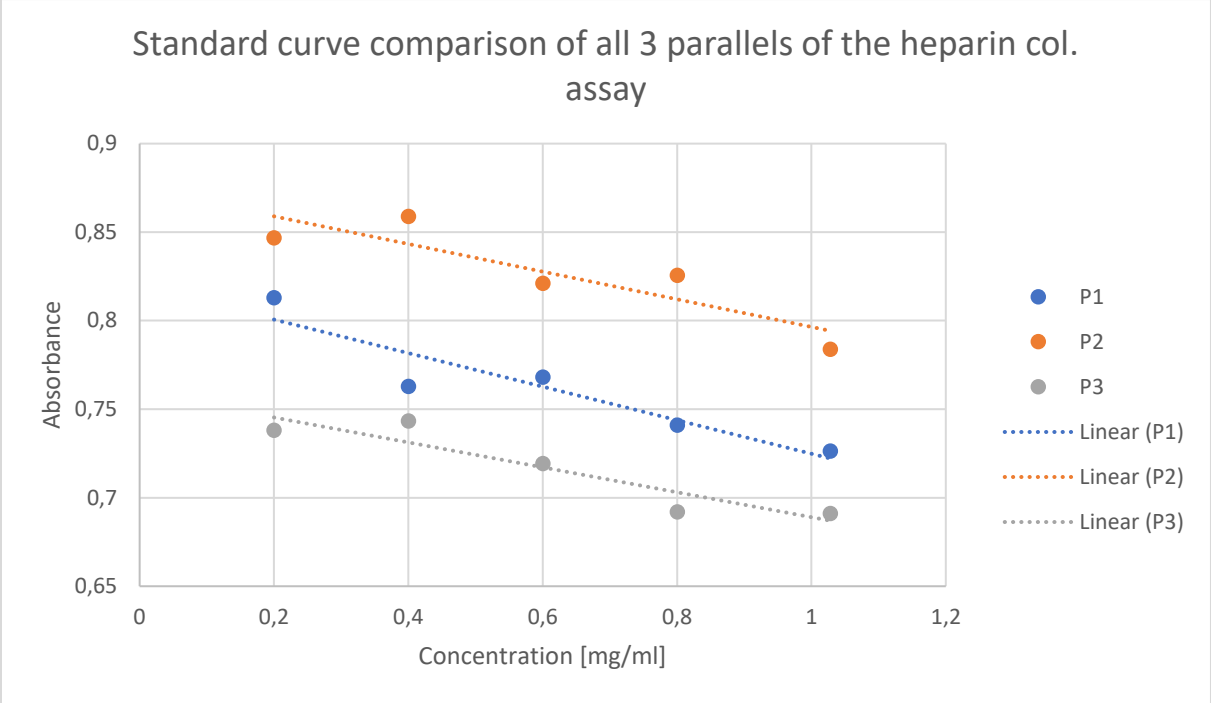

Figure 28: Comparison of heparin col. assay standard curves using Sigma Aldrich fucoidan P1, P2 and P3.

The first indication of a successful standardization came when the tintless solution changed colour from tintless to blue tint. This was the first indication of the heparin col. assay being successful in binding the dye to the sulphate groups of the fucoidans. From the standard curves in figure 32, 34 and 36 there is a clear degree of quantification. Relatively high levels of drift were observed in series 1 for P1 and in series 4 for all three parallels, shown in figure 33, 35 and 37. This is likely due to the reaction not being properly stopped with acetic acid. If the reaction was not properly stopped with acetic acid after its designated two minutes of reacting, the dye would still be free to bind to the sulphate groups, prolonging the reaction time. This would be shown as an increase in absorbance in the drift check. Another possible explanation of the drift could be that bubbles could have been formed when pipetting the solution into UV-VIS cuvettes.

The comparison of the standard curves in figure 38 show that the parallels had similar slope but started at different absorbances. The difference could be explained by small variations in reaction time due to human error. The dye had only 120 seconds to bind itself to the sulphate groups, meaning every second could have an impact on the measured absorbance. In this thesis the reaction time was left unchanged, however it would be highly recommended for future work to explore reaction time as a factor.

The implications of using a fucoidan standard from a different seaweed was addressed in the experimental methods. The difficulties in extracting fucoidan with high polymer degree (DP) and

degree of sulphation (DS), and how these properties matter to the anticoagulant ability was also addressed. The DP and DS of the Sigma Aldrich fucoidan standard is unknown. Extracting and isolating fucoidans is difficult and both polymer degree and sulphation degree are at risk of being lowered in the process of obtaining a fucoidan standard with high purity. Because of these difficulties, it is likely that the DP and DS of the fucoidan standard is lower than in a more crude fucoidan sample from the same seaweed species, delivered by the same manufacturer. The crude fucoidan samples had mass weights ranging from 20 kDa to 200 kDa, with an average of 134 kDa (Burbach, 2016). This corresponds to an average DP of 816. The sulphate content was found to be 7-11%, which means it is relatively far from the sulphate content in *L. hyp*. fucoidan. The DS for *L. hyp*. fucoidan has, as previously mentioned, been found to be 1.7 (Kopplin, 2018). Additionally, fucoidan from *L. hyp*. is known to have high molecular weight and high DS (Kopplin, 2018). In this thesis the fucoidan was assumed to be disulphated. The implication of standardizing the heparin col. assay with a fucoidan standard that likely has lower DP and DS than the fucoidans it is quantifying, should be investigated further. Fucoidan standards with relatively high DP and DS, preferably from *L. hyp.*, could be more viable than fucoidan from *F. ves.* when quantifying fucoidan from *L. hyp.* with heparin col. assay. Quantifying crude fucoidan solutions from *F. ves*. should also be investigated.

The standard curve with coefficient of determination was closer to 1 (P2) was chosen as the parallel used for quantification of the fine (OEWA-00289) and crude (OEWA-00039) fucoidan samples.

3.3.2 Quantification of fucoidan from fine fucoidan (OEWA-00289)

All relevant data for quantification of the fine fucoidan from Alginor is listed in table 13. The calculated fucoidan concentration found using the standard curve is marked in yellow and the fucoidan yield is marked in blue.

Table 13: Fine fucoidan (Alginor) solution using heparin col. assay

Fine fucoidan solution OEWA-00289			
	P1	P2	P3
m(Crude)[mg]	101	101	101
V(Total) [ml]	25	25	25
C(Crude) [mg/ml]	4.04	4.04	4.04
Absorbance	0.5881	0.6136	0.596
C(Fucoidan) Using std. curve [mg/ml]	2.445	2.175	2.361
m(Fucoidan) [mg]	61.114	54.382	59.029
Fucoidan in Crude [%]	60.509	53.844	58.444
Average [%]		57.60 ±3.41	

The results are highlighted in blue in table 13. The highest difference between two parallels for the heparin col. assay were found at 6.7% for two of the parallels (P1 and P2) and the lowest difference were at 2.1% (P1 and P3) for the fine fucoidan.

The heparin col. assay gave an average fucoidan yield of 57,6 ±3,4% for the fine fucoidan solution. The result is quite similar to the L-fucose col. assay at 57,1 ±0.7%. However, the average standard deviation using the L-fucose col. assay (±0.68%) is considerably lower than when using the heparin col. assay (±3.41%). The deviation could be caused by the short reaction time which makes small differences in pipetting and stirring more evident in the result or discrepancies in homogeneity in some of the reagents. Increasing the reaction time could let the dye bind itself more easily and more evenly to the sulphate groups.

The drift check of the heparin col. assay for P1, P2 and P3 is shown in figure 39.

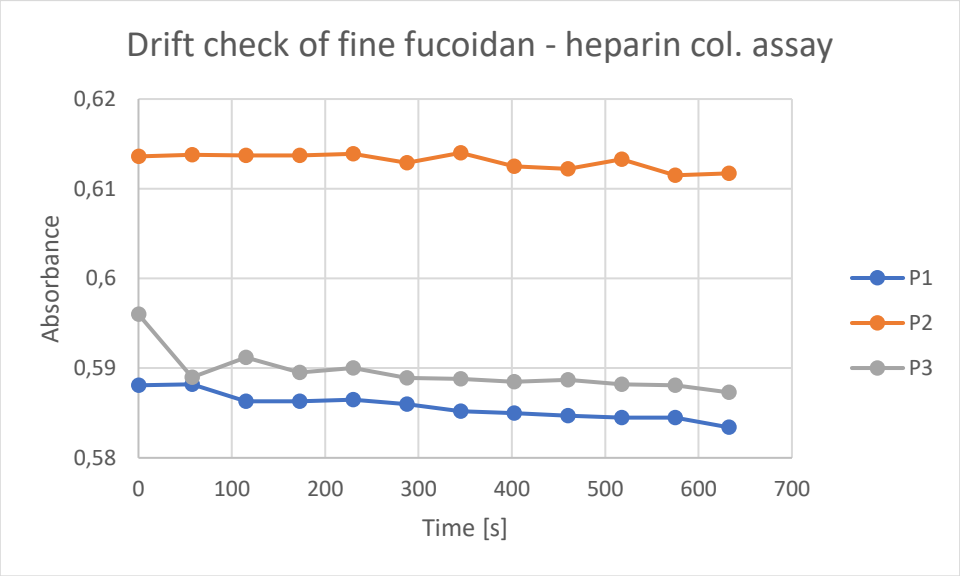

Figure 29: Drift check of fine fucoidan with the heparin col. assay. Measurements done every 60 seconds

The drift check shown in figure 39 indicate some level of drift, for instance for P3 where the absorbance shifted from about 0.597 to 0.587, a change of 0.01. However, this is not even close to the level of drift detected in series 4 for all parallels in the standard curve in figure 33, 35 and 37, where a change in absorbance of roughly 0.1 is observed.

The results from table 13 and the drift check in figure 39 indicate that the heparin col. assay can quantify the fine fucoidan (OEWA-00289) sample but is less precise than the L-fucose col. assay. Methods to optimize the quantification should be researched further.

3.3.3 Quantification of fucoidan from crude fucoidan (OEWA-00038)

All relevant data for quantification of the crude fucoidan from Alginor is listed in table 14. The calculated fucoidan concentration found using the standard curve is marked in yellow and the fucoidan yield is marked in blue.

Table 14: Crude fucoidan (Alginor) solution using heparin col. assay.

Crude Fucoidan OEWA-00038			
	P1	P2	P3
m(Crude)[mg]	106	106	106
V(Total) [ml]	25	25	25
C(Crude) [mg/ml]	4.24	4.24	4.24
Absorbance	0.6144	0.6563	0.6279
C(Fucoidan) Using std. Curve [mg/ml]	2.1668	1.7244	2.0243
m(Fucoidan) [mg]	54.171	43.110	50.607
Fucoidan in Crude [%]	51.105	40.670	47.743
Average [%]		46.51 ±5.33	

In figure 40 the drift check of all three parallels of the crude fucoidan quantification with heparin col. assay is shown.

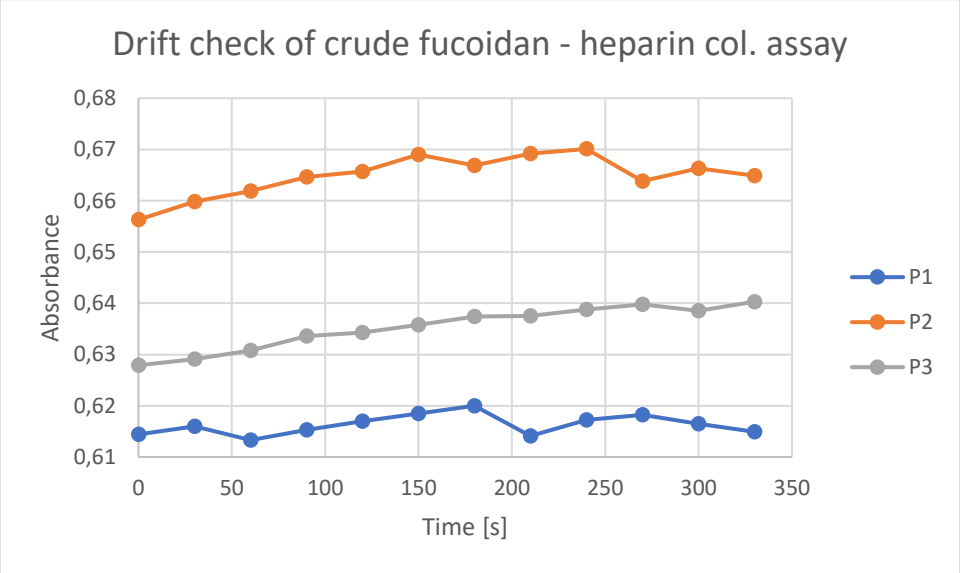

Figure 30: Drift check of crude fucoidan with the heparin col. assay with measurements every 30 seconds.

Quantification of the crude fucoidan (OEWA-00039) gave an average result of 46.5 ±5.3%, as seen in table 14. The highest difference between the parallels were 10,4% (P1 and P2) and the lowest difference was at 3,4% (P1 and P3). The average yield makes for a significantly higher result than observed from the L-fucose col. assay at 28.65 ±0.39%. The result from the heparin col. assay indicates

that it is possibly not as specific as the L-fucose assay, meaning that the dye is binding to contaminants in the sample, thus lowering the accuracy and precision. Another possible explanation could be differences in homogeneity in the fucoidan solution or, more likely, in the one or both of the reagents (S-2732 or FXa) since it is specified they need to be inverted before use.

A lack of precision for the heparin col. assay is observed with a standard deviation that is more than 10 times higher than for the L-fucose assay. The drift checks in figure 40 detected a shift in absorbance of roughly 0.01 for the crude fucoidan, which is small compared to the shift in absorbance measured in the drift check for the heparin col. assay standard curve of 0.1, shown in figure 33, 35 and 37.

It appears that with a lower purity of the fucoidan sample a less precise result is to be expected when quantifying with the heparin col. assay method. In extracts from *L. hyp*., only fucoidan have sulphate groups in its structure. The L-fucose col. assay measured roughly twice as much fucoidan in the fine solution than in the crude solution. The heparin col. assay measured 1.2 times more fucoidan in the fine solution than in the crude solution. The heparin col. assay seems to be less accurate and less specific than the L-fucose col. assay. By comparing the deviation of the fine and crude yield it would appear that for the heparin col. assay, the cruder the solution is, the less accurate the method is.

3.3.4 Improving the standard curve

A new standard curve for the heparin col. assay was made to improve the coefficient of determination and reduce drift. The concentration of fucoidan was doubled, solution 2 table 4, and the volumes of the reagents were quintupled instead of quadrupled to better avoid bubbles. The total volume of the reagents along with their respective concentrations and absorbances for each parallel and series are listed in table 15.

Table 15: Relevant concentrations of fucoidan (≥95%) from solution 2 and their respective absorbances used as an attempt to optimize standardization of heparin col. assay.

Sigma Aldrich fucoidan solution 2 opt. standard curve					
	Serie 1	Serie 2	Serie 3	Serie 4	Serie 5
V (Diluted fucoidan) [ml]	0.75	0.75	0.75	0.75	0.75
C (Fucoidan dilutions) [mg/ml]	2.02	1.8	1.4	1.0	0.6
P1 Absorbance	0.4991	0.5224	0.5281	0.5362	0.5628
P2 Absorbance	0.5613	0.5652	0.5704	0.5800	0.6023

The first parallel of the standard curve can be seen in figure 41. The drift check gave no indications of drift and can be seen in appendix 2.

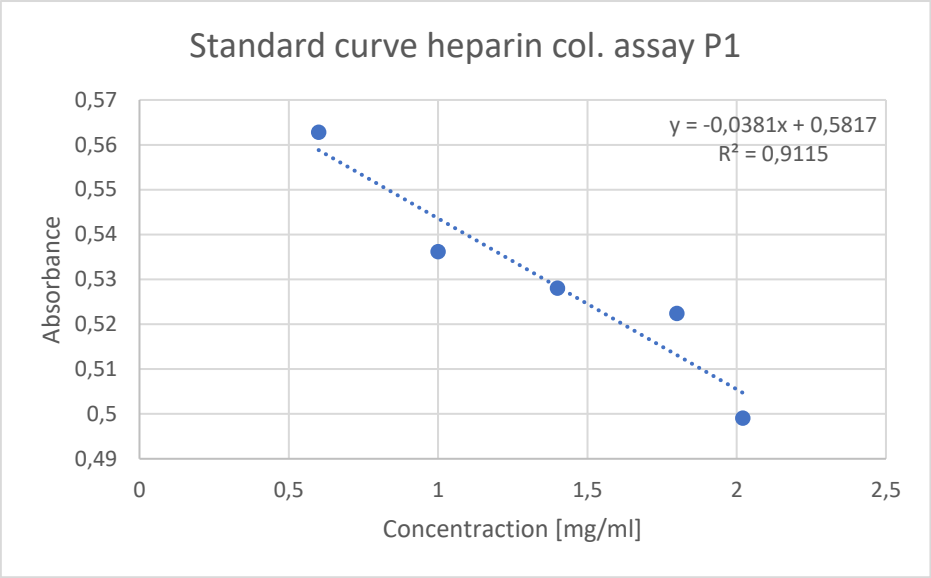

Figure 31: Standard curve with Sigma Aldrich fucoidan solution 2 P1.

The second parallel of the standard curve can be seen in figure 43. The drift check of said parallel gave no drift and can be seen in appendix 2.

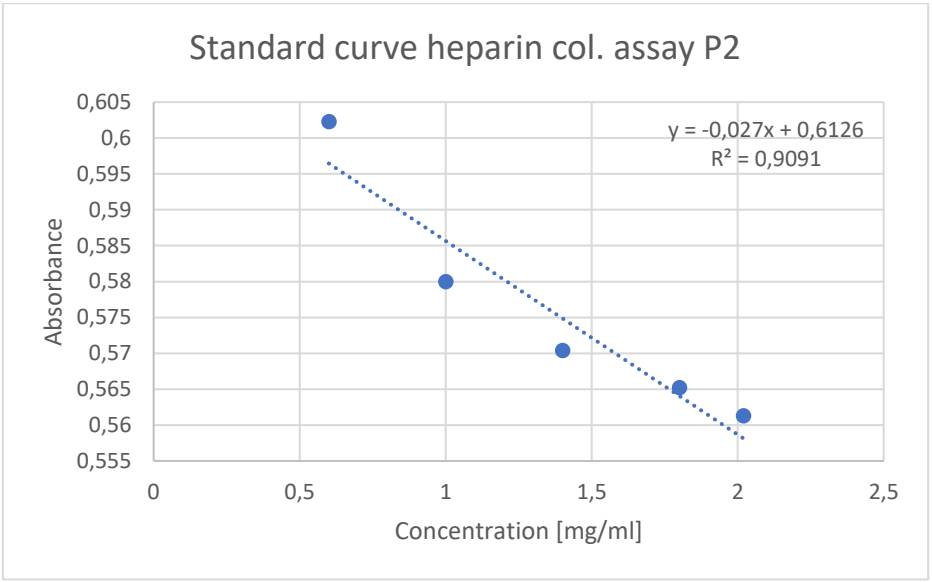

Figure 32: Standard curve with Sigma Aldrich fucoidan solution 2 P2.

A comparison of the two parallels is shown in figure 45.

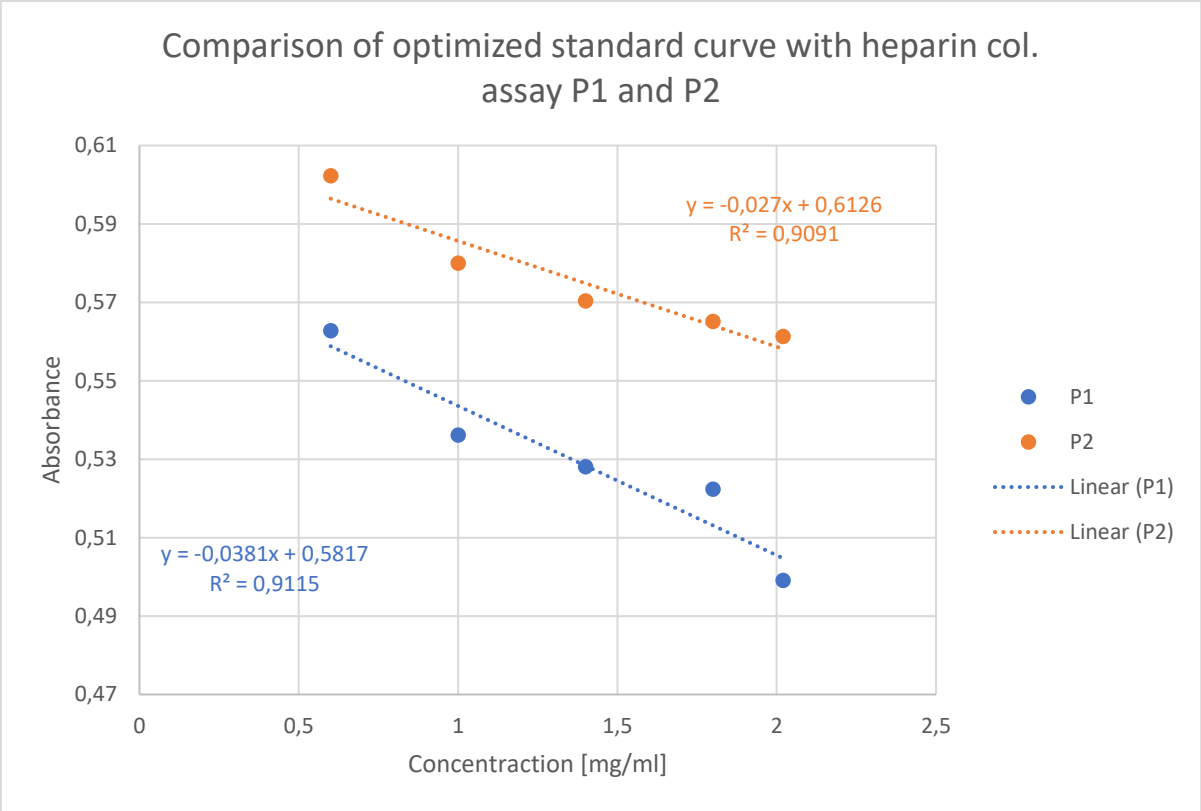

Figure 33: Comparison of standard curves with Sigma Aldrich fucoidan solution 2 P1 and P2.

The experience handling the assays led to an improved standard curve with both R^2 values way above the standard curve used for quantification, as shown in figure 41 and 43. The best parallel in the standard curve used for quantification had a R^2 value at 0,871 while R^2 value for the new standard curve for one of the parallels were at 0,911. Both parallels had no indication of drift, as seen in figure 42 and 44. A comparison of the two parallels is shown in figure 45.

3.3.5 Standardization at room temperature

To see whether the col. assay was affected by operating at room temperature (20°C) instead of 37°C, a third fucoidan solution was made. Solution 3 in table 4 was used and the volumes of the reagents were quintupled to better avoid bubbles. The total volume of the reagents along with their respective concentrations and absorbances for each parallel and series are listed in table 16. One outlier was removed from each parallel because they gave no absorbance, likely due to pipetting mistake.

*Table 16: Relevant concentrations and their respective absorbances for standardization of Sigma Aldrich fucoidan (≥95%) solution 3 with T=293K. *= Outliers.*

Fucoidan standard solution 3 with T=293K					
	Serie 1	Serie 2	Serie 3	Serie 4	Serie 5
V (Diluted fucoidan) [ml]	0.75	0.75	0.75	0.75	0.75
C (Fucoidan dilutions) [mg/ml]	2.20	1.80	1.40	1.00	0.60
P1 Absorbance	0.4806	*	0.4824	0.4866	0.4863
P2 Absorbance	0.4444	0.4444	0.4504	0.4552	*

The first parallel of the standard curve (T=293K) is shown in figure 46. The drift check gave no indications of drift and can be seen in appendix 2.

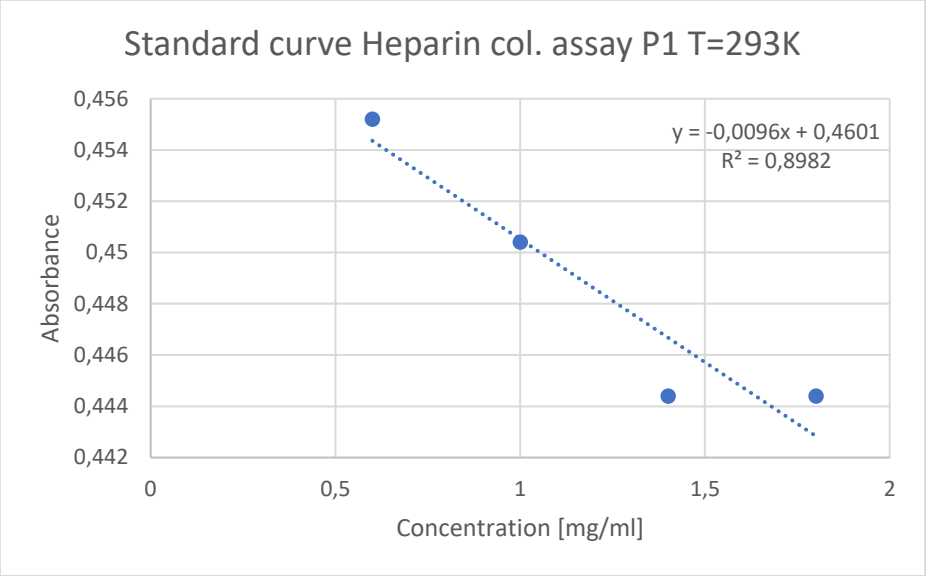

Figure 34: Standard curve with Sigma Aldrich fucoidan solution 3 P1 with room temperature.

The second parallel of the standard curve (T=293K) is shown in figure 48. The drift check gave no indications of drift and can be seen in appendix 2.

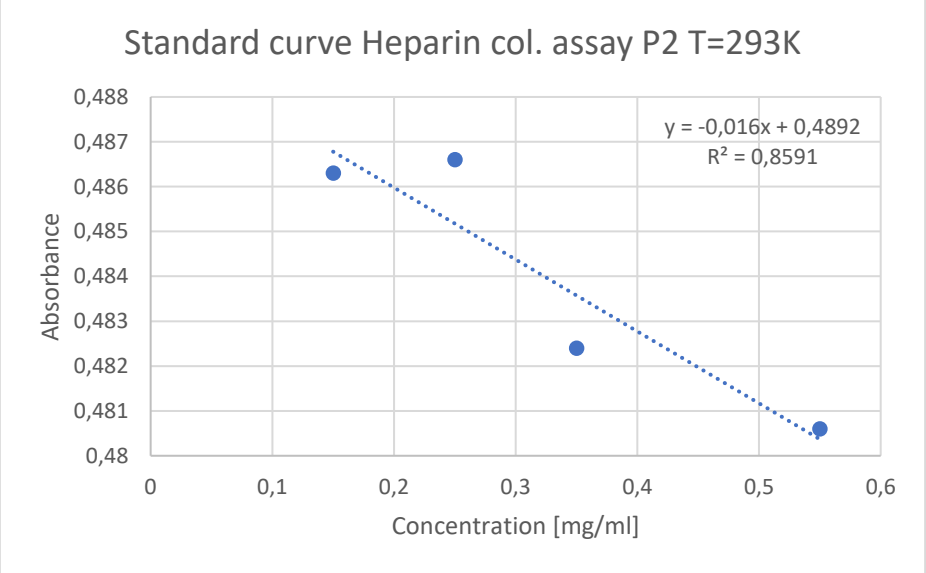

Figure 35: Standard curve with Sigma Aldrich fucoidan solution 3 P2 with room temperature.

A comparison of the two parallels is shown in figure 50.

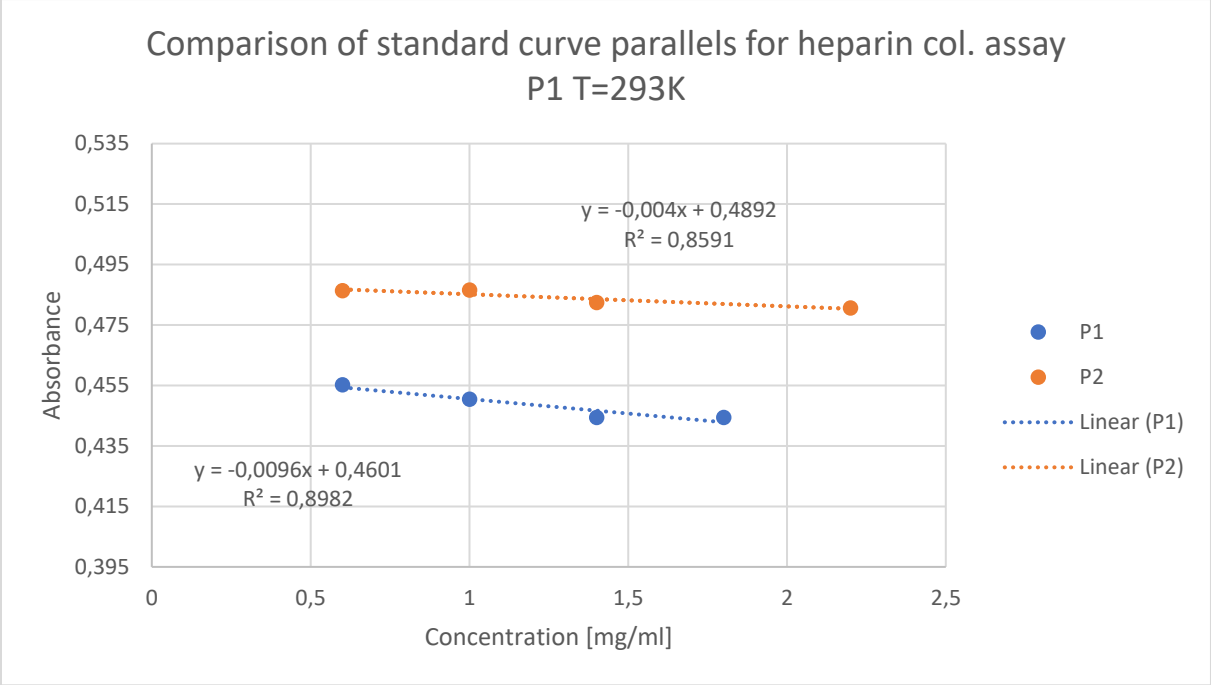

Figure 36: Comparison of standard curves P1 and P2 with T=293K.

A comparison of the standard curve parallels at normal operating temperature (310 K) and room temperature (293 K) is shown in figure 51.

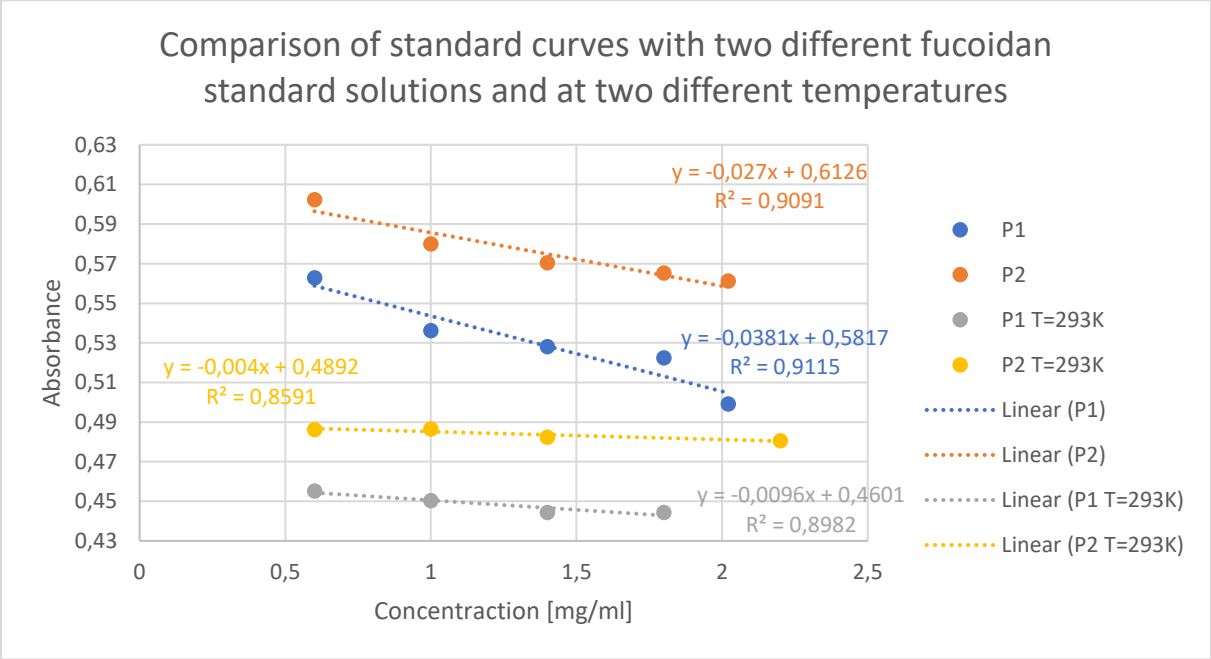

Figure 37: Standard curve comparison of fucoidan solution 2 (P1 and P2) and fucoidan solution 3 performed at room temperature (P1 T=293 K and P2 T=293 K).

From looking at the standard curves in figure 46, 48 and the comparisons in figure 50 and 51, it is evident that the lowered temperature seems to have an impact. The results showed a significant decrease of change in absorbance between the concentrations. The change in absorbance is so small that it is getting close to the limit of detection for the UV-VIS instrument (10^{-4} to 10^{-6}). Almost no drift was detected in either parallel, as seen in figure 47 and 48 in appendix 2. Comparing the improved standard curve with the room temperature standard curve, shown in figure 51, the difference in slope is evident. A higher temperature lets the polysaccharides move more easily around in the solution due to the added energy and thus easier bind to the dye within the 2-minute reaction time. From an article written by Zhao in 2017, it was proclaimed the heparin col. assay was not affected by temperature changes. In other words, theory contradicts the results. It should then be noted that the heparin col. assay is meant to be used with plasma, while in the experiments in this thesis it was used in deionized water. Some of the reagents may not work as intended when used in room temperature without plasma.

More experiments with the heparin col. assay could be performed, however there was a sudden stop from the distributor who delivered the assays, thereby limiting the experiments that could be performed.

3.4 Quantification of fucoidan using the quantitative NMR method

The peaks of interest for L-fucose and to which proton(s) they originate from is shown in figure 52, where calcium formate was used as standard. The same peaks are used when quantifying fucoidan. All NMR spectrums can be seen in appendix 1.

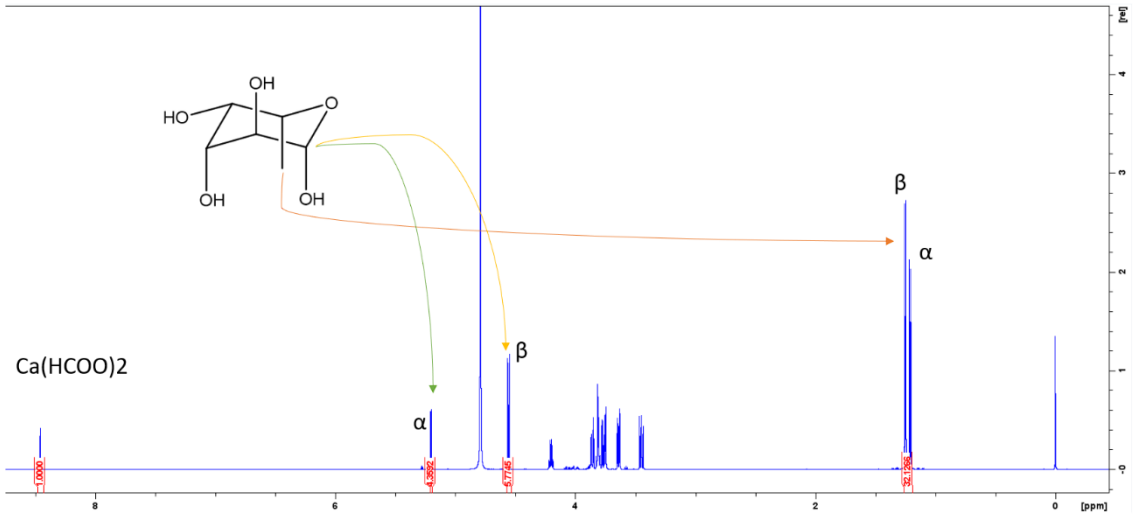

Figure 38: 1H NMR of L-fucose with calcium formate as standard. The alpha and beta C6 proton and the beta and alpha methyl group is highlighted.

To determine which qNMR standard to use for quantification of fucoidan, some consideration is needed. The standard should not react with the analyte, the pH in the solution should not change dramatically since this will change the fucoidan composition, the peaks of the standard should be either between 2-3ppm or -more preferably - further downfield than 6 ppm. The salt potassium phthalate (KHP) was first chosen as the standard. It is a known standard for qNMR and it should not precipitate in the solutions that are analyzed. Though KHP has a pH at 4, which could be problematic for fucoidan, it also gives two proton peaks, one from the two *para* protons and one from the two *meta* protons. If the peak from the *meta* protons and the peak from the *para* protons two peaks are similar, easy to integrate and give similar values, this could indicate that the spectrum has been processed well and integration is done correctly.

Relaxation time (T1) of fucose with, KHP as standard and D2O as solvent, was found to be 4.804 seconds. Proton NMR experiments should be theoretically set to 5 times higher than the T1 value. Since proton experiments are relatively fast it was set to more than 6 times T1 (30 seconds) to ensure the analyte were fully relaxed after each scan.

Integration was done in one of two ways. One way of integrating will be referred to as broad integration in this thesis and is only used as a supplement to the L-fucose standard quantification. This integration was done to see how close to the expected result it is possible to come when integrating all peaks in a broader manor. The other way of integrating had a high focus on similar slope, which is the standard way of integrating peaks in qNMR and was used for quantification of all samples. The broad integration gave results that made sense when quantifying the L-fucose, while sharper integration with higher focus in slope gave results that made sense for fucoidan. Thus, for L-fucose a

broader integration is included for the parallels not considered to be an outlier. Normal integration with high focus on slope is done in all fucoidan qNMR results. The area of the peaks highlighted with red in the table 17 to 25 and their respective concentrations highlighted with yellow, are used with formula (1.2) to calculate L-fucose yield, which is also highlighted in red at the bottom of each table.

3.4.1 qNMR of L-Fucose (≥99.9%) standard

Table 17 shows all relevant parameters to quantitatively determine the amount of a weighed L-fucose standard. The concentration of the internal standard (KHP) and L-fucose is marked in yellow. The area found when integrating the peaks in the spectrum is shown in red. The qNMR yield and deviation is also shown in red.

Table 17: ^{1}H NMR results from Sigma Aldrich L-Fucose (99.9% purity)
Calculation of yield is done using the average calculated concentration of the methyl- and alpha group.

L-Fucose proton NMR with KHP P1 (broad integration)						
	KHP (meta protons)	KHP (para protons)	Methyl group	Beta group	Alpha group meta	L-Fucose
Sigma Aldrich Purity [%]						≥99.9
m [g]	0.0026	0.0026				0.0111
Mw [g/mol]	204.22	204.22				164.16
n [mol]	1.273E-05	1.273E-05				6.762E-05
Sample volume [L]	0.00075	0.00075	0.00075	0.00075	0.00075	0.00075
C [mol/L]	0.01698	0.01698				0.09016
n [protons]	2	2	3	1	1	
Area in spectrum	1	1.0012	7.5474	1.6522	0.8600	
Factor alfa/beta (source)				0.55	0.45	
Calculated C [mol/L]			0.08541		0.0649	
Std. Deviation for calc. C					0.0145	
Average C [mol/L]						0.07515
Calculated m [g]						0.00925
qNMR yield [%]						83.4
Deviation in C [%]						16.65

The yield, highlighted in red in table 17, varies substantially on the integration of the peaks, also highlighted in red, and the areas can be difficult to integrate similarly. This should be put into consideration when evaluating the yield. The qNMR results of broad integration of KHP and L-fucose

(≥99.9%) standard in D2O gave a relatively high average deviation of 16.65% from the expected L-fucose yield. The deviation is likely caused by overlapping peaks in for the alpha and beta methyl groups.

In hopes of having less overlapping alpha and beta methyl peaks and lowering the average deviation at least below 10%, a parallel with the qNMR standard calcium formate was tested. Calcium formate is a salt that gives only one peak in the spectrum, it does not precipitate in solution and has the advantage of not lowering the pH like KHP. Broad integration of the peaks gave once again the lowest deviation. After the initial parallel with calcium formate, two more parallels were taken. Since calcium formate is the standard that is used later, both ways of integrating are shown for comparison.

Table 18 shows all relevant parameters for the first parallel to quantitatively determine the amount of a weighed L-fucose standard with calcium formate. The concentration of the internal standard (calcium formate) and L-fucose is marked in yellow. The area found when integrating the peaks in the spectrum is shown in red. The qNMR yield and deviation is also shown in red.

Table 18: ^{1}H NMR results from Sigma Aldrich L-Fucose (99.9% purity)
Calculation of yield is done using the average calculated concentration of the methyl- and alpha group.

L-Fucose standard proton NMR P1					
	$Ca(HCOO)_2$	Methyl group	Beta group	Alpha group	L-Fucose
Sigma Aldrich Purity [%]					≥99.9
m [g]	0.0005				0.0114
Mw [g/mol]	130.11				164.16
n [mol]	3.8429E-06				6.944E-05
Sample volume [L]	0.00075	0.00075	0.00075	0.00075	0.00075
C [mol/L]	0.00512				0.09259
n [protons]	2	3	1	1	
Area in spectrum	1	32.1266	5.7745	4.3592	
Factor alfa/beta (source)			0.55	0.45	
Calculated C [mol/L]		010974		0.0993	
Std. Deviation for calc. C				0.0074	
Average C [mol/L]					0.10451
Calculated m [g]					0.01287
qNMR yield [%]					112.9
Deviation in C [%]					12.87

Integration with high focus on slope gave a deviation of 12.87% at best when using calcium formate.

Table 19 shows a broad integration of the first qNMR parallel with calcium formate.

Table 19: ^{1}H NMR results from Sigma Aldrich L-Fucose (99.9% purity) with broad integration
Calculation of yield is done using the average calculated concentration of the methyl- and alpha group.

L-Fucose standard proton NMR P1 (broad integration)					
	$Ca(HCOO)_2$	Methyl group	Beta group	Alpha group	L-Fucose
Sigma Aldrich Purity [%]					≥99.9
m [g]	0.0005				0.0114
Mw [g/mol]	130.11				164.16
n [mol]	3.8429E-06				6.94E-05
Sample volume [L]	0.00075	0.00075	0.00075	0.00075	0.00075
C [mol/L]	0.00512				0.09259
n [protons]	2	3	1	1	
Area in spectrum	1	30.7884	5.7745	4.1152	
Factor alfa/beta (source)			0.55	0.45	
Calculated C [mol/L]		0.10517		0.0937	
Std. Deviation for calc. C				0.0081	
Average C [mol/L]					0.09944
Calculated m [g]					0.01224
qNMR yield [%]					107.4
Deviation in C [%]					7.40

The broad integration gave results closer to what was expected for the L-fucose standard. Using calcium formate as standard, the broad integration method had a lower deviation at 7.40% compared to the normal integration at 12.87% for the first parallel, shown in table 18 and 19.

Table 20 shows all relevant parameters for the second parallel to quantitatively determine the amount of a weighed L-fucose standard with calcium formate.

Table 20: ^{1}H NMR results from Sigma Aldrich Fucose (99.9% purity)
Calculation of yield using the average calculated concentration of the methyl- and alpha group.

L-Fucose standard proton NMR P2					
	$Ca(HCOO)_2$	Methyl group	Beta group	Alpha group	L-Fucose
Sigma Aldrich Purity [%]					≥99.9
m [g]	0.0009				0.0029
Mw [g/mol]	130.11				164.16
n [mol]	6.9172E-06				1.766E-05
Sample volume [L]	0.00075	0.00075	0.00075	0.00075	0.00075
C [mol/L]	0.00922				0.02355
n [protons]	2	3	1	1	
Area in spectrum	1	5.0361		0.566	
Factor alfa/beta (source)				0.45	
Calculated C [mol/L]		0.03097		0.0232	
Std. Deviation for calc. C				0.0055	
Average C [mol/L]					0.02708
Calculated m [g]					0.00333
qNMR yield [%]					115.0
Deviation in C [%]					14.98

Table 21 shows a broad integration of the second qNMR parallel of L-fucose with calcium formate.

Table 21: ^{1}H NMR results from Sigma Aldrich Fucose (99.9% purity) P2 broad integration
Calculation of yield is done using the average calculated concentration of the methyl- and alpha group.

L-Fucose standard proton NMR P2 (broad integration)					
	$Ca(HCOO)_2$	Methyl group	Beta group	Alpha group	L-Fucose
Sigma Aldrich Purity [%]					≥99.9
m [g]	0.0009				0.0029
Mw [g/mol]	130.11				164.16
n [mol]	6.9172E-06				1.766E-05
Sample volume [L]	0.00075	0.00075	0.00075	0.00075	0.00075
C [mol/L]	0.00922				0.02355
n [protons]	2	3	1	1	
Area in spectrum	1	4.5779		0.5727	
Factor alfa/beta (source)				0.45	
Calculated C [mol/L]		0.02815		0.0235	
Std. Deviation for calc. C				0.0033	
Average C [mol/L]					0.02581
Calculated m [g]					0.00318
qNMR yield [%]					109.6
Deviation in C [%]					9.58

Parallel 2 of L-fucose with calcium formate gave higher deviation than P1, as seen in table 20 and 21. Broad integration is, once again, around 5% closer to expected result when integrating in a broad manor for the second parallel.

Table 22 shows all relevant parameters for the third parallel to quantitatively determine the amount of a weighed L-fucose standard with calcium formate. The results are however considered an outlier and no broad integration was performed.

Table 22: ^{1}H NMR results from Sigma Aldrich Fucose (99.9% purity) P3. Calculation of yield is done using the average calculated concentration of the methyl- and alpha group.

L-Fucose standard proton NMR P3, outlier					
	$Ca(HCOO)_2$	Methyl group	Beta group	Alpha group	L-Fucose
Sigma Aldrich Purity [%]					≥99.9
m [g]	0.0016				0.0055
Mw [g/mol]	130.11				164.16
n [mol]	1.2297E-05				3.3504E-05
Sample volume [L]	0.00075	0.00075	0.00075	0.00075	0.00075
C [mol/L]	0.01640				0.04467
n [protons]	2	3	1	1	
Area in spectrum	1	8.0741		1.4453	
Factor alfa/beta (source)			0.55	0.45	
Calculated C [mol/L]		0.08826		0.1053	

Std. Deviation for calc. C	0.0121	
Average C [mol/L]		0.09679
Calculated m [g]		0.01192
qNMR yield [%]		216.7
Deviation in C [%]		116.67

The third parallel shown in table 22 had a spectrum that could not be processed properly and is thus considered an outlier. In general, calcium formate gave a yield closer to what was expected than KHP did.

In addition to possible discrepancies in integration, there is a factor that could have affected the result for L-fucose quantification; the C6 alpha/beta relation. The relation is relevant in L-fucose since it has both C6 alpha and C6 beta protons, while fucoidan has only C6 alpha protons. The alpha/beta relation for L-fucose is theoretically 0.45 when calculating the yield for the alpha group, as described by Francisco Bazerra (Bazerra, 2020). This means that there are 0.45 C6 alpha protons and 0.55 C6 beta protons, added together they make up 1 proton. Calculating the yield of the L-fucose equation 1.2 using only the alpha group, the result needs to be divided by 0.45 to make up for the fact that only the alpha group is being used. Deviations in this factor can have relatively large impacts on the results. A deviation of this factor could be the cause of the deviation observed, giving a result higher than 100%. In which case, the relation (0.45) is too low compared to true value. To exemplify, if the C6 alpha/beta relation was 0.59 instead of 0.45, the result of P1 would be 100.1% instead of 112.9%.

In the fucoidan qNMR experiments it will become evident that the deviation observed in L-fucose qNMR, seen in table 18, does not matter when quantifying fucoidan, table 23, 24 and 25, with the qNMR method.

3.4.2 qNMR analysis of fucoidan standard

As mentioned earlier, fucoidan has no C6 beta protons and the possibly problematic alfa/beta ratio is not an issue when quantifying fucoidan. In table 23 the fucoidan standard is quantified with qNMR using calcium formate.

Table 23: qNMR of Fucoidan standard from Fucus vesiculosus ≥95%
**= 95% purity was assumed when fucoidan was weighed in for quantification*

Fucoidan standard						
	Ca(HCOO)2	Methyl group	Beta group	Alpha group	L-Fucose	Fucoidan
Sigma Aldrich Purity [%]						≥95
m [g]	0.0008					0.0051
Mw [g/mol]	130.11				164.16	370.266

Fucose/Fucoidan factor					0.4434	0.4434
n [mol]	6.15E-06				3.11E-05	1.38E-05
Sample volume [L]	0.00075	0.00075	0.00075	0.00075	0.00075	0.00075
C [mol/L]	0.00820				0.04142	0.01837
n [protons]	2	3	1	1		
Area in spectrum	1	4.5146	0	0.7056		
Factor alfa/beta (source)			0.55	0.45		
Calculated C [mol/L]		0.024674		0.01157		
Std. Deviation for calc. C				0.00927		
Average C [mol/L]				0.01812		
Calculated m [g]						0.0050
qNMR Yield [%]						98.7
L-fucose col. assay yield [%]						98.0*
Deviation yield [%]						0.7%*

The fucoidan (≥95%) standard from *F. ves.* had a qNMR yield of 98.7%, as seen marked in red in table 23 and the L-fucose col. assay is highlighted in green along with the deviation between the two methods. For the qNMR method, the fucoidan standard was weighed in without the assumption of 95% purity as was with the L-fucose col. assay. Thus, comparing the qNMR result and the L-fucose col. assay result, it is important to remember that when quantifying with the L-fucose col. assay the fucoidan was weighed in assuming it was 95% clean, which then gave a 98% yield, while the qNMR is weighed in without assuming the fucoidan is 95% clean. This means that if the qNMR method is correct and the fucoidan standard is indeed 98.7%, the L-fucose col. assay result should in fact be slightly lower than 98.0%.

The yield from the L-fucose col. assay, where 95% purity was assumed, was 98%, giving a deviation to qNMR of 0.7%. The broad qNMR integration gave a lower yield at 95.6% and thus a deviation of 2.4% to the L-fucose col. assay. Integration with focus on slope is more accurate for fucoidan while broad integration is more accurate for L-fucose.

3.4.3 qNMR of fine fucoidan (OEWA-00289) sample

In table 24 the fine fucoidan from Alginor is quantified with qNMR using calcium formate.

Table 24: qNMR of the fine fucoidan from Alginor.

Fucoidan Fine solution						
	Ca(HCOO)2	Methyl group	Beta group	Alpha group	L-Fucose	Fucoidan
m [g]	0.0028					0.0045

Mw [g/mol]	130.11				164.16	370.266
Fucose/Fucoidan factor					0.4434	0.4434
n [mol]	2.152E-05				2.741E-05	1.215E-05
Sample volume [L]	0.00075	0.00075	0.00075	0.00075	0.00075	0.00075
C [mol/L]	0.02869				0.03655	0.01620
n [protons]	2	3	1	1		
Area in spectrum	1	0.663	0	0.1		
Factor alfa/beta (source)			0.55	0.45		
Calculated C [mol/L]		0.01268		0.00574		
Std. Deviation for calc. C				0.00491		
Average C [mol/L]				0.00921		
Calculated m [g]						0.0026
qNMR yield [%]						56.8
L-fucose col. assay yield [%]						57.1
Deviation in yield [%]						0.26

The fine Alginor fucoidan had a qNMR yield of 56.8% while the L-fucose col. assay had an average of 57.1%, giving an average deviation of 0.3%. It appears that qNMR and L-fucose col. assay are almost identical when quantifying solutions with little contamination.

3.4.4 qNMR of crude fucoidan (OEWA-00038) sample

In table 25 the crude fucoidan from Alginor is quantified with qNMR using calcium formate.

Table 25: qNMR of the crude fucoidan from Alginor.

Fucoidan Crude solution						
	Ca(HCOO)2	Methyl group	Beta group	Alpha group	L-Fucose	Fucoidan
m [g]	0.0015					0.0014
Mw [g/mol]	130.11				164.16	370.266
Fucose/Fucoidan factor					0.4434	0.4434
n [mol]	1.153E-05				8.527E-06	3.781E-06
Sample volume [L]	0.00075	0.00075	0.00075	0.00075	0.00075	0.00075
C [mol/L]	0.01537				0.01137	0.00504
n [protons]	2	3	1	1		
Area in spectrum	1	0.1963	0	0.0441		
Factor alfa/beta (source)			0.55	0.45		
Calculated C [mol/L]		0.00201		0.00136		
Std. Deviation for calc. C				0.00046		
Average C [mol/L]				0.00168		
Calculated m [g]						0.0005

qNMR yield [%]	33.4
L-fucose col. assay yield [%]	28.65
Deviation in yield [%]	4.75

The crude Alginor fucoidan gave a qNMR yield of 33.4%. This leaves a deviation of 4.75% to the L-fucose yield which was 28.65%. From the spectrum in appendix 3 it is evident that there is more contamination in the crude fucoidan than in the fine fucoidan. The crude qNMR spectrums are more difficult to integrate and are thus susceptible to contamination in the same area as the C6 alpha proton and the methyl group. This could lead to lower quantification accuracy and precision. The deviation between the col. assay and qNMR is higher for the crude fucoidan than the fine fucoidan, and it is perhaps more likely this is due to qNMR being more accurate in quantifying fucoidan than the L-fucose col. assay. When looking at the quantification of the Sigma Aldrich fucoidan standard, an assumption of 95% purity was taken, resulting in a yield of 98%. The same assumption was not done when quantifying the fucoidan standard with qNMR, which gave a yield of 98.7%. With this is mind, it is more likely that the qNMR yield is closer to true value. Especially when determining the yield of the fucoidan standard.

Chapter 4 – Conclusion and further work

The established L-fucose col. assay method of quantifying fucoidan seem to have relatively high accuracy and precision when enough time is spent hydrolyzing the polysaccharide into L-fucose units. Quantification of fucoidan by qNMR and heparin col. assay were introduced. Both methods were successful in quantifying fucoidan to varying degrees. The hypothesis is thus confirmed, heparin colorimetric assays can indeed quantify fucoidan to some extent. A compact table showing the average yield of the different methods is shown in table 26. The qNMR method seems to be highly accurate when quantifying the fucoidan samples. If quantification of the fucoidan standard with qNMR (98.7%) is the true fucoidan purity, it means that the assumption made when quantifying the fucoidan standard using the L-fucose col. assay, weighing in fucoidan based on 95% purity, is slightly incorrect. Thus, the L-fucose col. assay result from the fucoidan standard should in fact be slightly lower than the calculated yield (<98.0%).

Quantifying the fine fucoidan (OEWA-00289), the qNMR method gave a result almost identical to the L-fucose col. assay, as seen in table 26. For the crude fucoidan (OEWA-00038), qNMR gave a higher yield than the L-fucose col. assay, as seen in table 26. The crude fucoidan gives a more contaminated spectrum which could have an impact when integrating the peaks of interest. Additionally, it is likely that the hydrolyzation performed to break the polymer into L-fucose units also removes many of the impurities in the solution. It is however likely that qNMR becomes more accurate than the L-fucose col. assay the more filtered the solution is. Giving each method their respective strength.

*Table 26: Summary of the average results from the quantification methods. *= 95% purity was assumed during weighing.*

Quantification method	Fucoidan standard	Fine fucoidan	Crude fucoidan
L-fucose col. assay yield [%] (48-hh)	*98.0 ±0.17	57.1 ±0.7	28.65 ±0.4
Heparin col. assay yield [%]	x	57.6 ±3.4	46.5 ±5.3
qNMR yield [%]	98.7	56.8	33.4

The accuracy of the heparin col. assay is high for the fine fucoidan solution, with an average yield almost identical to the two other methods. However, the precision is lower with a standard deviation that is five times larger than the standard deviations of the L-fucose col. assay. With cruder, more contaminated fucoidan solutions, the precision of the L-fucose col. assay remains, while it falters for the heparin col. assay. The heparin col. assay gave a higher yield than both qNMR and L-fucose, which may suggest that the heparin method is more affected by contaminants in the crude fucoidan. In contrast to results from Zhao (Zhao, 2018), the heparin col. assay also seems to be affected by temperature change, as seen from the standard curve that was made in room temperature. The

difference may however be subject to the modification of the heparin col. assay, using samples in water without plasma.

A table of the advantages and disadvantages of the methods explored in the thesis is shown in table 27.

Table 27: Advantages and disadvantages of the methods explored.

Method	Advantages	Disadvantages
L-fucose col. assay	• Removes impurities during hydrolyzation. • Relatively accurate in solutions of varying purity. • High accuracy • Reliable proven method • Easy procedure	• Time consuming hydrolyzation and pH neutralization steps. • More energy required
Heparin col. assay	• Fast direct method • Seemingly accurate for more filtered solutions • Can be mechanized for higher accuracy • Potential to be more accurate if the method is optimized	• Unproven method • Hard procedure that is prone to human error • Acetic acid can easily form bubbles in cuvettes. • Unreliable in crude solutions
qNMR	• Fast • Reliable proven method • High accuracy in filtered solutions	• Contaminants may lead to integration errors • Expensive apparatus

Companies that aim to make use of seaweeds with high fucoidan content will always need methods to quantify the valuable content from their raw material. The heparin col. assay and qNMR method appears to be suitable methods of doing so. Both methods are direct ways of quantifying fucoidan, which means they are exceptionally faster than L-fucose col. assay. Several time-consuming steps such as hydrolyzation, filtration and pH neutralization are superfluous. These two direct methods would lead to a quicker way of determining the amount of fucoidan from extracts. However, it is likely that

only the heparin col. assay would be competitive to the L-fucose in terms of costs. Although qNMR seems like a solid method of quantifying polysaccharides, not all industries have easy access to it.

Companies, such as Alginor, that aim for total utilization of fucoidan rich seaweeds, could already benefit from the heparin col. assay method of quantification for the more filtered fucoidan, and furthermore if the method is optimized. The heparin col. assay, and possibly also qNMR, is however not as accurate when quantifying cruder fucoidan. To summarize, the cruder the fucoidan solution is the more viable the L-fucose col. assay is due to the hydrolyzation step. The more filtered the solution is the more viable the direct methods are.

Further research should aim to optimize the heparin col. assay for quantification of fucoidan. Increasing the precision and accuracy of the col. assay should be top priority. In that regard, experiments that determine the effect of temperature, reaction time, and fucoidan origin should be done. Standardization could be done with fucoidan standards from a different seaweed species that are already on the market such as *Macrocystis pyrifera*, or preferably from *L. hyp.* if it is available. Increasing reaction times above 2 minutes would give the reagent dye more time to bind itself to the sulphate groups, possibly leading to higher accuracy and precision. Performing quantification with different temperatures could influence how easily the dye binds itself to the sulphate groups and should be tested further, also in combination with different reaction times. It would also be interesting to see at what extent the degree of sulphation matters to the standardization and quantification of the heparin col. assay. Especially since the fucoidan used to standardize the heparin col. assay is expected to have a much lower sulphation degree than fucoidan from *L. hyp.*

Sources

1. Abels, K., Salvo-Halloran, E. M., White, D., Ali, M., Agarwal, N. R., Leung, V., Ali, M., Sidawi, M., Capretta, A., Brennan, J. D., Nease, J., & Filipe, C. D. M. (2021). Quantitative Point-of-Care Colorimetric Assay Modeling Using a Handheld Colorimeter. *ACS Omega*, *6*, 21. https://pubs.acs.org/doi/10.1021/acsomega.1c03460
2. Ahmad, T., B., S., Vårum, K. Mm, (2015). *Methods for quantification and extraction of fucoidan, and quantification of the release of total carbohydrate and fucoidan from the brown algae Laminaria hyperborean.* https://ntnuopen.ntnu.no/ntnu-xmlui/bitstream/handle/11250/2351634/10566_FULLTEXT.pdf?sequence=1
3. Ale, M. T., & Meyer, A. S. (2013). Fucoidans from brown seaweeds: an update on structures, extraction techniques and use of enzymes as tools for structural elucidation. *RSC Advances*, *3*(22), 8131–8141. https://doi.org/10.1039/C3RA23373A
4. *Algaebase: Listing the World's Algae*. Retrieved December 22, 2021, from https://www.algaebase.org/search/species/
5. *Alginate - an overview | ScienceDirect Topics*. Retrieved May 4, 2022, from https://www.sciencedirect.com/topics/materials-science/alginate
6. *Alginate Uses in Industry |ArtMolds*. Retrieved February 4, 2022, from https://www.artmolds.com/alginate-industrial-uses
7. Anastyuk, S. D., Shevchenko, N. M., Nazarenko, E. L., Imbs, T. I., Gorbach, V. I., Dmitrenok, P. S., & Zvyagintseva, T. N. (2010). Structural analysis of a highly sulfated fucan from the brown alga Laminaria cichorioides by tandem MALDI and ESI mass spectrometry. Carbohydrate Research, 345(15), 2206–2212. https://doi.org/10.1016/J.CARRES.2010.07.043
8. Angra, V., Sehgal, R., Kaur, M., & Gupta, R. (2021). Commercialization of bionanocomposites. *Bionanocomposites in Tissue Engineering and Regenerative Medicine*, 587–610. https://doi.org/10.1016/B978-0-12-821280-6.00017-9
9. Ardiana, N. A., & Husni, A. (2020). The impact of temperature on the antioxidant activity of fucoidan obtained from brown seaweed Sargassum hystrix extracted using EDTA. 13(6). http://www.bioflux.com.ro/docs/2020.3743-3753.pdf
10. Assis, J., Fragkopoulou, E., Frade, D., Neiva, J., Oliveira, A., Abecasis, D., Faugeron, S., & Serrão, E. A. (2020). A fine-tuned global distribution dataset of marine forests. *Scientific Data 2020 7:1*, *7*(1), 1–9. https://doi.org/10.1038/s41597-020-0459-x
11. Balboa, E. M., Conde, E., Moure, A., Falqué, E., & Domínguez, H. (2013). In vitro antioxidant properties of crude extracts and compounds from brown algae. *Food Chemistry*, *138*(2–3), 1764–1785. https://doi.org/10.1016/J.FOODCHEM.2012.11.026

12. Baraniraj, T., Philominathany, P., & Vijayanz, N. (2007). Growth and characterization of nonlinear optical para-nitroaniline (pNA) single crystals. *Modern Physics Letters B*, *21*(29), 2025–2032. https://doi.org/10.1142/S021798490701436X
13. Berteau, O., & Mulloy, B. (2003). Sulfated fucans, fresh perspectives: structures, functions, and biological properties of sulfated fucans and an overview of enzymes active toward this class of polysaccharide. Glycobiology, 13(6), 29R-40R. https://doi.org/10.1093/GLYCOB/CWG058
14. Beutler, J. A., McKee, T. C., Fuller, R. W., Tischler, M., Cardellina, J. H., Snader, K. M., McCloud, T. G., & Boyd, M. R. (1993). Frequent occurrence of HIV-inhibitory sulphated polysaccharides in marine invertebrates. *Antiviral Chemistry and Chemotherapy*, *4*(3), 167–172. https://doi.org/10.1177/095632029300400306
15. Bezerra, F. F., Vignovich, W. P., Aderibigbe, A. O. O., Liu, H., Sharp, J. S., Doerksen, R. J., & Pomin, V. H. (2020). Conformational properties of l-fucose and the tetrasaccharide building block of the sulfated l-fucan from Lytechinus variegatus. *Journal of Structural Biology*, *209*(1). https://doi.org/10.1016/J.JSB.2019.107407
16. Bilan, M. I., Grachev, A. A., Shashkov, A. S., Thuy, T. T. T., Thanh Van, T. T., Ly, B. M., Nifantiev, N. E., & Usov, A. I. (2013). Preliminary investigation of a highly sulfated galactofucan fraction isolated from the brown alga Sargassum polycystum. *Carbohydrate Research*, *377*, 48–57. https://doi.org/10.1016/J.CARRES.2013.05.016
17. Biology of the *macrocystis* resource in North America. (n.d.). Retrieved December 21, 2021, from https://www.fao.org/3/x5819e/x5819e0a.htm
18. Bohn, J. A., & BeMiller, J. N. (1995). (1→3)-β-d-Glucans as biological response modifiers: a review of structure-functional activity relationships. *Carbohydrate Polymers*, *28*(1), 3–14. https://doi.org/10.1016/0144-8617(95)00076-3
19. Brauder C*., CCGP — Macrocystis pyrifera (Giant Kelp)*. (n.d.). Retrieved January 28, 2022, from https://www.ccgproject.org/species/macrocystis-pyrifera-giant-kelp
20. Burbach, R. (2016). *Certificate of Analysis of crude fucoidan from fucus vesiculosus*. Sigma Aldrich. https://www.sigmaaldrich.com/certificates/COFA/F5/F5631/F5631-BULK_____SLBQ5071V_.pdf
21. Bürki, S., Brand, B., Escher, R., Wuillemin, W. A., & Nagler, M. (2018). Accuracy, reproducibility and costs of different laboratory assays for the monitoring of unfractionated heparin in clinical practice: a prospective evaluation study and survey among Swiss institutions. *BMJ Open*, *8*(6). https://doi.org/10.1136/BMJOPEN-2018-022943
22. Buschmann, A. H., Camus, C., Infante, J., Neori, A., Israel, Á., Hernández-González, M. C., Pereda, S. V., Gomez-Pinchetti, J. L., Golberg, A., Tadmor-Shalev, N., & Critchley, A. T. (2017).

Seaweed production: overview of the global state of exploitation, farming and emerging research activity. https://doi.org/10.1080/09670262.2017.1365175

23. Carvalho, G., L., Mcdougall, Gordon (2014). *(PDF) Laminaria hyperborea: Polysaccharide profiling and mapping.* (n.d.). https://www.researchgate.net/publication/309211208_Laminaria_hyperborea_Polysaccharide_profiling_and_mapping
24. Castaing, T., Bouillaud, D., Farjon, J., & Giraudeau, P. (2021). *Recent advances in benchtop NMR and its applications*. https://www.researchgate.net/publication/350177688_Recent_advances_in_benchtop_NMR_spectroscopy_and_its_applications
25. Chen, H., Cong, Q., Du, Z., Liao, W., Zhang, L., Yao, Y., & Ding, K. (2016). Sulfated fucoidan FP08S2 inhibits lung cancer cell growth in vivo by disrupting angiogenesis via targeting VEGFR2/VEGF and blocking VEGFR2/Erk/VEGF signaling. Cancer Letters, 382(1), 44–52. https://doi.org/10.1016/J.CANLET.2016.08.020
26. Chizhov, A. O., Dell, A., Morris, H. R., Reason, A. J., Haslam, S. M., McDowell, R. A., Chizhov, O. S., & Usov, A. I. (1998). Structural analysis of laminarans by MALDI and FAB mass spectrometry. *Carbohydrate Research*, *310*(3), 203–210. https://doi.org/10.1016/S0008-6215(98)00177-3
27. Chollet, L., Sabboural, P., Chauvierre, C., Villemin, J. N., Letourneur, D., Chaubet, F., & Laurienzo, P. (2016). Fucoidans in Nanomedicine. *Marine Drugs 2016, Vol. 14, Page 145*, *14*(8), 145. https://doi.org/10.3390/MD14080145
28. Chromogenix: Monitoring Heparin Therapy – A Role For The Chromogenic Anti-Factor Xa Assay Heparin. (1999). https://diapharma.com/wp-content/uploads/2016/01/K823393_K255539_Chromogenix_Monograph_Heparin.pdf
29. Chynoweth, D. P., Fannin, K. F., & Srivastava, V. J. (1987). Biological gasification of marine algae. *Developments in Aquaculture and Fisheries Science (Netherlands)*, 285–303. http://agris.fao.org/agris-search/search.do?recordID=NL8 80126188
30. *Colorimetry - an overview | ScienceDirect Topics*. Last accessed May 12, 2022, from https://www.sciencedirect.com/topics/medicine-and-dentistry/colorimetry
31. Cumashi, A., Ushakova, N. A., Preobrazhenskaya, M. E., D'Incecco, A., Piccoli, A., Totani, L., Tinari, N., Morozevich, G. E., Berman, A. E., Bilan, M. I., Usov, A. I., Ustyuzhanina, N. E., Grachev, A. A., Sanderson, C. J., Kelly, M., Rabinovich, G. A., Iacobelli, S., & Nifantiev, N. E. (2007). A comparative study of the anti-inflammatory, anticoagulant, antiangiogenic, and antiadhesive activities of nine different fucoidans from brown seaweeds. *Glycobiology*, *17*(5), 541–552. https://doi.org/10.1093/GLYCOB/CWM014

32. Cunha, L., & Grenha, A. (2016). Sulfated Seaweed Polysaccharides as Multifunctional Materials in Drug Delivery Applications. *Marine Drugs 2016, Vol. 14, Page 42*, *14*(3), 42. https://doi.org/10.3390/MD14030042
33. De Caro, C. A., (2015). *(PDF) UV-VIS Spectrophotometry - Fundamentals and Applications*. (n.d.). Retrieved March 3, 2022, from https://www.researchgate.net/publication/321017142_UVVIS_Spectrophotometry_-_Fundamentals_and_Applications
34. De Souza, A., C. (2017). Quantification of Food Polysaccharides by means of NMR. *Modern Magnetic Resonance*, 1–19. https://doi.org/10.1007/978-3-319-28275-6_5-1
35. Delwiche C. F. (2007). *Algae in the warp and weave of life: Bound by plastids | Request PDF*. (n.d.). Retrieved December 22, 2021, from https://www.researchgate.net/publication/287013415_Algae_in_the_warp_and_weave_of_life_Bound_by_plastids
36. Diffey, B. L. (2002). Sources and measurement of ultraviolet radiation. *Methods*, *28*(1), 4–13. https://doi.org/10.1016/S1046-2023(02)00204-9
37. Dodson, J. R., Budarin, V. L., Hunt, A. J., Shuttleworth, P. S., & Clark, J. H. (2013). Shaped mesoporous materials from fresh macroalgae. *Journal of Materials Chemistry A*, *1*(17), 5203–5207. https://doi.org/10.1039/C3TA10568G
38. Farndale, R. W., Buttle, D. J., & Barrett, A. J. (1986). Improved quantitation and discrimination of sulphated glycosaminoglycans by use of dimethylmethylene blue. *Biochimica et Biophysica Acta*, *883*(2), 173–177. https://doi.org/10.1016/0304-4165(86)90306-5
39. Fitton, J. H., Stringer, D. N., & Karpiniec, S. S. (2015). Therapies from Fucoidan: An Update. *Marine Drugs 2015, Vol. 13, Pages 5920-5946*, *13*(9), 5920–5946. https://doi.org/10.3390/MD13095920
40. Food and Agriculture Organization of the United Nations (FAO) (2018). The state of world fisheries and aquaculture- Meeting the Sustainable Development Goals. License; Rome, Italy: 2018. CC BY-NC-SA 3.0 IGO https://scholar.google.com/scholar_lookup?title=The+State+of+World+Fisheries+and+Aquaculture+2018%E2%80%94Meeting+the+Sustainable+Development+Goals&publication_year=2018&
41. Geiselman, J. A., & McConnell, O. J. (1981). Polyphenols in brown algae Fucus vesiculosus and Ascophyllum nodosum: Chemical defenses against the marine herbivorous snail, Littorina littorea. *Journal of Chemical Ecology 1981 7:6*, *7*(6), 1115–1133. https://doi.org/10.1007/BF00987632

42. *Goal 14 | Department of Economic and Social Affairs*. (n.d.). Retrieved January 2, 2022, from https://sdgs.un.org/goals/goal14
43. *Goal 14: Life Below Water | The Global Goals*. (n.d.). Retrieved January 2, 2022, from https://www.globalgoals.org/14-life-below-water
44. Graham, L. K. E., & Wilcox, L. W. (2000). The origin of alternation of generations in land plants: A focus on matrotrophy and hexose transport. *Philosophical Transactions of the Royal Society B: Biological Sciences*, *355*(1398), 757–767. https://doi.org/10.1098/RSTB.2000.0614
45. Grauffel, V., Kloareg, B., Mabeau, S., Durand, P., & Jozefonvicz, J. (1989). New natural polysaccharides with potent antithrombic activity: fucans from brown algae. *Biomaterials*, *10*(6), 363–368. https://doi.org/10.1016/0142-9612(89)90127-0
46. Guiry, M. D. (2012). *PERSPECTIVE HOW MANY SPECIES OF ALGAE ARE THERE? 1*. https://doi.org/10.1111/j.1529-8817.2012.01222.x
47. Hurd, C. L., Harrison, P. J., Bischof, K., & Lobban, C. S. (2014). Seaweed ecology and physiology, second edition. *Seaweed Ecology and Physiology, Second Edition*, 1–551. https://doi.org/10.1017/CBO9781139192637
48. Hwang, P. A., Phan, N. N., Lu, W. J., Hieu, B. T. N., & Lin, Y. C. (2016). Low-molecular-weight fucoidan and high-stability fucoxanthin from brown seaweed exert prebiotics and anti-inflammatory activities in Caco-2 cells. *Food & Nutrition Research*, *60*. https://doi.org/10.3402/FNR.V60.32033
49. *JEOL: What is qNMR (quantitative NMR)? | Applications | JEOL Ltd.* Retrieved March 27, 2022, from https://www.jeol.co.jp/en/applications/detail/1286.html
50. Justin Tom (2021). *UV-Vis Spectroscopy: Principle, Strengths and Limitations and Applications | Technology Networks*. (n.d.). Last accessed March 3, 2022, https://www.technologynetworks.com/analysis/articles/uv-vis-spectroscopy-principle-strengths-and-limitations-and-applications-349865
51. Kain, J. M., & Jones, N. S. (1976). The Biology of Laminaria Hyperborea. VIII. Growth on Cleared Areas. *Journal of the Marine Biological Association of the United Kingdom*, *56*(2), 267–290. https://doi.org/10.1017/S0025315400018907
52. Kasco Marine - Pond & Lake Zone Identification (n.d.). Retrieved December 21, 2021, from https://kascomarine.com/blog/pond-lake-zone-identification/
53. Kopplin, G., Rokstad, A. M., Mélida, H., Bulone, V., Skjåk-Bræk, G., & Aachmann, F. L. (2018). Structural Characterization of Fucoidan from Laminaria hyperborea: Assessment of Coagulation and Inflammatory Properties and Their Structure-Function Relationship. *ACS Applied Biomaterials*, *1*(6), 1880–1892. https://pubs.acs.org/doi/10.1021/acsabm.8b00436

54. Kraan, S. (2013). Mass-cultivation of carbohydrate rich macroalgae, a possible solution for sustainable biofuel production. *Mitigation and Adaptation Strategies for Global Change*, *18*(1), 27–46. https://link.springer.com/article/10.1007/s11027-010-9275-5
55. Kulshreshtha, G., Hincke, M. T., Prithiviraj, B., & Critchley, A. (2020). A review of the varied uses of macroalgae as dietary supplements in selected poultry with special reference to laying hen and broiler chickens. *Journal of Marine Science and Engineering*, *8*(7). https://doi.org/10.3390/JMSE8070536
56. Kusaykin, M., Bakunina, I., Sovo, V., Ermakova, S., Kuznetsova, T., Besednova, N., Zaporozhets, T., & Zvyagintseva, T. (2008). Structure, biological activity, and enzymatic transformation of fucoidans from the brown seaweeds. *Biotechnology Journal*, *3*(7), 904–915. https://doi.org/10.1002/BIOT.200700054
57. Lee, J. M., Shin, Z. U., Mavlonov, G. T., Abdurakhmonov, I. Y., & Yi, T. H. (2012). Solid-phase colorimetric method for the quantification of fucoidan. *Applied Biochemistry and Biotechnology*, *168*(5), 1019–1024. https://doi.org/10.1007/S12010-012-9837-Y
58. L-Fucose Assay Kit Test - *For the measurement of L-Fucose | Megazyme*. (n.d.). Retrieved January 28, 2022, from https://www.megazyme.com/l-fucose-assay-kit Alternative link: https://www.megazyme.com/documents/Assay_Protocol/K-FUCOSE_DATA.pdf
59. Li, B., Lu, F., Wei, X., & Zhao, R. (2008). Fucoidan: structure and bioactivity. *Molecules (Basel, Switzerland)*, *13*(8), 1671–1695. https://doi.org/10.3390/MOLECULES13081671
60. Liu, Q., & Jiao, Q. (2006). Mechanism of Methylene Blue Action and Interference in the Heparin Assay. *31*(5), 913–924. https://doi.org/10.1080/00387019808003271
61. Lorbeer, A. J., Tham, R., & Zhang, W. (2013). Potential products from the highly diverse and endemic macroalgae of Southern Australia and pathways for their sustainable production. *Journal of Applied Phycology 2013 25:3*, *25*(3), 717–732. https://doi.org/10.1007/S10811-013-0003-X
62. Mateos, R., Pérez-Correa, J. R., & Domínguez, H. (2020). Bioactive Properties of Marine Phenolics. *Marine Drugs*, *18*(10). https://doi.org/10.3390/MD18100501
63. Matsubara, K., Xue, C., Zhao, X., Mori, M., Sugawara, T., & Hirata, T. (2005). Effects of middle molecular weight fucoidans on in vitro and ex vivo angiogenesis of endothelial cells. *International Journal of Molecular Medicine*, *15*(4), 695–699. https://doi.org/10.3892/IJMM.15.4.695
64. Meneghetti, M. C. Z., Hughes, A. J., Rudd, T. R., Nader, H. B., Powell, A. K., Yates, E. A., & Lima, M. A. (2015). Heparan sulfate and heparin interactions with proteins. *Journal of The Royal Society Interface*, 12(110). https://doi.org/10.1098/RSIF.2015.0589

65. Mollah, M. Z. I., Zahid, H. M., Mahal, Z., Faruque, M. R. I., & Khandaker, M. U. (2021). The Usages and Potential Uses of Alginate for Healthcare Applications. *Frontiers in Molecular Biosciences*, *8*, 918. https://www.frontiersin.org/articles/10.3389/fmolb.2021.719972/full
66. *Mortensen S., Sustain.no: Species: Cuvie (Laminaria hyperborea)*. (n.d.). Retrieved January 3, 2022, from https://www.miljolare.no/nb/artstre/?or_id=3028
67. Mourao, P. (2005). Use of Sulfated Fucans as Anticoagulant and Antithrombotic Agents: Future Perspectives. *Current Pharmaceutical Design*, *10*(9), 967–981. https://doi.org/10.2174/1381612043452730
68. Nelson, T. E., & Lewis, B. A. (1974). Separation and characterization of the soluble and insoluble components of insoluble laminaran. *Carbohydrate Research*, *33*(1), 63–74. https://doi.org/10.1016/S0008-6215(00)82940-7
69. Nordhaug K. M., Havforskningsinstituttet, (2020). *Mot en ny havnæring for tare? | Havforskningsinstituttet*. Retrieved April 4, 2022, from https://www.hi.no/hi/nettrapporter/fisken-og-havet-2020-5
70. North, W. J., Evaluation, management, and cultivation of *Macrocystis* kelp forests (1978). https://www.osti.gov/servlets/purl/5007205
71. Ozaltin, K., Lehocký, M., Humpolíček, P., Pelková, J., & Sáha, P. (2016). A New Route of Fucoidan Immobilization on Low Density Polyethylene and Its Blood Compatibility and Anticoagulation Activity. *International Journal of Molecular Sciences 2016, Vol. 17, Page 908*, *17*(6), 908. https://doi.org/10.3390/IJMS17060908
72. Pangestuti, R., & Kim, S. K. (2011). Biological activities and health benefit effects of natural pigments derived from marine algae. *Journal of Functional Foods*, *3*(4), 255–266. https://doi.org/10.1016/J.JFF.2011.07.001
73. Piconi, P., Veidenheimer, R., (2020). *Edible Seaweed Market Analysis published by Island Institute - Island Institute*. (2020). Original source: Food and Agriculture Organization of the United Nations (FAO); Globefish Research Program; The Global Status of Seaweed Production, Trade and Utilization; Volume 124; 2018; Pentallect research. https://www.islandinstitute.org/2020/03/03/edible-seaweed-market-analysis/
74. Pozharitskaya, O. N., Shikov, A. N., Faustova, N. M., Obluchinskaya, E. D., Kosman, V. M., Vuorela, H., & Makarov, V. G. (2018). Pharmacokinetic and Tissue Distribution of Fucoidan from Fucus vesiculosus after Oral Administration to Rats. *Marine Drugs*, *16*(4). https://doi.org/10.3390/MD16040132
75. Quantitative NMR (qNMR) | Nuclear Magnetic Resonance (NMR) | [Analytical Chemistry] | Laboratory Chemicals-FUJIFILM Wako Chemicals Europe GmbH. (n.d.). Retrieved March 28,

2022, from https://labchem-wako.fujifilm.com/europe/category/analysis/nmr/qNMR/index.html

76. Ragan, M. A., & Jensen, A. (1979). Quantitative studies on brown algal phenols. III. Light-mediated exudation of polyphenols from Ascophyllum nodosum (L.) Le Jol. *Journal of Experimental Marine Biology and Ecology*, *36*(1), 91–101. https://doi.org/10.1016/0022-0981(79)90102-3
77. Rajauria, G. (2018). Optimization and validation of reverse phase HPLC method for qualitative and quantitative assessment of polyphenols in seaweed. *Journal of Pharmaceutical and Biomedical Analysis*, *148*, 230–237. https://doi.org/10.1016/J.JPBA.2017.10.002
78. Reis, R. L., Neves, N. M., Mano, J. F., Gomes, M. E., Marques, A. P., & Azevedo, H. S. (2008). Natural-based polymers for biomedical applications. In *Natural-Based Polymers for Biomedical Applications*. Elsevier Ltd. https://doi.org/10.1533/9781845694814 Alternative source: https://www.sciencedirect.com/topics/chemistry/heparin
79. Rioux, L. E., Turgeon, S. L., & Beaulieu, M. (2007). Characterization of polysaccharides extracted from brown seaweeds. Carbohydrate Polymers, 69(3), 530–537. https://doi.org/10.1016/J.CARBPOL.2007.01.009
80. Rocha, C. M. R., Genisheva, Z., Ferreira-Santos, P., Rodrigues, R., Vicente, A. A., Teixeira, J. A., & Pereira, R. N. (2018). Electric field-based technologies for valorization of bioresources. *Bioresource Technology*, *254*, 325–339. https://doi.org/10.1016/J.BIORTECH.2018.01.068
81. Rupérez, P., Ahrazem, O., & Leal, J. A. (2002). Potential antioxidant capacity of sulfated polysaccharides from the edible marine brown seaweed Fucus vesiculosus. *Journal of Agricultural and Food Chemistry*, *50*(4), 840–845. https://doi.org/10.1021/JF010908O
82. Ruyck, J., Famerée, M., Wouters, J., Perpète, E. A., Preat, J., & Jacquemin, D. (2007). Towards the understanding of the absorption spectra of NAD(P)H/NAD(P)+ as a common indicator of dehydrogenase enzymatic activity. *Chemical Physics Letters*, *450*(1–3), 119–122. https://doi.org/10.1016/J.CPLETT.2007.10.092
83. Schoenberger, T. (2019). *GUIDELINE FOR qNMR ANALYSIS*. https://www.jeol.co.jp/en/applications/detail/1286.html
84. Seaweed.ie: *Information on marine algae*. (n.d.). Retrieved December 27, 2021, from https://www.seaweed.ie/descriptions/Laminaria_hyperborea.php
85. Seaweed.ie*: Uses and Utilization*. (n.d.). Retrieved January 16, 2022, from https://seaweed.ie/uses_general/
86. Soedjak, H. S. (1994). Colorimetric Determination of Carrageenans and Other Anionic Hydrocolloids with Methylene Blue. *Analytical Chemistry*, *66*(24), 4514–4518. https://pubs.acs.org/doi/10.1021/ac00096a018

87. Soon-Ki Min, Kwon, O. C., Lee, S., Park, K. H., & Kim, J. K. (2012). An Antithrombotic Fucoidan, Unlike Heparin, Does Not Prolong Bleeding Time in a Murine Arterial Thrombosis Model: A Comparative Study of Undaria pinnatifida sporophylls and Fucus vesiculosus. *Phytotherapy Research*, *26*(5), 752–757. https://doi.org/10.1002/PTR.3628
88. Stévant, P., Rebours, C., & Chapman, A. (2017). Seaweed aquaculture in Norway: recent industrial developments and future perspectives. *Aquaculture International*, *25*(4), 1373–1390. https://doi.org/10.1007/s10499-017-0120-7
89. Stortare – *Store norske leksikon*. (n.d.). Retrieved December 28, 2021, from https://snl.no/stortare
90. Stortare | Havforskningsinstituttet. (2020). Retrieved December 27, 2021, from https://www.hi.no/hi/temasider/arter/stortare
91. Synytsya, A., Kim, W. J., Kim, S. M., Pohl, R., Synytsya, A., Kvasnička, F., Čopíková, J., & Il Park, Y. (2010). Structure and antitumour activity of fucoidan isolated from sporophyll of Korean brown seaweed Undaria pinnatifida. *Carbohydrate Polymers*, *81*(1), 41–48. https://doi.org/10.1016/J.CARBPOL.2010.01.052
92. Tarehøsting. (n.d.). Retrieved December 28, 2021, from https://www.fiskeridir.no/Yrkesfiske/Havmiljoe/Tarehoesting
93. Tomasik, P., & Schilling, C. H. (1998). Complexes of starch with inorganic guests. *Advances in Carbohydrate Chemistry and Biochemistry*, *53*(53), 263–343. https://doi.org/10.1016/S0065-2318(08)60046-3
94. Tsai, H. L., Tai, C. J., Huang, C. W., Chang, F. R., & Wang, J. Y. (2017). Efficacy of Low-Molecular-Weight Fucoidan as a Supplemental Therapy in Metastatic Colorectal Cancer Patients: A Double-Blind Randomized Controlled Trial. *Marine Drugs*, *15*(4), 122. https://doi.org/10.3390/MD15040122
95. Turan, G. (2017). Determination of the Seasonal Yields of Total Fucose and Fucoidan Yields in Brown Seaweeds (Order Fucales) Distributed along the Coast of Urla (izmir, Turkey). *Aquaculture & Fisheries*, *1*(1), 1–4. https://doi.org/10.24966/AAF-5523/100005
96. Ustyuzhanina, N. E., Bilan, M. I., Ushakova, N. A., Usov, A. I., Kiselevskiy, M. V., & Nifantiev, N. E. (2014). Fucoidans: Pro- or antiangiogenic agents? *Glycobiology*, *24*(12), 1265–1274. https://doi.org/10.1093/GLYCOB/CWU063
97. UV-VIS Spectroscopy - *an overview | ScienceDirect Topics*. (n.d.). Retrieved March 3, 2022, from https://www.sciencedirect.com/topics/chemistry/uv-vis-spectroscopy
98. Wang, Y., Xing, M., Cao, Q., Ji, A., Liang, H., & Song, S. (2019). Biological Activities of Fucoidan and the Factors Mediating Its Therapeutic Effects: A Review of Recent Studies. *Marine Drugs*, *17*(3). https://doi.org/10.3390/MD17030183

99. Warttinger, U., Giese, C., & Krämer, R. (2017). Comparison of Heparin Red, Azure A and Toluidine Blue assays for direct quantification of heparins in human plasma. https://doi.org/10.48550/arxiv.1712.03377

100. Wekre M., Kopplin G., Jordheim M., (PDF) Extraction optimization for high value products from *Laminaria hyperborea*. (n.d.). Retrieved January 2, 2022, DOI:10.3390/antiox8120612

101. Wekre M., Kåsin K., Underhaug J., Jordheim M., Holmelid B., (2019). Quantification of Polyphenols in Seaweeds: A Case Study of Ulva intestinalis. *Antioxidants*, *8*(12). https://doi.org/10.3390/ANTIOX8120612

102. Wu, H., Rebello, O., Crost, E. H., Owen, C. D., Walpole, S., Bennati-Granier, C., Ndeh, D., Monaco, S., Hicks, T., Colvile, A., Urbanowicz, P. A., Walsh, M. A., Angulo, J., Spencer, D. I. R., & Juge, N. (2021). Fucosidases from the human gut symbiont Ruminococcus gnavus. *Cellular and Molecular Life Sciences*, *78*(2), 675–693. https://doi.org/10.1007/S00018-020-03514-X

103. Yao, H. Y. Y., Wang, J. Q., Yin, J. Y., Nie, S. P., & Xie, M. Y. (2021). A review of NMR analysis in polysaccharide structure and conformation: Progress, challenge and perspective. *Food Research International*, *143*, 110290. https://doi.org/10.1016/J.FOODRES.2021.110290

104. Zargarzadeh, M., Amaral, A. J. R., Custódio, C. A., & Mano, J. F. (2020). Biomedical applications of laminarin. *Carbohydrate Polymers*, *232*, 115774. https://doi.org/10.1016/J.CARBPOL.2019.115774

105. Zayed A., M, E.-A., AS, I., & R, U. (2020). Fucoidan Characterization: Determination of Purity and Physicochemical and Chemical Properties. *Marine Drugs*, *18*(11). https://doi.org/10.3390/MD18110571

106. Zhao, J., Kong, Y., Zhang, F., & Linhardt, R. J. (2018). Impact of Temperature on Heparin and Protein Interactions. *Biochemistry & Physiology: Open Access*, *7*(2), 1–5. https://doi.org/10.4172/2168-9652.1000241

Appendix 1: Drift checks of selected L-fucose col. assay experiments

In figure 22, the drift check for the second parallel for the L-fucose col. assay standard curve is shown.

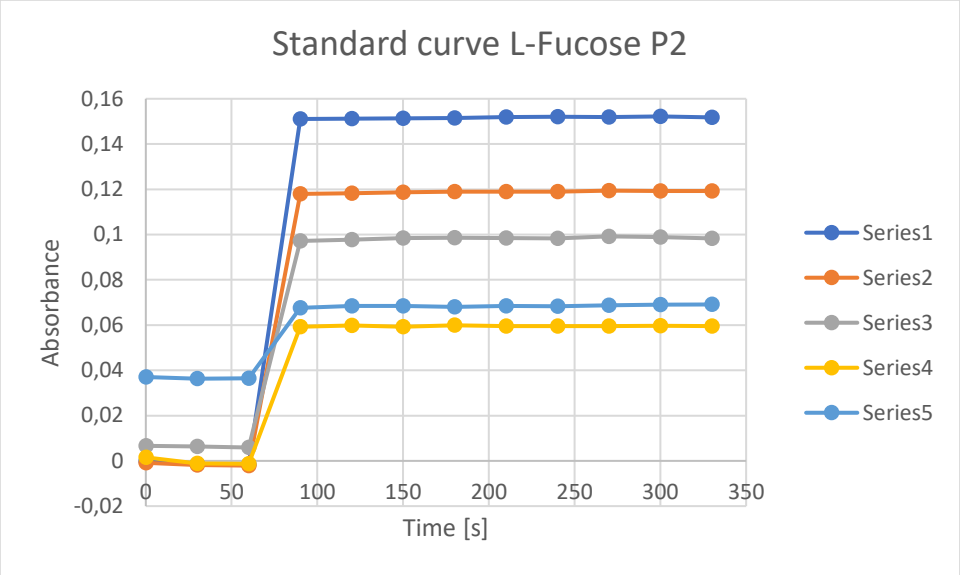

Figure 39: Drift check of L-fucose standard curve P2.

In figure 23 a drift check of the three parallels of the 6-hh L-fucose quantification of the Sigma Aldrich fucoidan standard is shown.

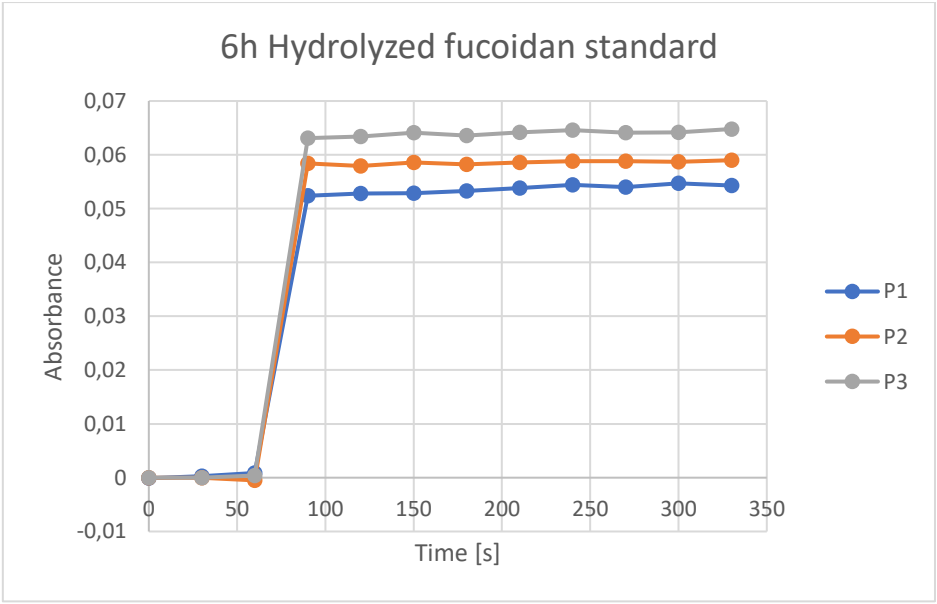

Figure 40: Drift check of the three parallels of the 6-hh fucoidan standard.

In figure 24 a drift check of the three parallels of the 24-hh L-fucose quantification of the Sigma Aldrich fucoidan standard is shown.

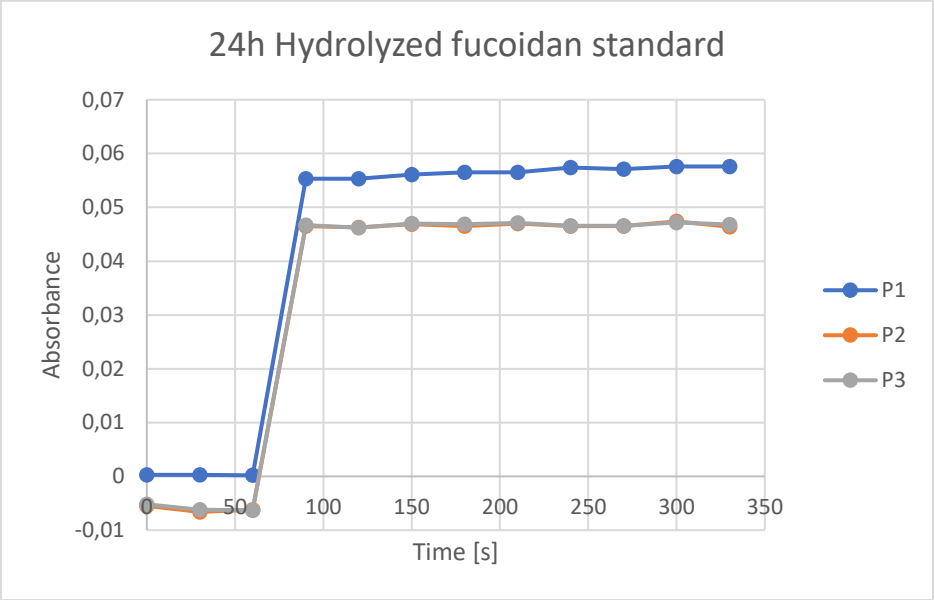

Figure 41: Drift check of the three parallels of the 24-hh fucoidan standard.

In figure 25 a drift check of the three parallels of the 48-hh L-fucose quantification of the Sigma Aldrich fucoidan standard is shown.

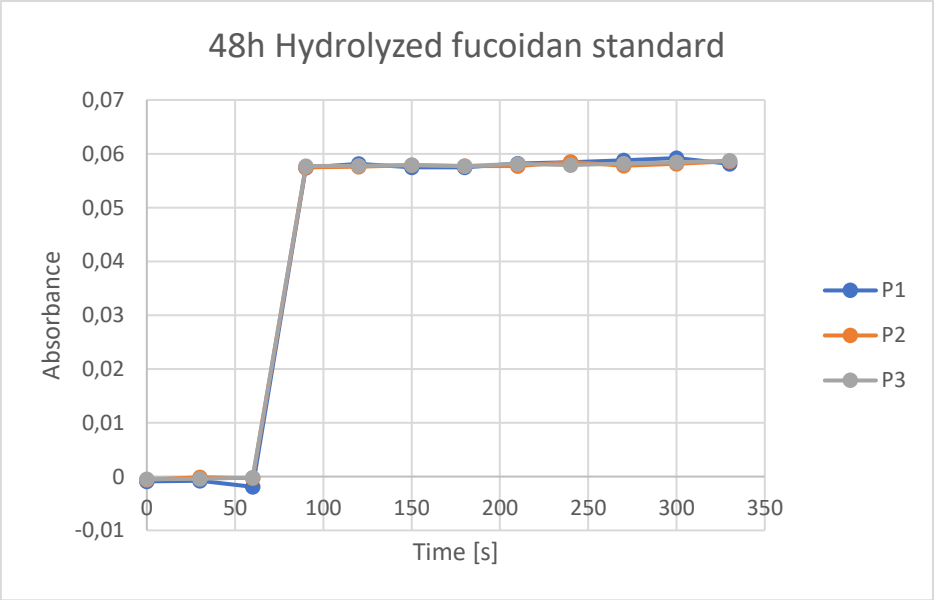

Figure 42: Drift check of the three parallels of the 48-hh fucoidan standard.

In figure 26 a drift check of the three parallels of the 6-hh L-fucose quantification of the fine fucoidan from Alginor is shown.

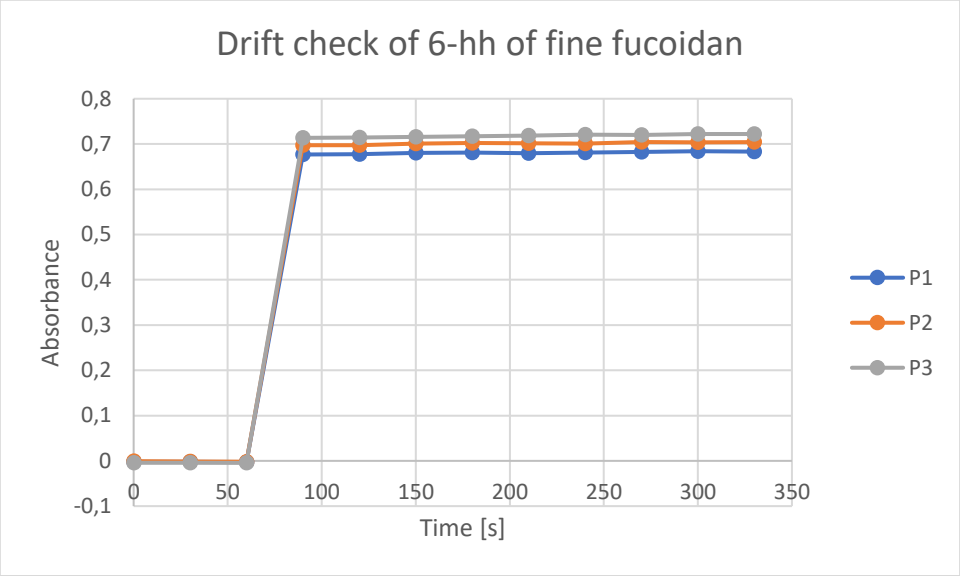

Figure 43: Drift check of the three parallels of the 6-hh fine fucoidan.

In figure 27 a drift check of the three parallels of the 24-hh L-fucose quantification of the fine fucoidan from Alginor is shown.

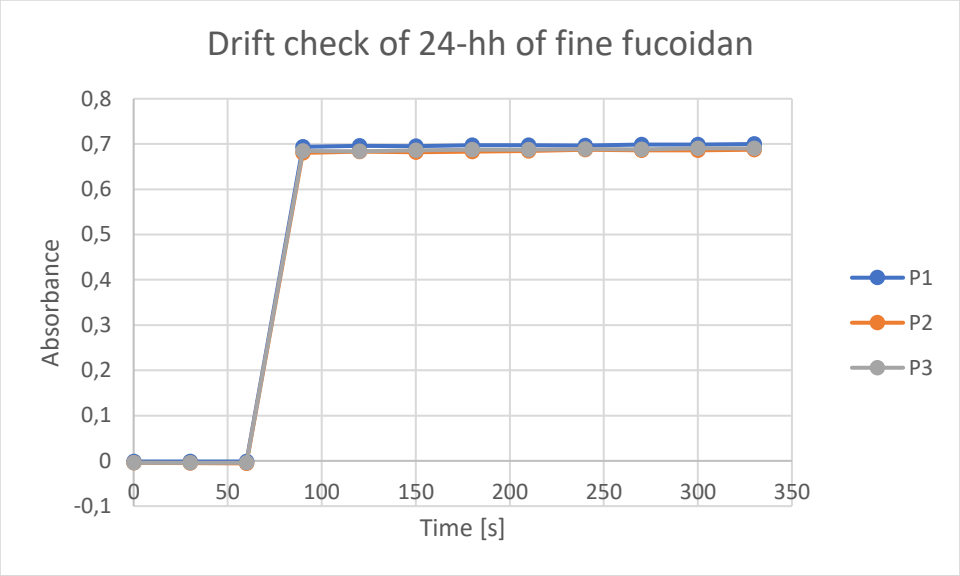

Figure 44: Drift check of the three parallels of the 24-hh fine fucoidan.

In figure 28 a drift check of the three parallels of the 48-hh L-fucose quantification of the fine fucoidan from Alginor is shown.

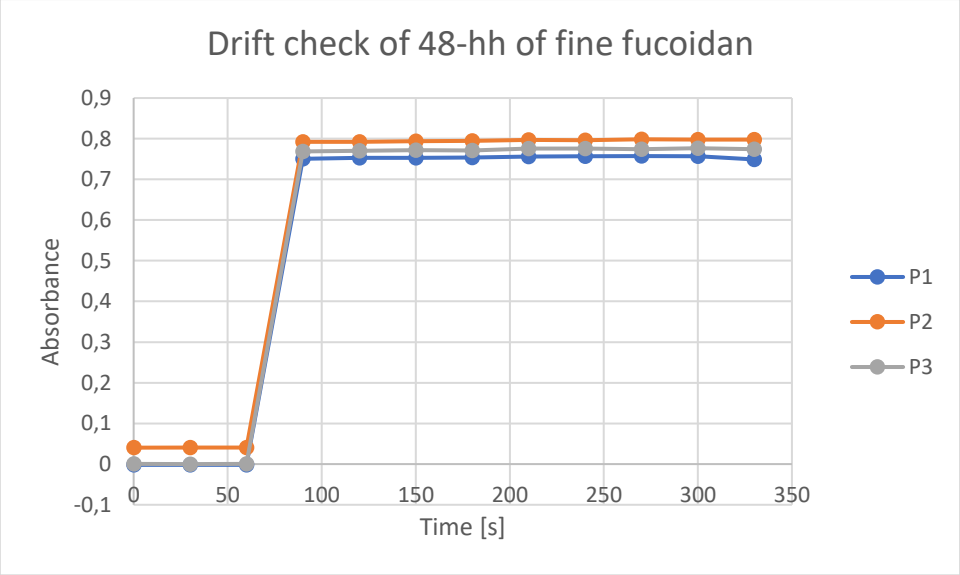

Figure 45: Drift check of the three parallels of the 48-hh fine fucoidan.

In figure 29 a drift check of the three parallels of the 6-hh L-fucose quantification of the crude fucoidan from Alginor is shown.

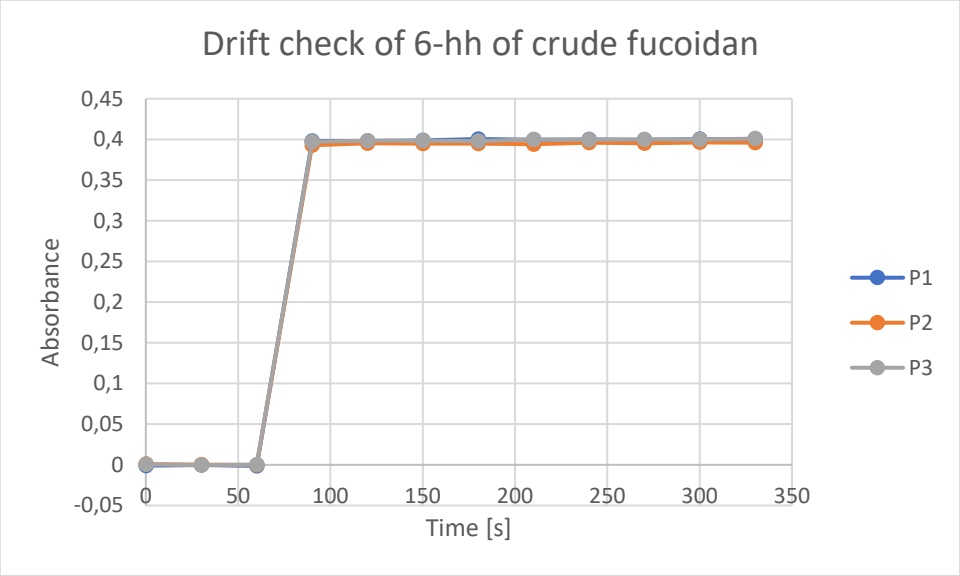

Figure 46: Drift check of the three parallels in 6-hh fucoidan crude.

In figure 30 a drift check of the three parallels of the 24-hh L-fucose quantification of the crude fucoidan from Alginor is shown.

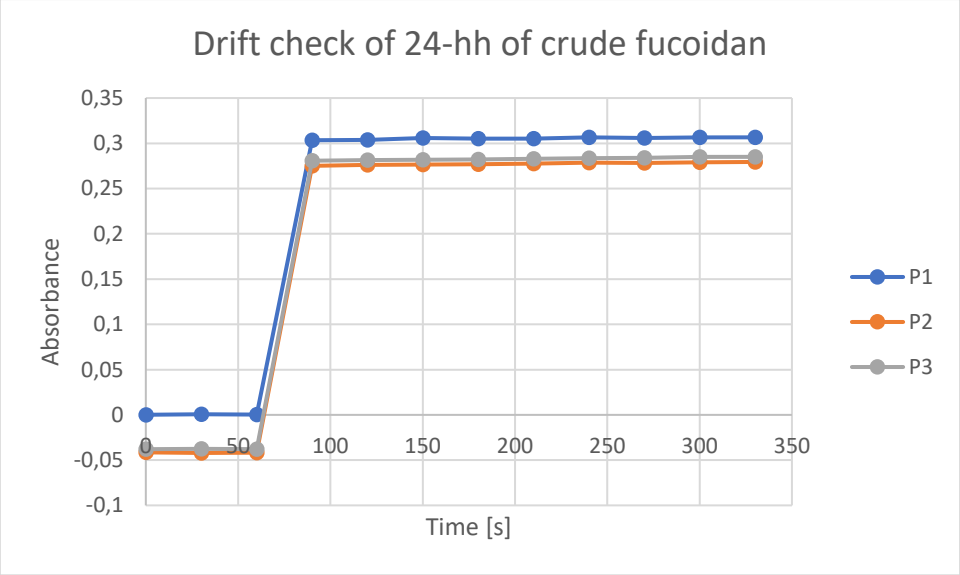

Figure 47: Drift check of the three parallels in 24-hh fucoidan crude.

In figure 31 a drift check of the three parallels of the 48-hh L-fucose quantification of the crude fucoidan from Alginor is shown.

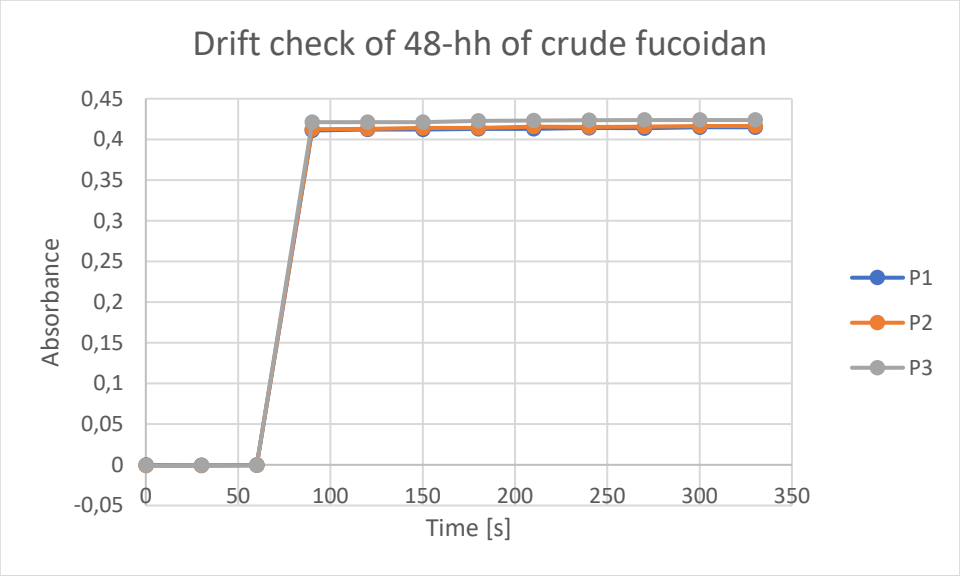

Figure 48: Drift check of the three parallels in 48-hh crude fucoidan.

Appendix 2: Drift check of optimized and room temperature heparin col. assay standard curves

In figure 42 a drift check of the five series in P1 for the optimized standard curve is shown. The standard curve is made using fucoidan solution 2 shown in table 4.

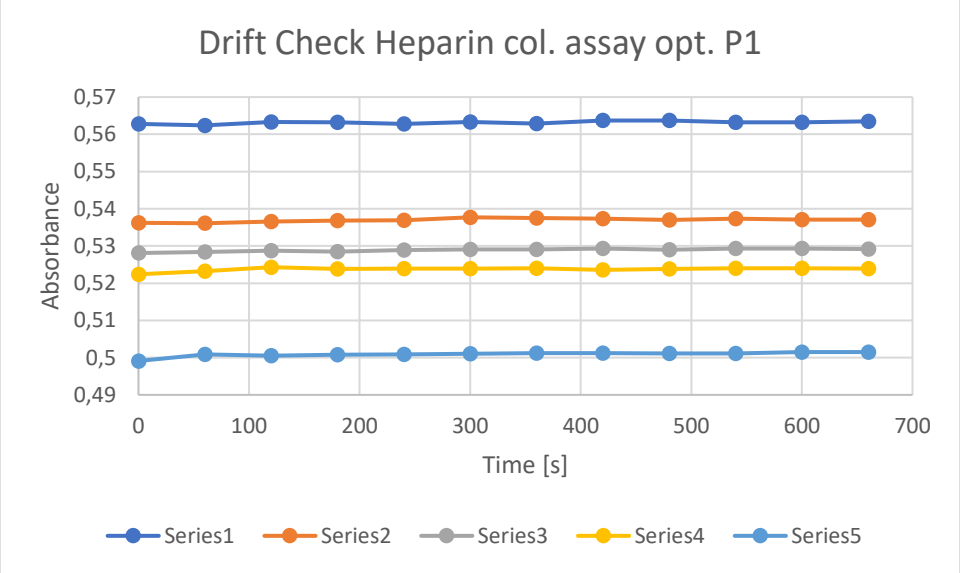

Figure 49: Drift check for standard curve with Sigma Aldrich fucoidan solution 2 P1

In figure 44 a drift check of the five series in P2 for the optimized standard curve is shown. The standard curve is made using fucoidan solution 2 shown in table 4.

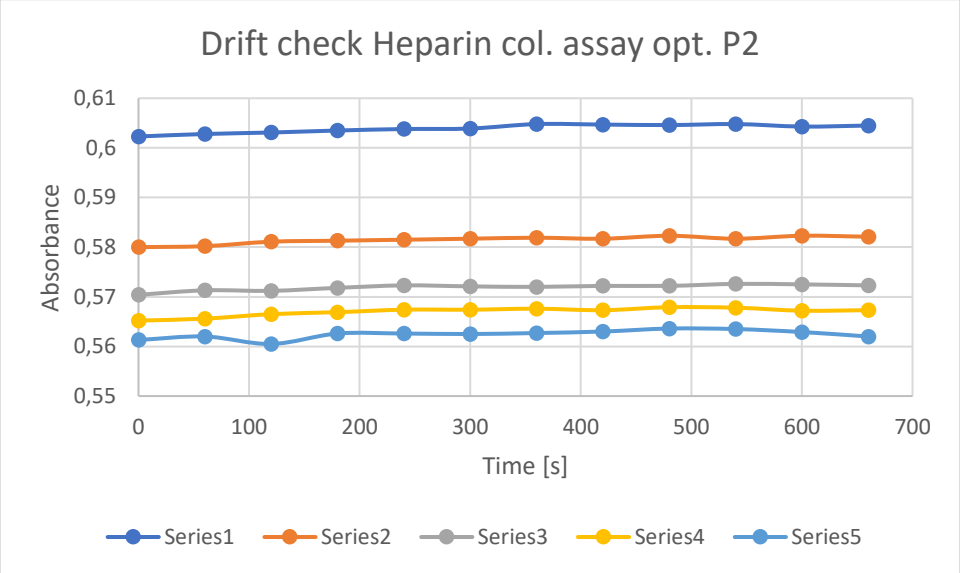

Figure 50: Drift check for standard curve with Sigma Aldrich fucoidan solution 2 P2.

In figure 47 a drift check of the five series in P1 for the room temperature standard curve is shown. The standard curve is made using fucoidan solution 3 shown in table 4.

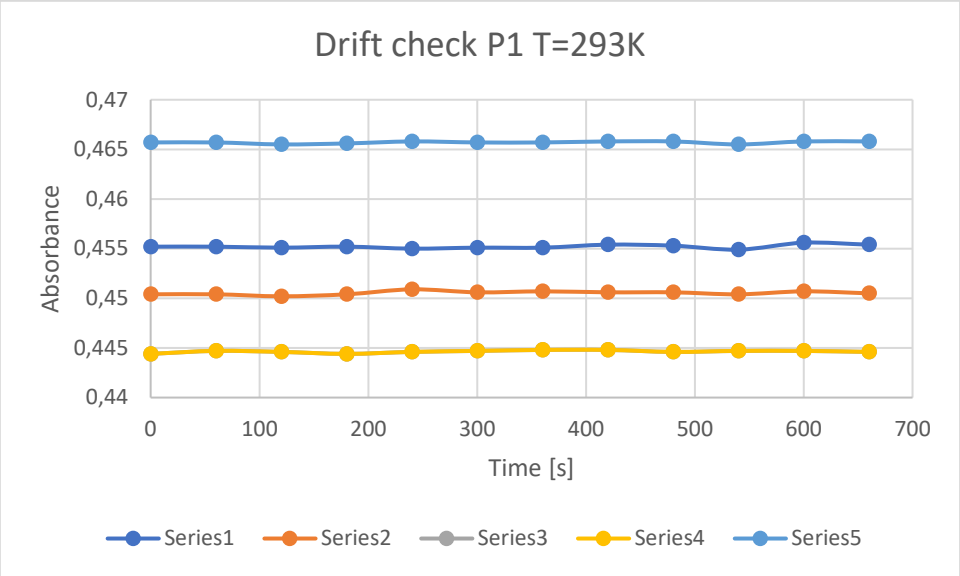

Figure 51: Drift check of standard curve with Sigma Aldrich fucoidan solution 3 P1 with room temperature.

In figure 49 a drift check of the five series in P2 for the room temperature standard curve is shown. The standard curve is made using fucoidan solution 3 shown in table 4.

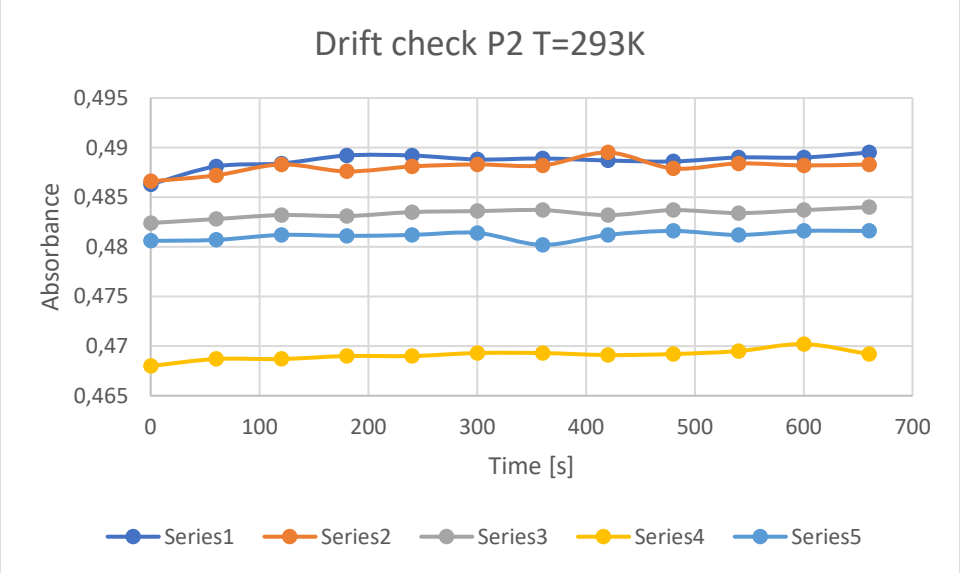

Figure 52: Drift check of standard curve with Sigma Aldrich fucoidan solution 3 P2 with room temperature.

Appendix 3: ^{1}H NMR and qNMR spectrums

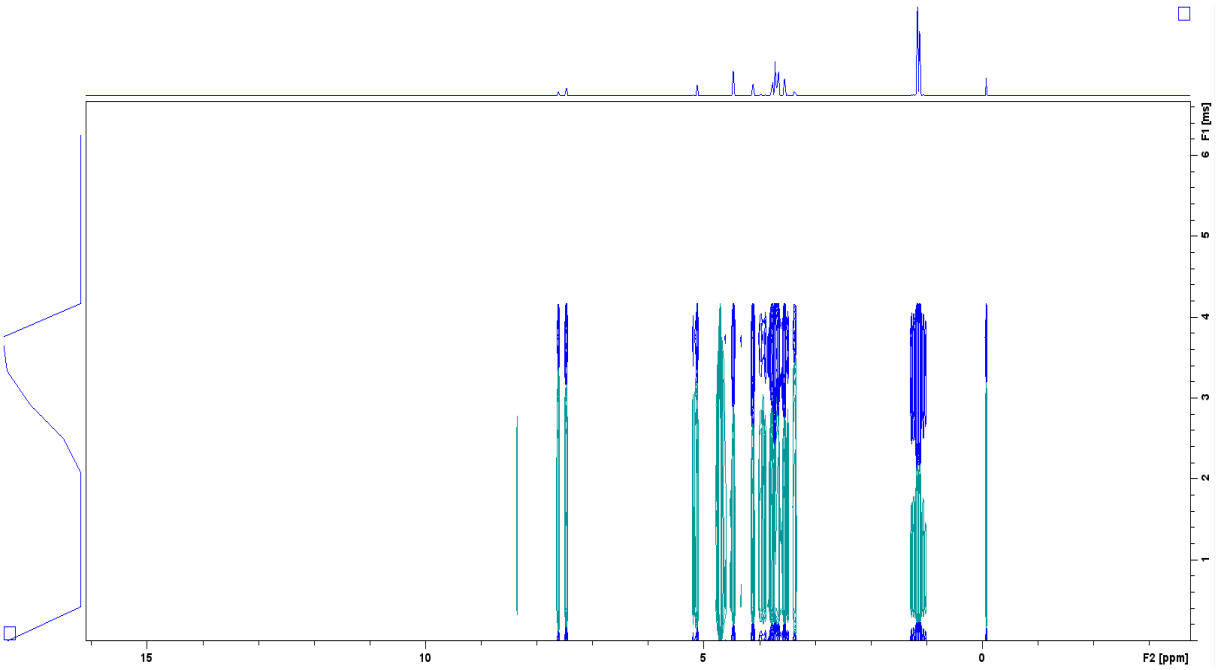

Figure 53: T1 experiment of fucose (≥99.9%), with KHP as internal standard and D2O as solved.

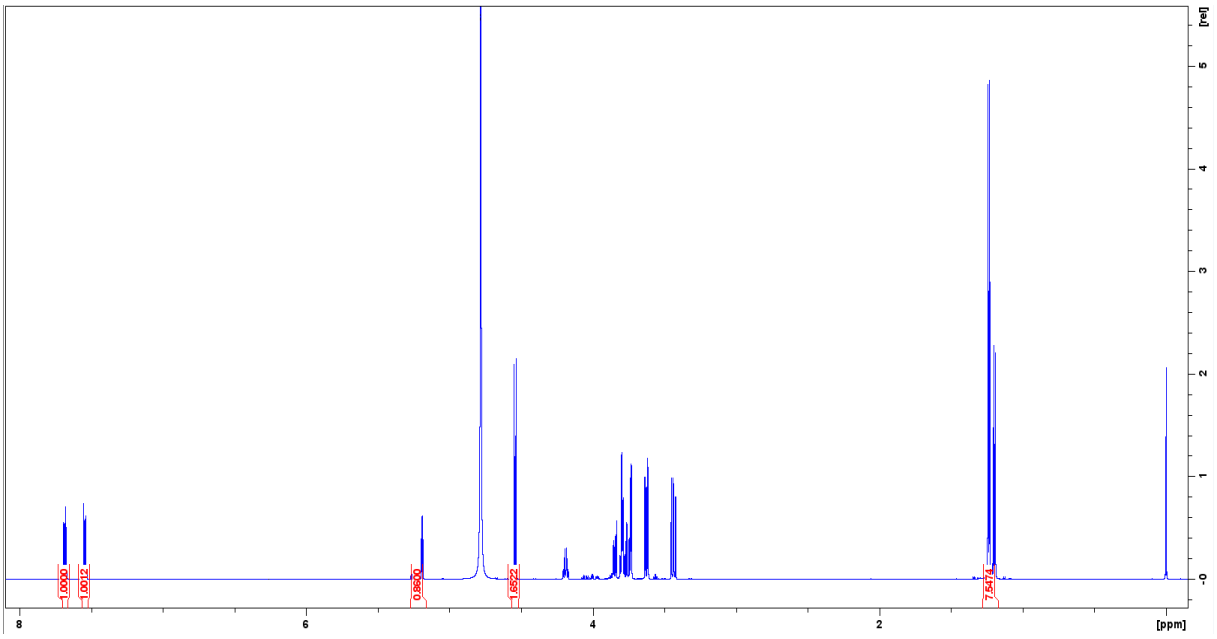

Figure 54: ^{1}H NMR of fucose (≥99.9%), with KHP as standard and D2O as solvent.

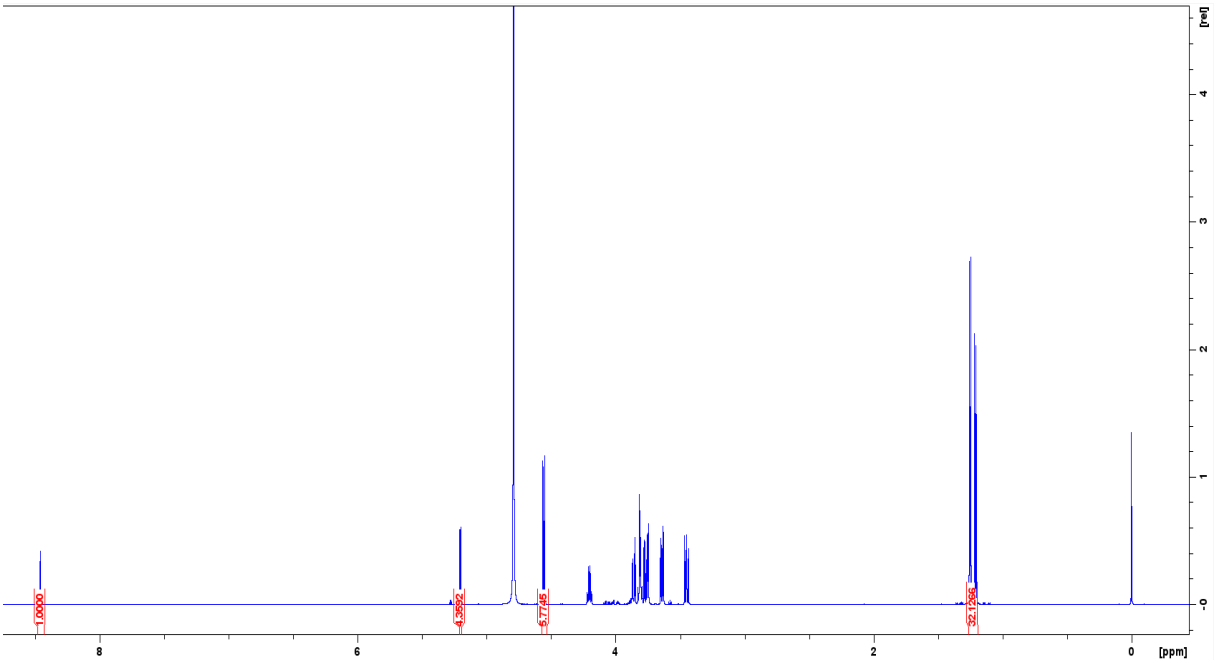

Figure 55: ^{1}H NMR of fucose (≥99.9%) with calcium formate as standard and D2O as solvent P1.

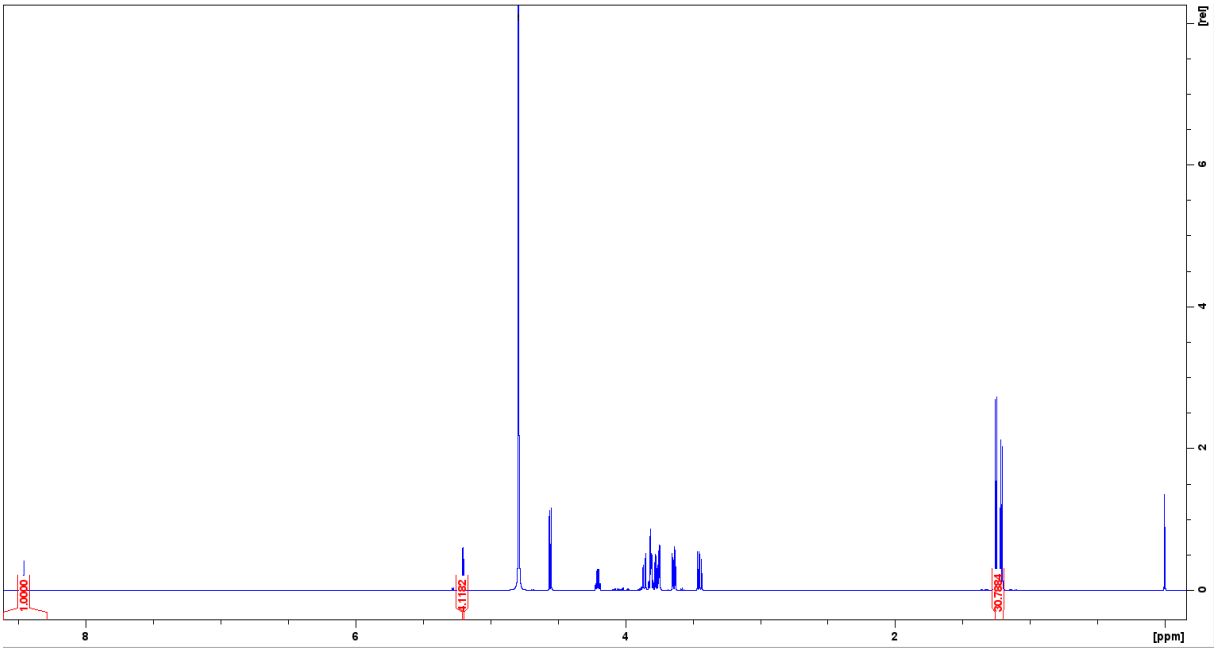

Figure 56: ^{1}H NMR of fucose (≥99,9%) with calcium formate as standard and D2O as solvent P1, broad integration.

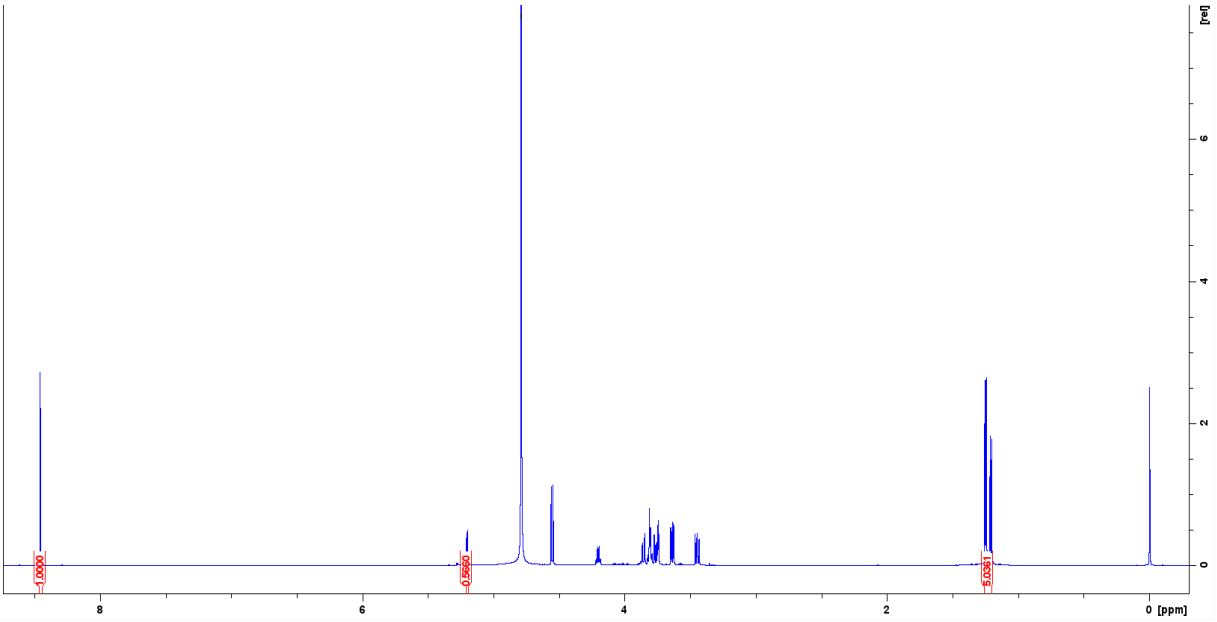

Figure 57: ^{1}H NMR of fucose (≥99,9%) with calcium formate as standard and D2O as solvent P2.

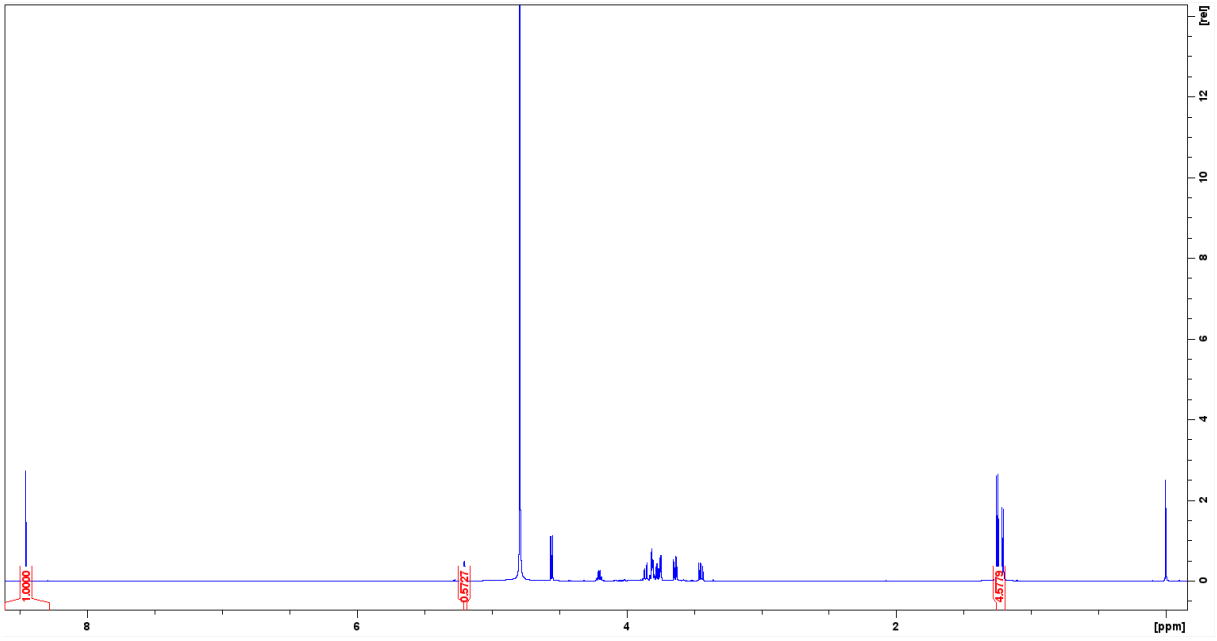

Figure 58: ^{1}H NMR of fucose (≥99,9%) with calcium formate as standard and D2O as solvent P2, broad integration.

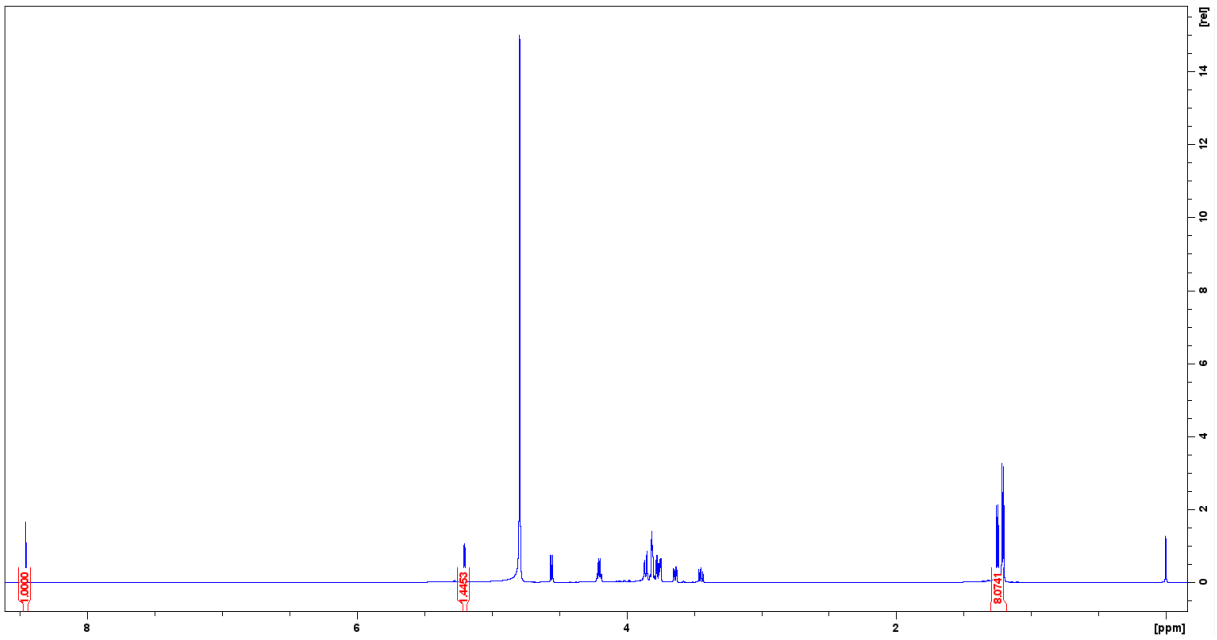

Figure 59: ^{1}H NMR of fucose (≥99,9%) with calcium formate as standard and D2O as solvent P3, considered an outlier.

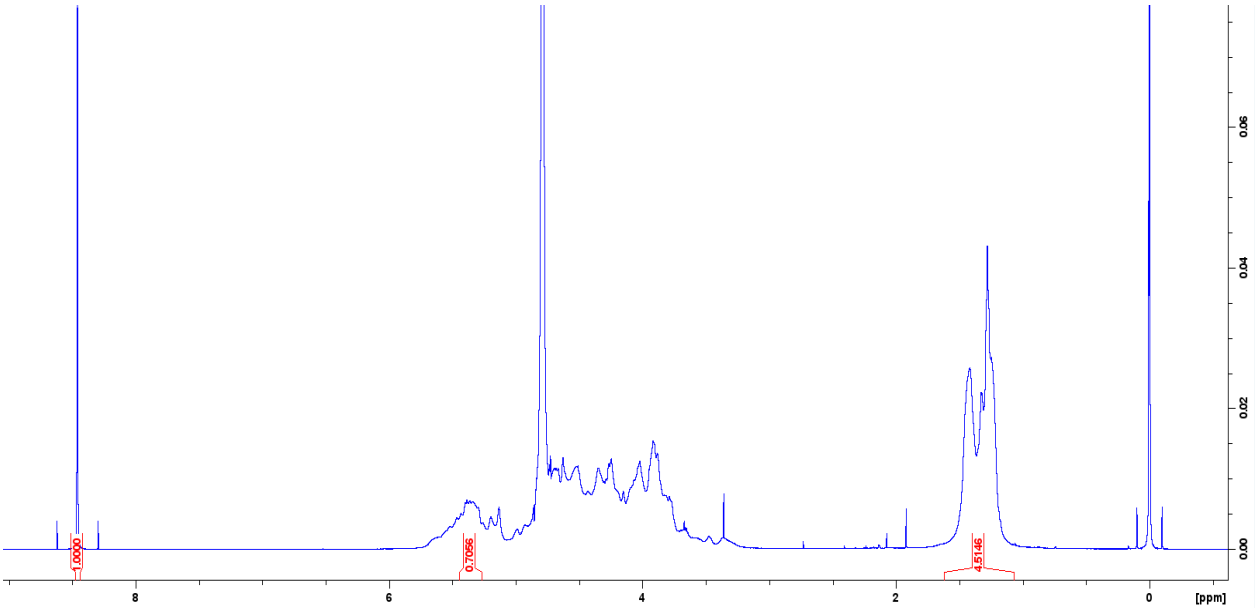

Figure 60: qNMR of fucoidan (≥95%) from Fucus vesiculosus, with calcium formate as standard and D2O as solvent.

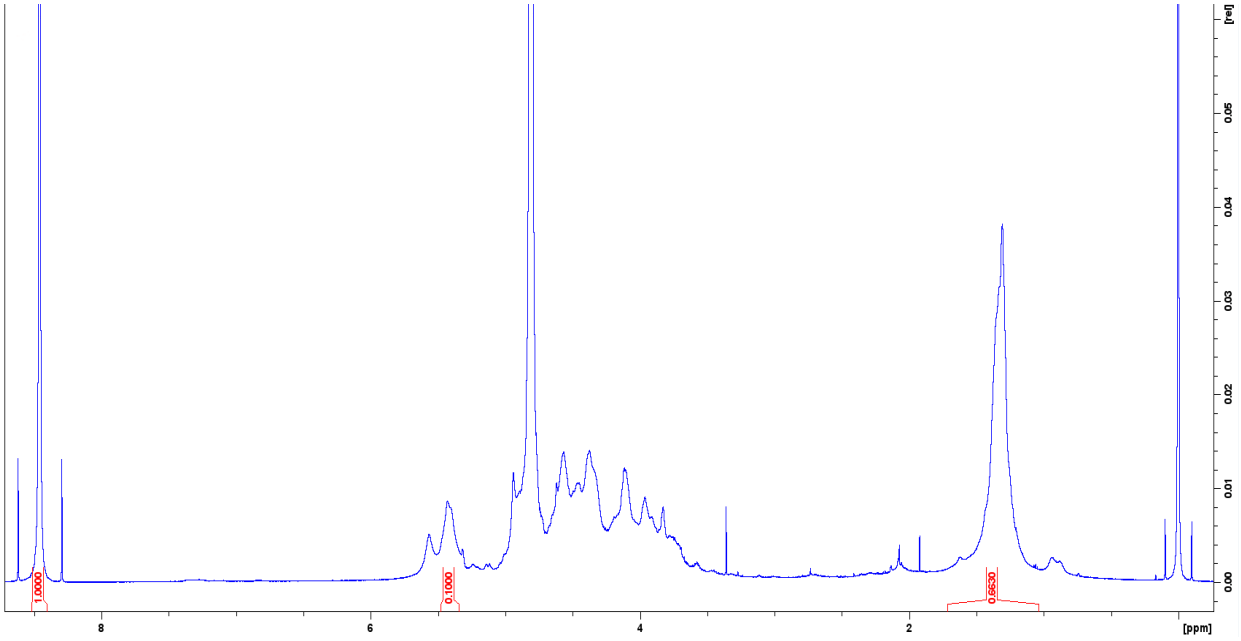

Figure 61: qNMR of fine fucoidan from Alginor, with calcium formate as standard and D2O as solvent.

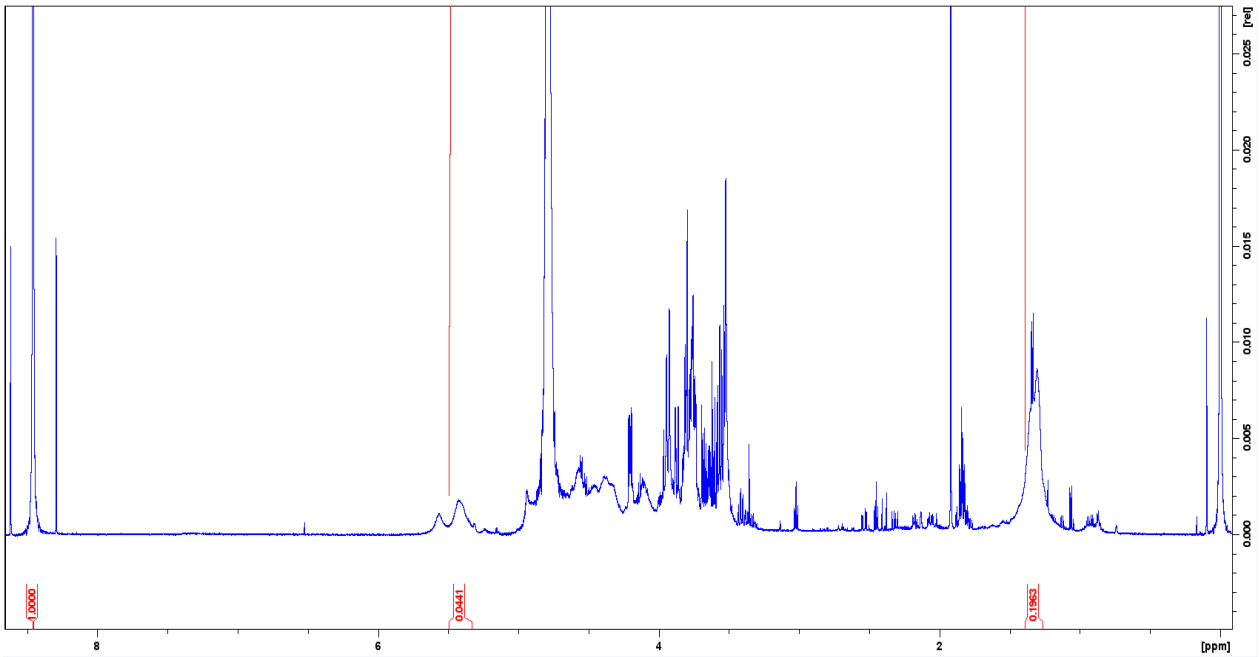

Figure 62: qNMR of crude fucoidan from Alginor, with calcium formate as standard and D2O as solvent.